Universidad Nacional Autónoma de México

Facultad de Ciencias

Topological Insulators: Quantum Phenomena of the Effective Theory

T E S I S

QUE PARA OBTENER EL TÍTULO DE:

Físico

P R E S E N T A :

Andrés Gómez Arias

TUTOR

Dr. Luis Fernando Urrutia Ríos

Ciudad Universitaria, CDMX, 2021

«See that the imagination of nature is far, far greater than the imagination of man.»

Richard P. Feynman

A mis padres, *Omar Gómez* y *Ana Rosa Arias*.

A mis hermanos, *Omar* y *Ana María*.

Agradecimientos

A los miembros del jurado: El *Dr. Chumin Wang Chen*, el *Dr. José Alberto Martín Ruiz*, el *Dr. Luis Fernando Urrutia Ríos*, el *Dr. José Eduardo Barrios Vargas* y el *Dr. Carlos Ramírez Ramos*.

Agradezco profundamente a mis padres, *Omar Gómez* y *Ana Rosa Arias*, quienes siempre alimentaron mi cuerpo y enriquecieron mi mente. Con cuidado y cariño construyeron los elementos fundamentales que hoy me definen. Con su esfuerzo y trabajo me permitieron realizar mis estudios en la UNAM, y sin ellos este trabajo no existiría.

A mis hermanos, *Omar* y *María*, por su acompañamiento y amistad, que desde sus diferentes perspectivas han complementado mi aprendizaje.

A mis amigos de GDL, *Carlos*, *José Antonio* (*Pepe*) y *Rubén*, que se han convertido en mis compañeros de la vida y que, a pesar de la distancia, nos hemos mantenido cercanos. Gracias por sus risas y alegrías en las incontables noches que hemos charlado y jugado.

A mis amigos de la CDMX, en especial a *Stefan*, *Alfonso*, *Jesús Eduardo* (*Eddy*), *André*, *Carlos* (*Charley*), *Eduardo* (*Chiapas*), *Harim*, *José Andrés* (*Parker*) y *Julián*, que me brindaron risas y compañía, y que se convirtieron en mi familia. Agradezco especialmente a *Stefan* por enseñarme, apoyarme, motivarme y guiarme en tantas cosas nuevas, tanto de la física como de la vida, así como por leer y ayudarme a pulir este escrito.

A todos los demás profesores, amigos y conocidos que han formado parte de mi vida que, directa o indirectamente, me han proporcionado enseñanzas tanto académicas como personales, y que de alguna manera han plasmado parte de su persona en la mía.

Abstract

The work presented in this Bachelor's thesis in physics focuses on a quantum system of electrons under the presence of a 3D topological insulator (TI). One of the main properties of TI's is that their microscopic effective electronic Hamiltonian can recover the free Dirac Lagrangian in exchange for the appearance of an additional effective electromagnetic action proportional to the fine structure constant, which produces the so-called axion electrodynamics. This feature is strongly exploited throughout this thesis, as one can effectively treat the electrons under the presence of a TI as a free electron gas, but within the effects of the effective electromagnetic response. This response, under the presence of external electromagnetic fields, creates induced electromagnetic fields inside the material, which affect the behaviour of the electrons.

When solving the respective Schrödinger equation, and under the presence of a finite plate of a TI in an external perpendicular magnetic field, bound states are produced. This happens because an electric field is induced inside the plate which in turn produces a finite triangle potential that constrains the electrons. The production of these bound states has two important consequences. First, the dependence in the magnetic field of the bound-state energies produces a non-trivial magnetization term in addition to the 2D analogue of the Landau magnetization. Second, this localization allows the treatment of this electron gas to be as if it was constrained to move in a bi-dimensional plate which, for this reason and for the presence of the perpendicular magnetic field, makes the system appropriate for the realization of the quantum Hall effect (QHE). An attempt to replicate the QHE on this system is made, but corrections to the Hall current are obtained. These discrepancies arise from the fact that the parallel electric field needed for the realization of the QHE also induces a parallel internal magnetic field. The corrections to the Hall current are treated via perturbation theory in terms of the small parameter given by the fine structure constant that accompanies each induced field. These corrections turn out to be non-trivial and of second-order on this parameter.

In both of the previous phenomenon, a discontinuous transition of the macroscopic variables is found, which arises from the sudden appearance of new energy states at particular values of the external magnetic field and thus resulting in quantum phase transitions of first order. This is the main result of this work, which as mentioned, is present both in the magnetization and in the corrections of the Hall current.

The thesis is organized as follows. In chapter 1 a review of the Hall effect is made, with special focus on its quantum version. In chapter 2 a general review of TI is also made, going from their general properties to the particular effective micro-

scopic Hamiltonian which produces the electromagnetic response. In chapter 3 the Schrödinger equation for the quantum system previously described is solved, obtaining the bound state solutions. Also, an extensive discussion over the occupation of the energy states is made as a preamble to the emergence of the phase transition. In chapter 4 the magnetization for this system is calculated. First for a thin-plate where only one energy band is present, then close to the first critical point from which a second energy band appears and produces the phase transition, and finally, for a general critical point from which the nth energy band appears. In chapter 5, the parallel electric field is introduced and the corrections to the QHE via perturbation theory are obtained. Numerical analysis for these corrections are made to visualize the presence of the phase transitions. The conclusions are presented in chapter 6. Appendix A enlists the constants and variables used throughout this work. Appendix B manages the corrections to all of the results produced by the presence of spin, as it is for simplicity generally ignored. Appendix C briefly presents the Airy functions and their properties, and shows how they are involved in the wave function solutions in the case of a constant electric field. Appendix D reviews the WKB approximation and applies it to our particular system to obtain a closed formula for the bound state energies. Appendix E clarifies some non-trivial limits which appear in the matrix elements of chapter 5.

Resumen

El trabajo presentado en esta tesis de licenciatura en física se enfoca en sistemas cuánticos de electrones bajo la presencia de un aislante topológico (AT) 3D. Una de las principales propiedades de los AT es que su Hamiltoniano microscópico efectivo puede recuperar la Lagrangiana de Dirac a cambio de la aparición de una acción electromagnética efectiva adicional proporcional a la constante de estructura fina, la cual produce la así llamada electrodinámica axiónica. Esta propiedad es constantemente aprovechada a lo largo de esta tesis puesto que uno puede tratar a los electrones bajo la presencia de un AT como un gas de electrones libres, pero bajo los efectos de la respuesta electrodinámica efectiva. Esta respuesta, bajo la presencia de campos electromagnéticos externos, crea campos electromagnéticos inducidos dentro del material, los cuales afectan el comportamiento de los electrones.

Al resolver la ecuación de Schrödinger respectiva, y bajo la presencia de una placa finita de un AT con un campo magnético perpendicular externo, hay una aparición de estados ligados. Esto sucede debido a que un campo eléctrico es inducido dentro de la placa, que en consecuencia produce un potencial triangular finito que constriñe a los electrones. La producción de estos estados ligados tiene dos consecuencias importantes. Primero, la dependencia en el campo magnético de las energías de los estados ligados produce un término de magnetización no trivial además del análogo en 2D de la magnetización de Landau. Segundo, esta localización permite que el manejo de este gas electrones sea como si estuviera constreñido a moverse en una placa bidimensional que, por esta razón y debido a la presencia del campo magnético perpendicular, hace que el sistema sea apropiado para la realización del efecto Hall cuántico (EFC). Se hace un intento para replicar el EFC en este sistema, pero se encuentran correcciones a la corriente Hall. Estas discrepancias surgen debido a que el campo eléctrico adicional necesario para la realización del EFC también induce un campo magnético paralelo interno. Las correcciones a la corriente Hall son tratadas mediante teoría de perturbaciones en términos del parámetro pequeño dado por la constante de estructura fina que acompaña a cada campo inducido. Éstas resultan ser no triviales y de segundo orden en este parámetro.

En ambos fenómenos previos se encuentra una transición discontinua de las variables macroscópicas, que surge de la aparición espontánea de nuevos estados de energía en valores particulares del campo magnético externo y que entonces resulta en transiciones de fase cuánticas de primer orden. Este es el resultado principal de este trabajo, que como fue mencionado, está presente tanto en la magnetización como en las correcciones a la corriente Hall.

La tesis tiene la siguiente organización. En el capítulo 1 se hace una revisión del efecto Hall, con especial enfoque en su versión cuántica. En el capítulo 2 se hace también una revisión general de los AT, abarcando desde sus propiedades generales hasta el Hamiltoniano microscópico efectivo particular que produce la respuesta electromagnética. En el capítulo 3 se resuelve la ecuación de Schrödinger para el sistema cuántico previamente descrito, obteniendo las soluciones de estados ligados. Además, se hace una discusión extensiva sobre la ocupación de los estados de energía como un preámbulo de la emergencia de la transición de fase. En el capítulo 4 la magnetización para este sistema es calculada. Primero para una placa delgada donde sólo una banda de energía está presente, luego cerca del primer punto crítico a partir del cual aparece una segunda banda de energía y produce la transición de fase y finalmente, para un punto crítico general a partir del cual aparece la n-ésima banda. En el capítulo 5 el campo eléctrico paralelo es introducido y las correcciones al EFC mediante teoría de perturbaciones son obtenidas. Se hace un análisis numérico para estas correcciones para visualizar la presencia de las transiciones de fase. Las conclusiones se presentan en el capítulo 6. El apéndice A enlista las constantes y variables usadas a lo largo de este trabajo. El apéndice B maneja las correcciones a todos los resultados producidas por la presencia del espín, pues por simplicidad es generalmene ignorado. El apéndice C presenta brevemente a las funciones de Airy y sus propiedades, y muestra como estas están involucradas en las funciones de onda para el caso de un campo eléctrico constante. En el apéndice D se hace una revisión de la aproximación WKB, junto con su aplicación a nuestro sistema en particular para obtener una fórmula cerrada de las energías de los estados ligados. Finalmente, el apéndice E aclara algunos limites no triviales que aparecen en los elementos de matriz en el capítulo 5.

Contents

1 Introduction to the Hall effect

The Hall effect (HE) takes place on systems of electrons restricted to move on a bidimensional surface where a perpendicular magnetic field B_z is present. When an electric current I_x is induced on the plate, a transverse voltage V_y appears [1] (see Fig. 1.1).
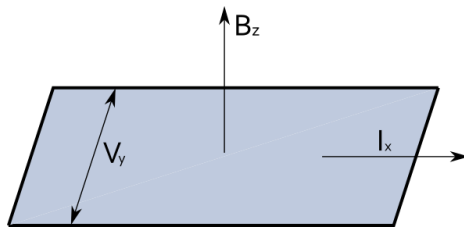
Figure 1.1: Hall effect system.

Classically, this transverse voltage is linearly dependent on the magnetic field, such that the transverse resistivity takes the form

$$\rho_{xy} \equiv -V_y/I_x = \frac{B_z}{n_e e}, \tag{1.1}$$

where e is the fundamental charge and n_e the electronic surface density. This is the classical Hall effect, discovered by Edwin Hall in 1879 [2]. This effect is peculiar, as the resistivity above-defined does not depend on the collision time between electrons. A more detailed description of the classical Hall effect can be found in section 1.1.

When the plate presents disorder [3], in the presence of strong magnetic fields (around $15\,\mathrm{T}$) and at low temperatures (around $3\,\mathrm{K}$) [4], the behavior of the system completely changes. The Hall voltage forms constant plateaus, each with the distinct value

$$\boxed{\rho_{xy} = \frac{2\pi\hbar}{e^2}\frac{1}{\nu}, \quad \nu \in \mathbb{N}}, \tag{1.2}$$

where $\hbar$ is Planck's constant. Furthermore, the longitudinal resistivity becomes zero[1], $\rho_{xx} = 0$. This is the integer quantum Hall effect (QHE). It was discovered experimentally by Klaus von Klitzing in 1980 [4], which earned him the 1985 Nobel Prize. This effect motivated the definition of $R_K = 2\pi\hbar/e^2$ as the *quantum of resistivity* (also

---

[1]It actually presents peaks around each transition point between plateaus, but we will not focus on this phenomenon.

known as the von Klitzing constant); the QHE precisely allows the measurement of this constant with incredible precision. With the 2018 redefinition of the fundamental constants h and e, it has a defined value of [5] $R_K = 25812.80745... \Omega$. A more detailed description of the QHE will be made in section 1.2. A comparison between the classical and quantum Hall effect's transverse resistivity is shown in Fig. 1.2.
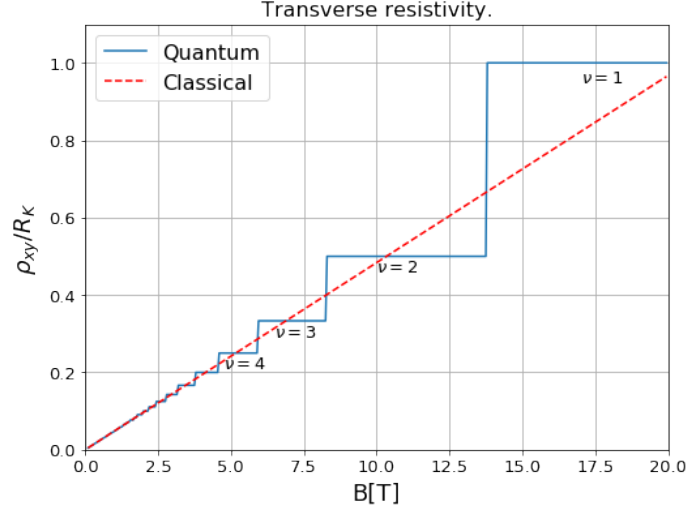
Figure 1.2: Classical and quantum transverse resistivity in the HE, divided by the quantum of resistivity R_K. A typical value [3] of $n_e = 5 \times 10^{15} \, \mathrm{m}^{-2}$ was used.

With the reduction of impurities, the quantum behaviour of the resistivity breaks, but in the process, fractional valued plateaus arise. This was discovered by Tsui and Störmer in 1982 [6], and is known as the fractional quantum Hall effect[2]. It is a midpoint between the integer-valued plateaus and the classical linearly-behaved HE. This phenomenon is best described when the interactions between electrons are taken into account [3]. Nonetheless, this will not be discussed here as it escapes the purposes of this thesis.

1.1 Classical Hall effect

Take the system of Fig. 1.1. The Lorentz force gives the equation of motion for electrons

$$m\frac{d\mathbf{v}}{dt} = -e(\mathbf{E} + \mathbf{v} \times \mathbf{B}), \tag{1.3}$$

where m is the electron mass, $\mathbf{v}$ its velocity, and $\mathbf{E}$, $\mathbf{B}$ the electric and magnetic fields respectively. In absence of electric fields, and with $\mathbf{B} = B\hat{e}_z$ the solution to the equation is

$$x(t) = x_0 + r_0 \sin(\omega_B t - \varphi), \quad y(t) = y_0 + r_0 \cos(\omega_B t - \varphi), \tag{1.4}$$

---

[2]The fractional case is still technically a quantum Hall effect. Yet, for simplicity and unless stated otherwise, on this thesis the quantum Hall effect will only denote the integer case.

where x_0, y_0, r_0, φ are arbitrary integration constants, and

$$\omega_B = \frac{eB}{m}. \tag{1.5}$$

This motion is called cyclotron motion, where electrons move in circles at a frequency given by ω_B, denoted as the cyclotron frequency. This variable carries the sign of B and thus, the electrons go clockwise for $\mathbf{B}$ in the $\hat{z}$ direction, and counterclockwise in the $-\hat{z}$ direction.

But when the electrons are trapped in a finite plate such as in Fig. 1.1, the movement of the electrons in the boundary changes. Instead of completing their circular motion, they collide with the boundary of the plate, bouncing with opposite velocity, which sets off a new displaced turn. In summary, the electrons on the bulk move in circular orbits, while the ones on the boundaries propagate across them. This can be seen in Fig. 1.3. Even with the unidirectional displacement of electrons in the boundaries, no net current is induced because opposite borders carry opposite current.
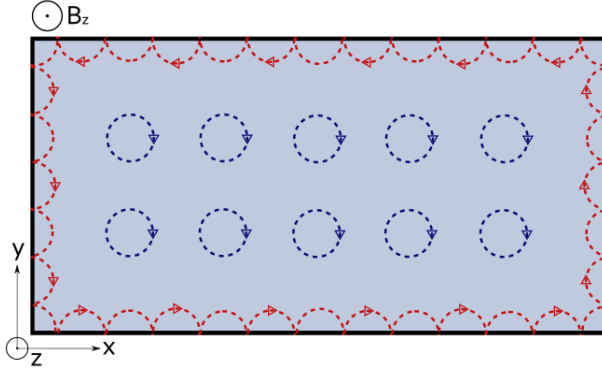
Figure 1.3: Cyclotron motion of electrons in the bulk and edges of the plate. In the edges, chiral states (constrained to move in one direction) appear.

If we take the plate infinite in the x direction, we get electrons constrained to move to the right (left) in the lower (upper) edge of the plate. These are called chiral states [7]. The left and right states usually don't mix, as they are separated by the bulk. But when a current in the y-direction is induced, the number of chiral states in one direction diminishes, while the other one increases. Electronic charge is conserved, but chirality is not. In the context of quantum field theory, this phenomena is called the chiral anomaly [8] and is a pure quantum effect. Yet, in this context, this can be seen classically! This anomaly will be discussed in section 2.2.2, as it is the responsible of the effective electromagnetic theory in topological insulators.

We introduce an electric field in the plate $\mathbf{E} = E_x \hat{e}_x + E_y \hat{e}_y$. To form a static current we also need to introduce the mean free time between collisions τ, which accounts for the collisions between electrons in the material. Thus, the macroscopic classical equation of motion they obey is given by the Drude model [9, 10]

$$m\frac{d\mathbf{v}}{dt} = -e(\mathbf{E} + \mathbf{v} \times \mathbf{B}) - \frac{m\mathbf{v}}{\tau}. \tag{1.6}$$

At equilibrium the velocity is constant, therefore

$$\mathbf{v} = -\frac{\omega_B \tau}{B}(\mathbf{E} + \mathbf{v} \times \mathbf{B}). \tag{1.7}$$

Substituting the velocity on the same equation,

$$\mathbf{v} = \frac{\omega_B \tau}{B}(\mathbf{E} - \frac{\omega_B \tau}{B}\mathbf{E} \times \mathbf{B} - \frac{\omega_B \tau}{B}(\mathbf{v} \times \mathbf{B}) \times \mathbf{B}), \tag{1.8}$$

where in this case

$$\begin{aligned}(\mathbf{v} \times \mathbf{B}) \times \mathbf{B} &= (\mathbf{v} \cdot \mathbf{B})\mathbf{B} - B^2\mathbf{v} \\ &= -B^2\mathbf{v},\end{aligned} \tag{1.9}$$

because $\mathbf{v}$ is perpendicular to $\mathbf{B}$.

Now, in matrix form,

$$\mathbf{E} \times \mathbf{B} = \begin{pmatrix} 0 & B_z \\ -B_z & 0 \end{pmatrix} \begin{pmatrix} E_x \\ E_y \end{pmatrix}. \tag{1.10}$$

With this, and introducing the electronic current density[3] $\mathbf{J} = -n_e e\mathbf{v}$, Eq. (1.8) becomes Ohm's law in (2D) matrix form

$$\mathbf{J} = \sigma_e \mathbf{E}, \tag{1.11}$$

with

$$\sigma_e = \frac{\sigma_{DC}}{1 + \omega_B^2 \tau^2} \begin{pmatrix} 1 & -\omega_B \tau \\ \omega_B \tau & 1 \end{pmatrix}, \tag{1.12}$$

where

$$\sigma_{DC} = \frac{n_e e \tau}{m} = n_e e \frac{\omega_B \tau}{B} \tag{1.13}$$

is the usual Drude conductivity.

Inverting the conductivity matrix produces the resistivity matrix,

$$\rho \equiv \sigma_e^{-1} = \frac{1}{\sigma_{DC}} \begin{pmatrix} 1 & \omega_B \tau \\ -\omega_B \tau & 1 \end{pmatrix}. \tag{1.14}$$

The longitudinal term

$$\rho_{xx} = \frac{1}{\sigma_{DC}}, \tag{1.15}$$

corresponds to the usual resistivity of the Drude model. For a perfect conductor (limit $\tau \longrightarrow 0$), we obtain $\rho_{xx} = 0$, which corresponds to the one of the QHE. The transverse term

$$\rho_{xy} = \frac{B}{n_e e}, \tag{1.16}$$

corresponds to the classical transverse resistivity (1.1) of the HE. This is completely independent of the scattering time. Thus, from the classical level we have an indication that this term is associated with the geometry of the system, and not its impurities.

---

[3]Because we take the electronic surface density $n_e = N/A$, this current density in reality possesses units of A$/m$, which is in correspondence with working in a 2D system.

1.2 Quantum Hall effect

A theoretical description of the QHE calls for the use of quantum mechanics. At first instance, it will appear as if this is enough. But careful consideration will reveal that nevertheless, the classical current should be recovered. This is not unexpected. Quantum mechanics usually predicts the quantization of microscopic variables such as the energy or the angular momentum of an individual particle, and thus one would not expect that macroscopic variables like the resistivity can also be quantized. It will be seen that the presence of disorder plays a key role. But ultimately, it will be seen that the QHE is of topological character [3].

In the following discussion (and from now on) we will completely ignore the effect of spin on the QHE. A brief discussion over the effects of spin can be found in Appendix B.

1.2.1 Landau Levels

Take the time-independent Schrödinger equation $\hat{H}\Psi = \mathcal{E}\Psi$. The Hamiltonian of electrons under the action of electromagnetic fields is [11]

$$\hat{H} = \frac{1}{2m}\big(\hat{\mathbf{p}} + e\mathbf{A}(\hat{\mathbf{x}})\big)^2 - e\,\phi(\hat{\mathbf{x}}), \tag{1.17}$$

where $\hat{\boldsymbol{\pi}} = \hat{\mathbf{p}} + e\mathbf{A}(\hat{\mathbf{x}})$ is the canonical momentum operator and $\mathbf{A}(\hat{\mathbf{x}})$, $\phi(\hat{\mathbf{x}})$ are the operators of the respective electromagnetic potentials. That is, for static fields, $\mathbf{E} = -\nabla\phi$ and $\mathbf{B} = \nabla \times \mathbf{A}$. In this section it will not be necessary to fix a gauge.

For now we will stay only with the magnetic field $\mathbf{B} = B\hat{e}_z$, without the electric field. In this case, the canonical momentum obey

$$[\hat{\pi}_x, \hat{\pi}_y] = -ie\hbar B. \tag{1.18}$$

Defining the operators

$$\hat{a}^\dagger = \frac{1}{\sqrt{2e\hbar B}}(\hat{\pi}_x + i\hat{\pi}_y), \quad \hat{a} = \frac{1}{\sqrt{2e\hbar B}}(\hat{\pi}_x - i\hat{\pi}_y), \tag{1.19}$$

we get, through Eq. (1.18), the commutation relation

$$[\hat{a}, \hat{a}^\dagger] = 1. \tag{1.20}$$

Furthermore, the (2D) Hamiltonian can be expressed as

$$\hat{H} = \frac{1}{2m}\hat{\boldsymbol{\pi}} \cdot \hat{\boldsymbol{\pi}} = \hbar\omega_B\Big(\hat{a}^\dagger\hat{a} + \frac{1}{2}\Big). \tag{1.21}$$

This is exactly the Hamiltonian of the quantum harmonic oscillator, whose frequency is the cyclotron frequency. The solutions are then expressed by the well known Hermite polynomials [11, 12] with energies given by

$$\boxed{\mathcal{E}_n = \hbar\omega_B\Big(n + \frac{1}{2}\Big), \quad n = 0, 1, 2, ...} \tag{1.22}$$

These are the Landau levels. They are in correspondence with the classical solutions, where for a constant magnetic field, the electrons move in cyclotron orbits. We can go even further in this relation. Classically, from Eq. (1.4), the center of the orbits is given by

$$x_0 = x(t) - r_0 \sin(\omega_B t - \varphi) = x + \frac{\dot{y}}{\omega_B} = x + \frac{\pi_y}{m\omega_B},$$
$$y_0 = y(t) - r_0 \cos(\omega_B t - \varphi) = y - \frac{\dot{x}}{\omega_B} = y - \frac{\pi_x}{m\omega_B}. \tag{1.23}$$

Thus, we can define the *center of mass operators* as

$$\hat{X} = \hat{x} + \frac{\hat{\pi}_y}{m\omega_B}, \quad \hat{Y} = \hat{y} - \frac{\hat{\pi}_x}{m\omega_B}. \tag{1.24}$$

They commute with the Hamiltonian,

$$i\hbar \frac{\partial}{\partial t} \langle \hat{X} \rangle = \langle [\hat{X}, \hat{H}] \rangle = 0, \quad i\hbar \frac{\partial}{\partial t} \langle \hat{Y} \rangle = \langle [\hat{Y}, \hat{H}] \rangle = 0, \tag{1.25}$$

and thus are constants of evolution. That is, their expectation value is constant. Nevertheless, the operators do not commute with each other,

$$[\hat{X}, \hat{Y}] = -i\ell_B^2, \tag{1.26}$$

where

$$\ell_B = \sqrt{\frac{\hbar}{eB}} = \sqrt{\frac{\hbar}{m\omega_B}} \tag{1.27}$$

is called the magnetic length.

Eq. (1.26) has a direct physical interpretation. In a semi-classical quantization of phase space[4], the uncertainty relation between these two variables is

$$\Delta X \Delta Y = 2\pi \ell_B^2. \tag{1.28}$$

This means that each wave-function occupies an area of $2\pi\ell_B^2$. Because the electrons are fermions, they cannot occupy both the same energy level, and the same spatial area. Therefore, a plate of area A can only harbor

$$g = \frac{A}{\Delta X \Delta Y} = \frac{A}{2\pi\ell_B^2} = \frac{eBA}{2\pi\hbar} = \frac{AB}{\Phi_0} \tag{1.29}$$

electrons on each energy state. g is thus the degeneracy of each Landau level. The quantity

$$\Phi_0 = \frac{2\pi\hbar}{e} \tag{1.30}$$

is called the flux quantum. This means that the necessary electron's surface density required to exactly fill ν Landau levels is

$$n_e = \frac{B}{\Phi_0}\nu. \tag{1.31}$$

---

[4]We say this because in Eq. (1.28) we don't use the usual uncertainty relation $\Delta X \Delta Y \geq \left| \frac{1}{2i} \langle [\hat{X}, \hat{Y}] \rangle \right|$, but instead quantize the area as $\Delta X \Delta Y = \left| \frac{2\pi}{i} \langle [\hat{X}, \hat{Y}] \rangle \right|$, which can be shown to be equivalent to a semi-classical quantization of phase space [13]. All arguments treating the degeneracy of the Landau levels use, in one way or another, semi-classical approximations.

1.2.2 Quantum Current

Now we turn on the electric field $\mathbf{E} = E\hat{e}_x$, such that $\phi(\mathbf{x}) = -Ex$. We also fix the gauge as the Landau gauge, where $\mathbf{A}(\mathbf{x}) = xB\hat{e}_y$. Thus, the Hamiltonian becomes

$$\hat{H} = \frac{1}{2m}\left(\hat{p}_x^2 + (\hat{p}_y + eB\hat{x})^2\right) + eE\hat{x}. \tag{1.32}$$

There is a translational invariance in the y-coordinate, so we can use the *ansatz* wave function

$$\Psi_{n,k_y}(\mathbf{x}) = Ae^{ik_y y}\phi_n(x), \tag{1.33}$$

then

$$\begin{aligned}
\hat{H} &= \frac{1}{2m}\left(\hat{p}_x^2 + (\hbar k_y + eB\hat{x})^2\right) + eE\hat{x} \\
&= \frac{\hat{p}_x^2}{2m} + \frac{1}{2}m\omega_B^2\left(\hat{x} + k_y\ell_B^2 + \frac{mE}{eB^2}\right)^2 - eE\left(k_y\ell_B^2 + \frac{mE}{2eB^2}\right).
\end{aligned} \tag{1.34}$$

This is the Hamiltonian of the harmonic oscillator with its center and energies shifted. Thus

$$\Psi_{n,k_y}(\mathbf{x}) = Ce^{ik_y y}\phi_n\left(x + k_y\ell_B^2 + \frac{mE}{eB^2}\right), \tag{1.35}$$

with C a normalization constant and

$$\phi_n(x) = \frac{1}{\sqrt{2^n n!\ell_B}}\frac{1}{\pi^{1/4}}e^{-x^2/(2\ell_B^2)}H_n(x/\ell_B), \tag{1.36}$$

the eigenfunctions of the harmonic oscillator, which also called Hermite functions [14]. Furthermore, the energies are

$$\mathcal{E}_{n,k_y} = \hbar\omega_B\left(n + \frac{1}{2}\right) - eE\left(k_y\ell_B^2 + \frac{mE}{2eB^2}\right). \tag{1.37}$$

We now compute the electric current. If we consider the system as a gas of electrons, the average current is

$$\mathbf{I} = -e\langle\dot{\mathbf{x}}\rangle = -\frac{e}{m}\langle\hat{\mathbf{p}} + e\mathbf{A}(\hat{\mathbf{x}})\rangle = -\frac{e}{m}\sum_{\text{O.S.}}\langle\Psi_{n,k_y}| - i\hbar\nabla + e\mathbf{A}(\hat{\mathbf{x}})|\Psi_{n,k_y}\rangle, \tag{1.38}$$

where the sum is made over the occupied states.

The allowed k_y values still need careful treatment. Suppose we have a plate of lengths L_x and L_y. Because the system is free in the y-direction, the borders have the effect of quantizing the allowed values of k_y in units of $2\pi/L_y$. For the other direction, we have the restriction $-L_x/2 \leq x \leq L_x/2$. As the wave-functions are localized around $x = -k_y\ell_B^2 - \frac{mE}{eB^2}$, then

$$\frac{L_x}{2} \geq k_y\ell_B^2 + \frac{mE}{eB^2} \geq -\frac{L_x}{2}. \tag{1.39}$$

Then $k_y \in [a, b]$, with

$$a = -\frac{1}{\ell_B^2}\left(\frac{L_x}{2} + \frac{mE}{eB^2}\right),$$
$$b = \frac{1}{\ell_B^2}\left(\frac{L_x}{2} - \frac{mE}{eB^2}\right). \tag{1.40}$$

With this, the sum over k_y for an occupied Landau level becomes

$$\sum_{k_y}(...) \longrightarrow \frac{L_y}{2\pi}\int_a^b (...)\mathrm{d}k_y. \tag{1.41}$$

For this section, only the trivial integral will be required,

$$\frac{L_y}{2\pi}\int_a^b \mathrm{d}k_y = \frac{L_y}{2\pi}(b-a) = \frac{L_x L_y}{2\pi\ell_B^2} \equiv N. \tag{1.42}$$

This recovers the degeneracy of each Landau level (1.29). Nevertheless, this should be treated as the number of states allowed in each Landau level, because the electric field has lifted the degeneracy of the energy in Eq. (1.37), as now each level also depends linearly on k_y.

It is worth noting that, by only considering the difference $(b-a)$, a careful treatment with the cumbersome limits given by (1.40) should not be needed. It would be sufficient to take $a = -L_x/(2\ell_B^2)$ and $b = L_x/(2\ell_B^2)$ like previous authors have done [3]. Yet, it will be seen in section 5.4.2, where we compute the current for topological insulators, that these cumbersome limits are actually relevant.

Proceeding with the calculation of the current (1.38) in the y direction,

$$I_y = -\frac{e}{m}\sum_{(n,k_y)}\langle\Psi_{n,k_y}|\hbar k_y + e\hat{\mathrm{x}}B|\Psi_{n,k_y}\rangle. \tag{1.43}$$

The wave functions are assumed normalized. The expectation value in $\hat{\mathrm{x}}$ of the harmonic oscillator (1.36) is zero, so the expectation value in $\hat{\mathrm{x}}$ of the wave function (1.35) is

$$\langle\Psi_{n,k_y}|\hat{\mathrm{x}}|\Psi_{n,k_y}\rangle = -\left(k_y\ell_B^2 + \frac{mE}{eB^2}\right). \tag{1.44}$$

Thus

$$I_y = -\frac{e}{m}\sum_{(n,k_y)}\left[\hbar k_y - eB\left(k_y\ell_B^2 + \frac{mE}{eB^2}\right)\right]$$
$$= \sum_{(n,k_y)}\frac{eE}{B} \tag{1.45}$$
$$= N\frac{eE}{B}\nu.$$

Eqs. (1.41) and (1.42) were used, and ν Landau levels were assumed to be completely occupied.

Dividing by the area to get the current density,

$$J_y = \frac{e^2}{2\pi\hbar} E\nu. \tag{1.46}$$

The current in the x-direction is zero, for the expectation value of the momentum operator is zero in the harmonic oscillator. The treatment for both currents is analogous in the case of an electric field in the y-direction. Thus,

$$\mathbf{J} = \begin{pmatrix} 0 & -\sigma_{xy} \\ \sigma_{xy} & 0 \end{pmatrix} \begin{pmatrix} E_x \\ E_y \end{pmatrix}, \quad \mathbf{E} = \begin{pmatrix} 0 & \rho_{xy} \\ -\rho_{xy} & 0 \end{pmatrix} \begin{pmatrix} J_x \\ J_y \end{pmatrix}, \tag{1.47}$$

where

$$\rho_{xy} = \sigma_{xy}^{-1} = \frac{2\pi\hbar}{e^2} \frac{1}{\nu} \tag{1.48}$$

is the QHE resistivity (1.2). This tells us that the integer ν of the resistivity has a direct physical meaning: It corresponds to the number of Landau levels completely filled.

Nonetheless, this calculation does not explain what happens when a Level is partially occupied. In this case, one would not get the complete integral (1.42), only a fraction of it. The so-called "robustness of the Hall states" appears to break in those cases. There are thus additional phenomena that must be taken into account.

1.2.3 The influence of disorder

The origin of the robustness of the Hall states was first proposed by Ando [15]. In short, as remarked by Klitzing [4], "[...] the electrons in impurity bands, arising from short range scatterers, do not contribute to the Hall current; whereas the electrons in the Landau level give rise to the same Hall current as that obtained when all the electrons are in the level and can move freely". In this section we will make a simple calculation in the semi-classical approximation, proposed by Tong [3], to prove the first assertion: There exist some impurity bands which do not contribute to the current. In the next section we will discuss the second assertion: Even when only part of the electrons contribute to the current, its value is the same as if all of the electrons were to move freely.
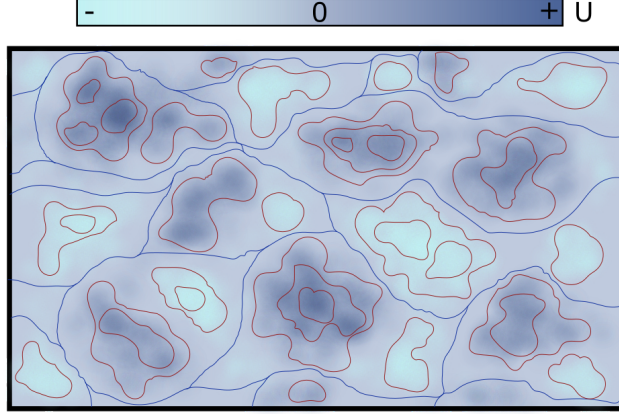
Figure 1.4: Microscopic picture of the random potential $U(x, y)$, which models the disorder on the plate. Its equipotentials constitute the paths through which the electrons are allowed to move. There are localized states (red curves) and extended states (blue curves).

For modelling the disorder, we can take a continuous potential $U(x, y)$ with random (and small) values distributed along the plate. We study the effect of this potential on the Landau levels described by the Hamiltonian $\hat{H}$ of Eq. (1.21). That is, we consider the movement in the x-y plane with a magnetic field in the z direction. Taking again the center of mass operators $\hat{X}$ and $\hat{Y}$ of Eq. (1.24), the addition of the potential $\hat{U} \equiv U(\hat{X}, \hat{Y})$ modifies their motion so that

$$i\hbar\frac{\partial}{\partial t}\langle\hat{X}\rangle = \langle[\hat{X}, \hat{H} + \hat{U}]\rangle = \langle[\hat{X}, \hat{U}]\rangle, \quad i\hbar\frac{\partial}{\partial t}\langle\hat{Y}\rangle = \langle[\hat{Y}, \hat{H} + \hat{U}]\rangle = \langle[\hat{Y}, \hat{U}]\rangle. \quad (1.49)$$

Performing an Taylor expansion of the operator $\hat{U}$ around $(x_0, y_0) \equiv (\langle\hat{X}\rangle, \langle\hat{Y}\rangle)$, at first order[5],

$$\hat{U} \approx U(x_0, y_0)\hat{\mathbb{1}} + (\hat{X} - x_0\hat{\mathbb{1}})\frac{\partial U}{\partial x} + (\hat{Y} - y_0\hat{\mathbb{1}})\frac{\partial U}{\partial y}. \quad (1.50)$$

Therefore, using Eq. (1.26),

$$i\hbar\frac{\partial}{\partial t}\langle\hat{X}\rangle \approx \langle[\hat{X}, \hat{Y}]\rangle\frac{\partial U}{\partial y} = -i\ell_B^2\frac{\partial U}{\partial y}, \quad i\hbar\frac{\partial}{\partial t}\langle\hat{Y}\rangle \approx \langle[\hat{Y}, \hat{X}]\rangle\frac{\partial U}{\partial y} = i\ell_B^2\frac{\partial U}{\partial y}. \quad (1.51)$$

Thus, $(\dot{X}, \dot{Y})$ is perpendicular to ∇U, and so the expected movement of the center of mass takes place along the equipotentials of U.

Now, picture the landscape of this potential, such as in Fig. 1.4. The electrons located around the "cliffs" and "valleys" of the potential will be constrained to move in close paths. Thus, these states will not contribute to the current. These are called *localized states* in Ref. [3]. On the other hand, the electrons in the intermediate points (where U is close to zero) have paths connected all around the plate, and so are allowed to move freely between the cliffs and valleys of the potential. These states are called *extended states* in the same reference.

---

[5]For this, we are assuming that $|\nabla U| \ll \hbar\omega_B/l_B$, which holds for small perturbations.
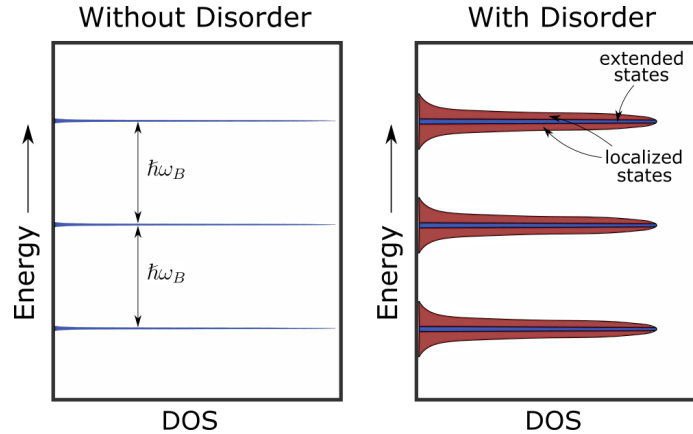
Figure 1.5: Density of states of the original Landau Levels without and with the disorder potential. On the right, the localized states correspond to the tails of the distributions (red), while the extended states correspond to the centers (blue).

The potential has also an impact on the energies. As it breaks translational symmetry, the degeneracy of the Landau levels is lifted. Still, we assume that the potential is small enough ($U \ll \hbar\omega_B$), so that the levels don't mix. This can be seen in Fig. 1.5, where the density of states (DOS) changes from delta distributions to extended distributions on the energy through the introduction of disorder. Furthermore, as we saw in Fig. 1.4, the localized states arise at the perturbed energy levels of the potential, so they correspond to the tails of the distributions. Meanwhile, the extended states stay at the zero energy levels of the potential, so they correspond to the center of the distributions, at the same energies of the Landau levels.

Overall, we can then conclude that the impurities are the responsible for the robustness of the Hall states. Because, even when a Landau level (distribution) may be partially filled, the current will not change until the filling arrives to the level of the extended states. That is, until it arrives to the energies of the original Landau levels.

1.2.4   The Corbino geometry

We now discuss the reasons behind why, even when only some electrons contribute to the current, the values of the conductivity are as if all of the electrons of a Landau level were filled. To do this, we must take into account a full geometrical description of the system.

One very convenient arrangement is the Corbino geometry (or Corbino ring) [16]. This consists of taking the HE system of Fig. 1.1 and bending it over itself in a ring, such as in Fig. 1.6. In a way, we can think of the original rectangular plate as a section of a very big ring. Thus, the $\hat{e}_x$ direction becomes the angular direction $\hat{e}_\phi$, and the $\hat{e}_y$ direction becomes the negative[6] radial direction $-\hat{e}_r$. The perpendicular magnetic field B is still in the z direction in all space. Furthermore, instead of directly placing an electric field around the angular direction, we can induce it through the

---

[6]This is to get a right-handed system, so that at the end all of the signs are consistent.

time variation of a magnetic flux Φ which goes through the center of the ring (like in a solenoid).
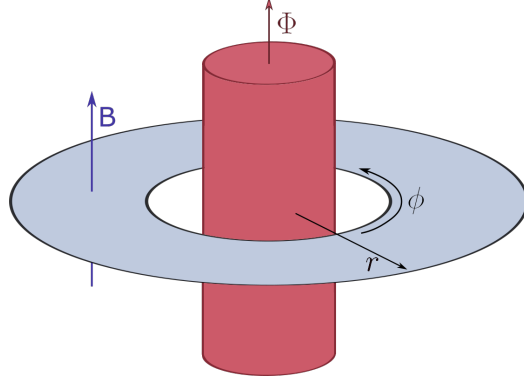
Figure 1.6: The Corbino ring.

This setup has many advantages. First, we don't have to worry about externally setting an input and output of electrical charge around the edges of the x direction to make the current, as it is now in an angular direction which circles back around itself. Second, the chiral currents (seen in Fig. 1.3) now are naturally separated, so a distinction between the two chiral currents can be made. Lastly, as we will see, the action of the electric field will couple more naturally to the system through the variation of the central flux, which will ultimately allow us to completely describe the QHE.

In cylindrical (polar) coordinates, the Hamiltonian takes the form

$$\hat{H} = \frac{1}{2m}\left[-\frac{\hbar^2}{r}\frac{\partial}{\partial r}\left(r\frac{\partial}{\partial r}\right) + \left(\frac{\hbar}{ir}\frac{\partial}{\partial \phi} + eA_\phi\right)^2\right]. \tag{1.52}$$

Here, the potential A_ϕ contains two terms: One corresponding to the constant magnetic field in the z direction, and another one from the central flux Φ. Taking the Coulomb gauge $\nabla \cdot \mathbf{A} = 0$, A_ϕ will only depend on r, and thus for a circular contour C over the ring,

$$\oint_C \mathbf{A} \cdot d\mathbf{r} = 2\pi r A_\phi(r) \equiv \pi r^2 B + \Phi, \quad A_\phi(r) = \frac{Br}{2} + \frac{\Phi}{2\pi r}. \tag{1.53}$$

There are special values of the flux for which we recover the Landau levels. Unsurprisingly, these are given by integer multiples of the quantum of flux. This can be seen from the following procedure: When $\Phi = k\Phi_0$ with $k \in \mathbb{Z}$ and Φ_0 the quantum of flux of Eq. (1.30), one can perform a gauge transformation such that

$$\Psi(r, \phi) \longrightarrow \exp\left[\frac{e\Phi\phi}{2\pi i\hbar}\right]\Psi(r, \phi) = \exp[-ik\phi]\Psi(r, \phi),$$

$$A_\phi(r) \longrightarrow A_\phi(r) + \frac{\hbar}{ir}\frac{e\Phi}{2\pi i\hbar} = \frac{Br}{2}. \tag{1.54}$$

This maintains the periodicity of the wave functions in ϕ and cancels the flux term of the vector potential, so that the Hamiltonian describing electrons under a constant

magnetic field B is consistently recovered. We thus expect that the spectrum of the Hamiltonian (1.52) corresponds to the Landau levels for these cases.

Having noticed this we analyse the general case where the flux takes an arbitrary value. From the rotational symmetry of the system, angular momentum is conserved, and so we can take the *ansatz* wave functions

$$\Psi_{n,l}(r, \phi) = e^{-il\phi}\psi_{n,l}(r). \tag{1.55}$$

With this, the Hamiltonian then takes the form

$$\hat{H} = -\frac{\hbar^2}{2m}\frac{1}{r}\frac{\partial}{\partial r}\left(r\frac{\partial}{\partial r}\right) + V(r), \quad V(r) \equiv \frac{1}{2m}\left(-\frac{\hbar}{r}l + \frac{eBr}{2} + \frac{e\Phi}{2\pi r}\right)^2. \tag{1.56}$$

Here, l is an integer, as the wave functions are periodic in ϕ. For the label n, because the aforementioned procedure allows us to remove the presence of the flux when $\Phi = k\Phi_0$, we can generally identify it with the label of the Landau levels.

Now, in general, the radial components will be localized around a radius r_l. This happens when the radial differential operator (that is, the kinetic operator) is maximum. As the sum of this operator with the potential is the constant energy, this happens when the potential is null: $V(r_l) = 0$. The solutions to this condition are

$$r_l = \ell_B\sqrt{2(l - \Phi/\Phi_0)}. \tag{1.57}$$

We now perform a slow variation of the flux Φ over a time interval T, such that $\Phi(t = 0) = 0$ and $\Phi(t = T) = \Phi_0$. This produces an electric field around the ring following Lenz's law,

$$\mathbf{E} = -\frac{1}{2\pi r}\frac{\partial\Phi}{\partial t}\hat{e}_\phi = -\frac{1}{2\pi r}\frac{\Phi_0}{T}\hat{e}_\phi, \tag{1.58}$$

which plays the role of the longitudinal electric field. Furthermore, the adiabatic theorem [11] ensures us that each wave function remains an eigenstate of the Hamiltonian with the same quantum numbers n and l. Thus, each state $|n, l\rangle$ goes from being localized at $r_l = \ell_B\sqrt{2l}$ at $t = 0$ to being localized at $r_l = \ell_B\sqrt{2(l - 1)}$ at t=T, which corresponds to the position that the $|n, l - 1\rangle$ state had at $t = 0$. This creates a one particle radial current from the outer edge of the ring to the inner edge,

$$\mathbf{J} = \frac{1}{2\pi r}\frac{(-e)}{T}(-\hat{e}_r). \tag{1.59}$$

This phenomenon is independent of the quantum number n, and so each Landau level filled produces a current of this kind. If ν Landau levels are full, then

$$\rho_{xy} = \frac{E_\phi}{J_{-r}} = \frac{\Phi_0}{e}\frac{1}{\nu}, \tag{1.60}$$

which recovers the QHE resistivity of Eq. (1.2). Even when the charge transfer builds a one-particle current (for each Landau level), this is done exactly in a time such that the QHE current is produced.

For the cases where the Landau levels are partially filled, the disorder comes into rescue. Introducing a random potential $U(\mathbf{x})$ such as in the one in the last section, the Hamiltonian is now

$$\hat{\mathrm{H}} = \frac{1}{2m}\left[-\frac{\hbar^2}{r}\frac{\partial}{\partial r}\left(r\frac{\partial}{\partial r}\right) + \left(\frac{\hbar}{ir}\frac{\partial}{\partial \phi} + eA_\phi\right)^2\right] + U(r,\phi). \qquad (1.61)$$

This, in principle, breaks the rotational symmetry, which induces the localized states, but leaves some extended states just as it was discussed in the last section. But before we continue, we must clarify the concept of localized states in this context. The existence of these new localized states must not come into confusion with the existence of the localization radius r_l. The localization radius exists for both the extended and localized states. The difference between these two is that the localized states are bounded not only in a radius, but also in an angular region. The extended states are only localized around a radius, but they are extended through the whole angular region of the disk (see Fig. 1.7).
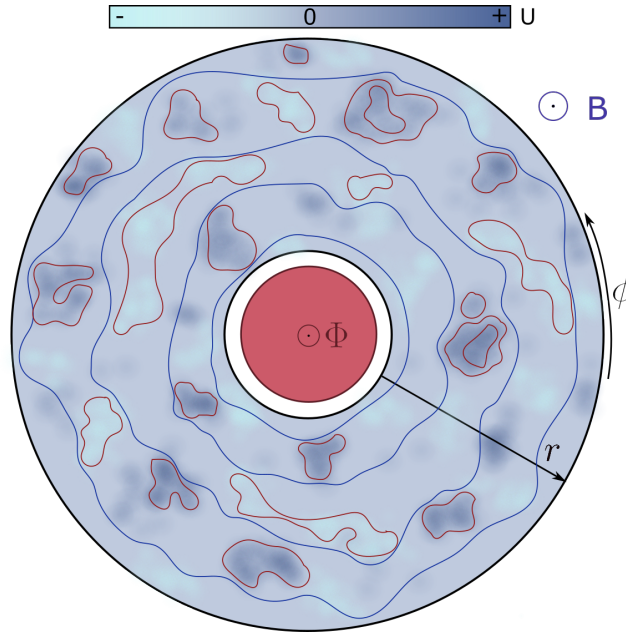
Figure 1.7: Microscopic picture of the effect of random potential $U(x,y)$ in the Corbino ring. Just as before, there are localized states (red curves) and extended states (blue curves). The localized states are bounded in a radius and in an angle. The extended states are unbounded in the angular coordinate, but are localized around a radius.

The angular localization of the localized states nullifies the restriction for the periodicity of the ϕ coordinate [3], so the gauge transformation of Eq. (1.54) can be performed for arbitrary values of the flux (k can be real). This means that the localized states are unaffected by the flux, and therefore do not contribute to the current (just as in the last section). This cannot be performed for the extended states, as the periodicity in ϕ coordinate is still needed for them. And so the extended states are still affected by the flux, while the localized states are not.

Despite this, we can directly see here how the remaining extended states still build the same value of the current. Through the process of the flux changing from $\Phi = 0$ to $\Phi = \Phi_0$, we can still see that the extended states transform from (extended states of) Landau levels to themselves. We show this by noticing that the condition for the localization radius is now $V(r) + U(r) = 0$, which will be particularly satisfied for states that are both extended ($U(r) = 0$) and have a localization radius ($V(r) = 0$). As the localized states remain unchanged, the extended states must then transform into the next extended state neighbour, skipping any "gaps" left by a localized state. In total we will then recover the same current (1.59), independently of whether the Landau levels are full or not, and as long as all of the extended states are filled. This is sufficient, as one can see from the density of states of Fig. 1.5.

2 Introduction to topological insulators (TI)

The notion of topological insulators as a new phase of matter was first introduced by Kane and Mele [17, 18] in 2005, and further developed in subsequent studies [19–22]. Some of the first materials capable of presenting the TI phase were theoretically predicted to be $Bi_{1-x} Sb_x$ [23] and the HgTe quantum well [24], as well as $Bi_2 Se_3$, $Bi_2 Te_3$ and $Sb_2 Te_3$ [25]. Later studies confirmed these predictions (such as for $Bi_{0.9} Sb_{0.1}$ [26] or the HgTe quantum well [27] for example).

In this chapter we will give a brief introduction to the basic properties that define topological insulators (section 2.1), as well as the origins and consequences of the effective electromagnetic theory of these materials (section 2.2). The resulting changes in the boundary conditions for electromagnetic fields will be the key tools for the setups studied in the next chapters.

2.1 Definition and basic properties of TI

Topological insulators are crystalline systems which have two defining properties:

1. Their Hamiltonian possesses time reversal symmetry.

2. They are insulators in the bulk, but possess topologically non-trivial conduction states in the edges.

In section 2.1.1 we will make a short review of time reversal symmetry and its physical consequences on the general energy levels of a system. In section 2.1.2 we will study the physical consequences of time reversal symmetry on the energy bands of a crystal system, and distinguish the case where these effects originate the topologically non-trivial edge states of a TI.

2.1.1 Time reversal symmetry

The time reversal transformation is generally defined as,

$$\mathcal{T} : t \longrightarrow -t. \tag{2.1}$$

For example, for classical variables of movement such as mass m, electric charge q, momentum $\mathbf{p}$, and angular momentum $\mathbf{L}$,

$$\begin{aligned}
\mathcal{T} &: m \longrightarrow m, \\
\mathcal{T} &: q \longrightarrow q, \\
\mathcal{T} &: \mathbf{p} \longrightarrow -\mathbf{p}, \\
\mathcal{T} &: \mathbf{L} \longrightarrow -\mathbf{L}.
\end{aligned} \tag{2.2}$$

Thus, for the electromagnetic fields and potentials [28],

$$\begin{aligned}
\mathcal{T} &: \mathbf{E} \longrightarrow \mathbf{E}, \\
\mathcal{T} &: \mathbf{B} \longrightarrow -\mathbf{B}, \\
\mathcal{T} &: A^0 \longrightarrow A^0, \\
\mathcal{T} &: A^i \longrightarrow -A^i.
\end{aligned} \tag{2.3}$$

Kramers theorem

In quantum mechanics, the time reversal transformation is represented as an anti-unitary[1] linear operator [11],

$$\Theta = \mathrm{U}\,\mathrm{K}, \tag{2.4}$$

where K represents complex conjugation on the coefficients of a wave-function (not on the kets that form the basis) and U is a unitary operator. The transformations of (2.2) and (2.3) are preserved when taking the action of time reversal on the respective operators. For wave-functions, its explicit representation depends completely on the basis at hand. Nevertheless, there exists an important general property for this operator. If j denotes the total spin of the wave-function, then

$$\Theta^2 = (-1)^{2j}. \tag{2.5}$$

That is, it is 1 for boson and -1 for fermion systems.

Now, suppose that a Hamiltonian possesses time reversal symmetry. That is,

$$[\,\mathrm{H}, \Theta\,] = 0. \tag{2.6}$$

Then, if $|n\rangle$ is an eigen-ket of H with energy E_n, so will $\Theta|n\rangle$ be. It could be the case that $\Theta|n\rangle$ results in the original ket, but it could also be the case that this is a different eigen-ket with a degeneracy in the energy. We probe the possibility of the first case. At most, recovering the original ket would mean that $\Theta|n\rangle = e^{i\delta}|n\rangle$. But, using that Θ is anti-unitary, this would mean that

$$\Theta^2|n\rangle = \Theta e^{i\delta}|n\rangle = e^{-i\delta}\Theta|n\rangle = e^{-i\delta}e^{i\delta}|n\rangle = +|n\rangle. \tag{2.7}$$

From relation (2.5), this is forbidden for fermion systems. Thus, for fermions, $\Theta|n\rangle$ must be a different eigen-ket and so every energy level of H is doubly degenerate. This is Kramers theorem, originally noted by him while studying crystal systems [29], but related to time inversion symmetry by Wigner [30].

---

[1]If Θ were purely unitary, Hamiltonians which commute with it (such as the free particle Hamiltonian) would have a boundless negative energy spectrum. As this is unacceptable, it is then taken as anti-unitary.

2.1.2   Topologically non-trivial edge states

In crystalline systems, the discrete translational symmetry allows the eigen-states to be described by the so-called energy band structure. This consists of expressions for the eigen-energies as functions of the so-called crystalline momentum $\mathbf{k}$, which lives in reciprocal space (just as the position vector $\mathbf{r}$ lives in the real space) and also presents a translational symmetry. That is, the energies of the system are given by energy bands $E = E_s(\mathbf{k})$, with $s = 0, 1, 2...$ the band index. If the reciprocal space is invariant under a discrete translation given by a vector $\mathbf{G}$, then $E_s(\mathbf{k} + \mathbf{G}) = E_s(\mathbf{k})$. For example, for 1D systems, $G = 2\pi/a$, where a is the lattice constant associated with the translational symmetry of real space.

(a) Topologically equivalent to a normal insulator.   (b) Topologically non-trivial edge states.
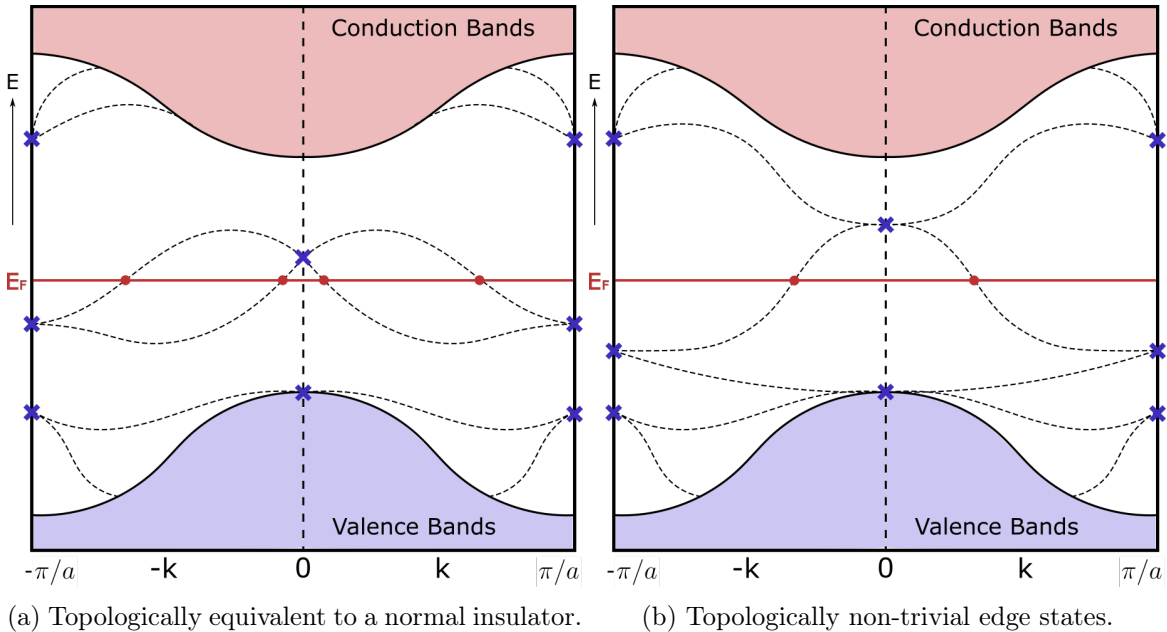
Figure 2.1: Two possible energy spectra for Hamiltonians with time reversal symmetry plotted in one direction in reciprocal space. The shaded regions depict the bulk states proper of an insulator, while the dashed lines depict the edge states with conduction bands. The intersections with the Fermi level are given by red dots. By the time reversal symmetry, the spectra must be symmetric around the origin, and must have intersecting bands at special points (blue crosses).

Just as the usual momentum, the crystalline momentum (non-trivially[2]) transforms as $\mathcal{T} : \mathbf{k} \longrightarrow -\mathbf{k}$. Thus, for Hamiltonians of crystalline systems which also possess time reversal symmetry, the band structure is symmetric with respect to the origin,

$$E_s(\mathbf{k}) = E_s(-\mathbf{k}). \tag{2.8}$$

---

[2]A way to see this is by recalling that Bloch's theorem [1] implies that the wave functions can be expressed as $\Psi_{\mathbf{k}}(\mathbf{r}) = e^{i\mathbf{k}\cdot\mathbf{r}} u_{\mathbf{k}}(\mathbf{r})$, with $u(\mathbf{r})$ a function with the periodicity of the crystal. Thus, as time reversal implies complex conjugation, its action is equivalent to taking $\mathbf{k} \longrightarrow -\mathbf{k}$.

This is consistent with the double-degeneracy of the energies described by the Krammers theorem seen in section 2.1.1. Nevertheless, there are two special cases for which, in Eq. (2.8), $\mathbf{k}$ was already identified with $-\mathbf{k}$. These are $\mathbf{k} = \mathbf{0}$ and $\mathbf{k} = \mathbf{G}/2$. For these points, Krammers theorem implies that two separate energy bands must intersect to give the double degeneracy. This is completely independent of the shape of the Hamiltonian, as long as the time reversal symmetry is maintained. That is, the shape of the band structure can be tuned in any continuous way, but the double degeneracy points in $\mathbf{k} = \mathbf{0}$ and $\mathbf{k} = \mathbf{G}/2$ will always exist.

This property has important consequences, for it allows us to make a classification of the Hamiltonians of insulators which are related by smooth transformations that do not close the energy gap in the bulk. That is, we can relate energy spectra which are topologically equivalent and distinguish those who are not. We focus on the easiest of these classifications, which corresponds to the so-called Z_2 classification of topological insulators belonging to 2D space [17].

Two cases are depicted in Fig. 2.1. In both, we consider an arbitrary spectrum with valence and conduction bands in the bulk separated by an energy gap (shaded regions). Depending on the details of the Hamiltonian, there could exist edge states inside the gap (dashed lines). As discussed before, the time reversal symmetry restricts the spectrum to be symmetric around the origin, and to have intersections of two different band structures at the special points $\mathbf{k} = \mathbf{0}$ and $\mathbf{k} = \mathbf{G}/2$. For the edge states, these points are marked by blue crosses. For the first case (Fig. 2.1a), the edge states near the Fermi energy intersect each other at both of the special points. Thus, we can perform a smooth deformation to lower these bands and recover a normal insulator. For the second case (Fig. 2.1b), the edge states near the Fermi energy connect instead to both the conduction and valence bands, closing the gap and thus obtaining a conductor in the edges. No smooth transformation preserving time reversal symmetry can be performed to recover an insulator state (it is said to be symmetry protected), and so it is a different topological phase of matter: The topological insulator.

Now, note the number of times that the edge states cross the Fermi energy level for both cases (red dots). As the symmetry around the origin always doubles this number, we can just focus on one side. With this, Fig. 2.1a possesses two independent intersections, while Fig. 2.1b only one. If we translate or deform the bands, either no intersection points, or an even number of points are added. Thus, the number of independent intersection points

$$N = \frac{1}{2}|\{E_s(\mathbf{k}) = E_F\}| \pmod 2 \tag{2.9}$$

form a topological invariant. For this, it is said that we obtain a Z_2 classification of the band structure for 2D TI [17]. The classification for 3D TI can be found in Ref. [19].

2.2 Effective electromagnetic theory in TI

The notion that the topological insulators' response to external electromagnetic fields can be completely described by the so-called θ-term was first proposed theoretically by Qi, Hughes and Zhang [31] in 2008. In 2017, Dziom, Shuvaev and Pimenov et al. made the first experimental confirmation of this phenomenon [32] by measuring that the Faraday rotation angle of electromagnetic waves going through TI media was universal and equal to the fine structure constant $\alpha = e^2/4\pi$, in accordance to the predictions of the θ-term [33, 34].

In the study of Xiao et al., they first demonstrated the existence of TI in $(4+1)$ dimensions and, based on an energy band model with the desired topological properties, obtained the electromagnetic response. From there, they performed a procedure called dimensional reduction, in which they chose a gauge such that translational invariance is present in one direction. That way, one of the crystalline moments can be chosen as a good quantum number, and thus could be related to a intrinsic parameter of the system called θ. Their electromagnetic effective theory could now be represented by the θ-term, which is an effective Lagrangian

$$\mathcal{L}_\theta = -\frac{e^2}{32\pi^2}\theta(x)F_{\mu\nu}F_{\rho\sigma}\varepsilon^{\mu\nu\rho\sigma}, \qquad (2.10)$$

where $F_{\mu\nu} = \partial_\mu A_\nu - \partial_\nu A_\mu$ is the electromagnetic field tensor, e is the fundamental charge and $\varepsilon^{\mu\nu\rho\sigma}$ is the totally anti-symmetric tensor in $(3+1)$ dimensions with $\varepsilon^{0123} = 1$. $\theta(x)$ is the intrinsic parameter which characterizes TIs. Although this parameter is constant within each TI, its space-time dependence comes from the fact that different TI media could be arranged in space-time. As it could be inferred, in this section we work in natural units $(c = \hbar = 1)$.

Here, in sections 2.2.1 and 2.2.2, we will directly compute this term in a model in $(3+1)$ dimensions. We follow the procedure summarized by Sekine and Nomura [34], which takes an effective Hamiltonian proposed by Zhang et al. [25] and applies the Fujikawa method [8] to determine the θ-term.

2.2.1 Effective microscopic Hamiltonian

Here we take for example Bi_2Se_3 (Bismuth Selenide). By looking at its crystal structure, one can see that a pair of Se atoms and a pair of Bi atoms possess inversion symmetry around a point where the third Se atom is located [25]. Thus, definite parity eigenstates can be constructed. It turns out that, around the Γ point, the lowest energy orbitals are the p orbitals. A basis can then be constructed as $|P1^+_{x,y,z}\rangle$ and $|P1^-_{x,y,z}\rangle$ states for the p orbitals of the pair of Bi atoms (where $\pm$ denotes parity), $|P2^+_{x,y,z}\rangle$ and $|P2^-_{x,y,z}\rangle$ states for the pair of Se atoms, and a $|P0^-_{x,y,z}\rangle$ state for the central Se atom[3]. Nevertheless, taking into account chemical bonding and the total

---

[3]This central atom state with only negative parity comes from the fact that p orbitals are odd around the orbit's center.

charge distributions, the degeneracy is split such that $|P1_z^+\rangle$ and $|P2_z^-\rangle$ turn out to be the lowest energy eigenstates [25].

An effective Hamiltonian for the resulting $\{|P1_z^+,\uparrow\rangle, |P1_z^+,\downarrow\rangle, |P2_z^-,\uparrow\rangle, |P2_z^-,\downarrow\rangle\}$ basis (where $\uparrow, \downarrow$ denotes spin) can then be built. At lowest order in the crystalline momentum $\mathbf{k}$, it can be expressed as [34]

$$\hat{H}_{TI} = v_F \mathbf{k} \cdot \boldsymbol{\alpha} + m_0 \alpha_4, \tag{2.11}$$

where v_F is the Fermi velocity and $m_0 < 0$ is a constant parameter of the crystal (For $Bi_2 Se_3$, $m_0 \sim -0.28\,\text{eV}$ [34]). α_μ are 4×4 matrices in the Dirac representation, given by

$$\alpha_i = \begin{pmatrix} 0 & \sigma_i \\ \sigma_i & 0 \end{pmatrix}, \quad \alpha_4 = \begin{pmatrix} 1 & 0 \\ 0 & -1 \end{pmatrix}, \tag{2.12}$$

which satisfy the relation $\{\alpha_\mu, \alpha_\nu\} = 2\delta_{\mu\nu}\mathbb{1}$.

The Hamiltonian (2.11) would represent the Dirac Hamiltonian if not for the negative mass term m_0. We thus pass to field theory, defining the gamma matrices

$$\gamma^i \equiv \alpha_4 \alpha_i = \begin{pmatrix} 0 & \sigma_i \\ -\sigma_i & 0 \end{pmatrix}, \quad \gamma^0 \equiv \alpha_4 = \begin{pmatrix} 1 & 0 \\ 0 & -1 \end{pmatrix}, \quad \gamma^5 \equiv i\gamma^0\gamma^1\gamma^2\gamma^3 = \begin{pmatrix} 0 & 1 \\ 1 & 0 \end{pmatrix}, \tag{2.13}$$

which satisfy $\{\gamma^\mu, \gamma^\nu\} = 2g^{\mu\nu}\mathbb{1}$, with $g^{\mu\nu} = \text{diag}(1, -1, -1, -1)$ the Minkowski metric. The pseudoscalar γ^5 anticommutes with each γ matrix, $\{\gamma^\mu, \gamma^5\} = 0$. Introducing the fermionic fields Ψ and $\bar{\Psi} \equiv \Psi^\dagger \gamma^0$, the Legendre transformation of (2.11) in field theory gives the Lagrangian density

$$\mathcal{L} = \Psi^\dagger \big[-k_0 - H \big] \Psi = \bar{\Psi} \big[-\gamma^\mu k_\mu - m_0 \big] \Psi, \tag{2.14}$$

where we absorbed the Fermi velocity in the spatial crystalline momentum. Now, taking the Fourier transformation and introducing the electromagnetic coupling $-k_\mu \longrightarrow i\partial_\mu \longrightarrow iD_\mu \equiv i(\partial_\mu - ieA_\mu)$, with $\Psi = \Psi(x)$, the action is

$$S[\Psi, \bar{\Psi}] = \int \mathrm{d}^4 x\, \bar{\Psi} \big[i\gamma^\mu D_\mu - m_0 \big] \Psi, \tag{2.15}$$

which would be the usual Dirac action if not for the negative mass. Note that this action describes only the bulk states, completely ignoring the presence of the edge states.

2.2.2 The θ-term

In the case $m_0 = 0$, the classical action (2.15) is invariant under the chiral transformation

$$\Psi(x) \longrightarrow \Psi'(x) = e^{i\theta\gamma^5/2}\Psi(x), \quad \bar{\Psi}(x) \longrightarrow \bar{\Psi}'(x) = \bar{\Psi}(x)e^{i\theta\gamma^5/2}, \tag{2.16}$$

defined by a global (constant) chiral angle θ. This implies that the associated Noether current, the chiral current $j_5^\mu \equiv \bar{\Psi}\gamma^\mu\gamma^5\Psi$, is conserved: $\partial_\mu j_5^\mu = 0$.

The astonishing result, which was first a problem encountered by H. Fukuda, Y. Miyamoto, S. Tomonaga and J. Steinberger, but finally resolved by J. Bell, R. Jackiw and S. Adler [8], is that this conservation is not fulfilled when moving from classical field theory to quantum field theory (QFT). This is the so-called chiral anomaly, and it is in fact the mechanism through which the θ-term arises (even when classically, the chiral current is not conserved, as $m_0 \neq 0$). A classical picture of this phenomenon was already seen in the Hall effect, particularly in Fig. 1.3, but the quantum analogue could also be visualised in the Corbino ring setup (Fig. 1.6). In all of these systems, the common elements are the presence of electromagnetic fields and border regions. These will be in fact, the necessary elements for the realization of the θ-term.

The chiral anomaly

One interpretation of the chiral anomaly in QFT can be found by analysing the Feynman path integral [8]

$$\mathcal{Z}[A_\mu] \equiv \int \mathcal{D}\Psi \mathcal{D}\bar{\Psi} \exp\left(iS[\Psi, \bar{\Psi}]\right), \tag{2.17}$$

where the integration is to be taken over all of the configurations[4] of the fermionic fields Ψ and $\bar{\Psi}$. The vector potential A_μ is taken as an external non-dynamical field. One can show that any correlation function of the fermionic fields can be computed in terms of the path integral [8]. In this way, this object completely describes the quantization of the theory.

Now we consider a change of integration variables, taking the chiral transformation, but now we take the chiral angle as a local and small parameter $\delta\theta(x)$,

$$\Psi(x) \longrightarrow \Psi'(x) = e^{i\delta\theta(x)\gamma^5/2}\Psi(x), \quad \bar{\Psi}(x) \longrightarrow \bar{\Psi}'(x) = \bar{\Psi}(x)e^{i\delta\theta(x)\gamma^5/2}. \tag{2.18}$$

Under this transformation, the Lagrangian in Eq. (2.15) changes like

$$\begin{aligned} \mathcal{L}' &= \bar{\Psi}'e^{i\delta\theta(x)\gamma^5/2}[i\gamma^\mu D_\mu - m_0]e^{i\delta\theta(x)\gamma^5/2}\Psi \\ &= \bar{\Psi}[i\gamma^\mu D_\mu - m_0]\Psi - \frac{1}{2}\bar{\Psi}\gamma^\mu\gamma^5\Psi\partial_\mu(\delta\theta(x)) - i\delta\theta(x)\bar{\Psi}\gamma^5 m_0\Psi \\ &= \mathcal{L} - \frac{1}{2}j_5^\mu\partial_\mu(\delta\theta(x)) - i\delta\theta(x)\bar{\Psi}\gamma^5 m_0\Psi \end{aligned} \tag{2.19}$$

Thus, integrating by parts, the action transforms as

$$S[\Psi', \bar{\Psi}'] = S[\Psi, \bar{\Psi}] + \int \mathrm{d}^4x\, \delta\theta(x)\left[\frac{1}{2}\partial_\mu j_5^\mu - i\bar{\Psi}\gamma^5 m_0\Psi\right]. \tag{2.20}$$

---

[4]The formal way to do this is to expand the fields in terms of a basis $\phi_n(x)$, with coefficients a_n defined as Grassmann numbers (that is, numbers such that $a_n a_m \equiv -a_m a_n$) so that the Pauli exclusion principle is fulfilled. Thus, the integral over all field configurations is translated to an integral over all of the coefficients a_n.

If we assumed that the measure of the path integral $\mathcal{D}\Psi\mathcal{D}\bar{\Psi}$ remained unchanged under this change of variables, then we would have that

$$\begin{aligned} \mathcal{Z}[A_\mu] &= \int \mathcal{D}\Psi'\mathcal{D}\bar{\Psi}' \exp\left(iS[\Psi',\bar{\Psi}']\right) \\ &= \int \mathcal{D}\Psi\mathcal{D}\bar{\Psi} \exp\left(iS[\Psi,\bar{\Psi}] + i\int \mathrm{d}^4x\,\delta\theta(x)\left[\frac{1}{2}\partial_\mu j_5^\mu - i\bar{\Psi}\gamma^5 m_0\Psi\right]\right). \end{aligned} \tag{2.21}$$

As the integral cannot depend on the arbitrary variation of the fields (because we integrate over all of the field configurations) described by $\delta\theta(x)$, we must have that

$$\partial_\mu j_5^\mu = 2i\bar{\Psi}\gamma^5 m_0\Psi, \tag{2.22}$$

which recovers the conservation of the chiral current for the massless case. Nonetheless, the detail noted by Fujikawa was that the measure could change in this transformation. That is, one can get

$$\mathcal{D}\Psi'\mathcal{D}\bar{\Psi}' = \mathcal{J}[\Psi,\bar{\Psi},A_\mu]\mathcal{D}\Psi\mathcal{D}\bar{\Psi}, \tag{2.23}$$

with a non-trivial Jacobian $\mathcal{J}[\Psi,\bar{\Psi},A_\mu]$. Using the so-called Fujikawa method [8] one can find that this Jacobian is given by

$$\mathcal{J}[\Psi,\bar{\Psi},A_\mu] \equiv \mathcal{J}[A_\mu] = \exp\left(-i\int \mathrm{d}^4x\,\delta\theta(x)\mathcal{A}(x)\right), \quad \mathcal{A}(x) = \frac{e^2}{32\pi^2}F_{\mu\nu}F_{\rho\sigma}\varepsilon^{\mu\nu\rho\sigma}. \tag{2.24}$$

This creates an additional contribution in Eq. (2.21) when comparing the path integral under this change of variables. For the same reasons as before, we must have that

$$\partial_\mu j_5^\mu = \frac{e^2}{16\pi^2}F_{\mu\nu}F_{\rho\sigma}\varepsilon^{\mu\nu\rho\sigma} + 2i\bar{\Psi}\gamma^5 m_0\Psi. \tag{2.25}$$

That is, even in the massless case, the quantization of the theory breaks the conservation of the chiral current.

The effective macroscopic action

In our context, the chiral anomaly can be used to our advantage to modify the negative mass term of (2.15) and in turn obtain an effective electromagnetic response. We do that by once again applying a change of variables given by the global chiral transformation (2.16). Under this, the action is now

$$S[\Psi',\bar{\Psi}'] = \int \mathrm{d}^4x\,\bar{\Psi}\left[i\gamma^\mu D_\mu - m_\mathrm{eff}\right]\Psi, \tag{2.26}$$

with an effective mass

$$m_\mathrm{eff} = e^{i\theta\gamma^5}m_0. \tag{2.27}$$

We will later see that this effective mass will make us recover the free Dirac action with a positive mass term. On the other side, the electromagnetic response is given

by integrating the infinitesimal parameter $\delta\theta(x)$ in the Jacobian (2.24), which in turn gives us the effective Lagrangian $\mathcal{L}_\theta$ of Eq. (2.10). We have thus obtained the equivalence

$$\bar{\Psi}\big[i\gamma^\mu D_\mu - m_0\big]\Psi \equiv \bar{\Psi}\big[i\gamma^\mu D_\mu - m_{\text{eff}}\big]\Psi - \frac{e^2}{32\pi^2}\theta F_{\mu\nu}F_{\rho\sigma}\varepsilon^{\mu\nu\rho\sigma}. \qquad (2.28)$$

We remark once again that the chiral angle is constant within each TI, and its spatial dependence comes from the arrangement of different TI media in space-time. In fact, each TI can possess a different microscopic Hamiltonian. Nevertheless, we will see in the next section that *all* of the TI media possess the same value for the parameter θ, while the trivial insulators can be seen like TI with $\theta = 0$. Specifically, the vacuum gives us both $\theta = 0$ and the original Dirac Lagrangian with a positive mass term.

The allowed values of θ

As $(\gamma^5)^2 = \mathbb{1}$, the chiral transformation term can expressed as

$$
\begin{aligned}
e^{i\theta\gamma^5/2} &= \sum_{n=0}^{\infty}\frac{(i\theta\gamma^5/2)^n}{n!} = \sum_{n=0}^{\infty}\frac{(i\theta\gamma^5/2)^{2n}}{(2n)!} + \sum_{n=0}^{\infty}\frac{(i\theta\gamma^5/2)^{2n+1}}{(2n+1)!}\\
&= \mathbb{1}\sum_{n=0}^{\infty}(-1)^n\frac{(\theta/2)^{2n}}{(2n)!} + i\gamma^5\sum_{n=0}^{\infty}(-1)^n\frac{(\theta/2)^{2n+1}}{(2n+1)!}\\
&= \mathbb{1}\cos(\theta/2) + i\gamma^5\sin(\theta/2).
\end{aligned}
\qquad (2.29)
$$

Thus, taking $\theta \longrightarrow \theta + 2\pi$ changes the transformation as

$$e^{i(\theta+2\pi)\gamma^5/2} = e^{i\pi\gamma^5}e^{i\theta\gamma^5/2} = -e^{i\theta\gamma^5/2}. \qquad (2.30)$$

This extra minus sign cancels when taking both of the field transformations of Eq. (2.16). Thus, adding 2π to θ does not change the theory. That is, θ is defined modulo 2π; for example in the interval $(-\pi, \pi]$. This was also found to hold in the context of TI when speaking about different θ-media [31].

Now, the time reversal symmetry present in TI further restricts the allowed values of θ. The term $F_{\mu\nu}F_{\rho\sigma}\varepsilon^{\mu\nu\rho\sigma}$ can be expressed as proportional to $\mathbf{E}\cdot\mathbf{B}$. As this term transforms as $\mathcal{T}:\mathbf{E}\cdot\mathbf{B}\longrightarrow -\mathbf{E}\cdot\mathbf{B}$, the θ parameter must transform as $\mathcal{T}:\theta\longrightarrow -\theta$ to keep the action invariant. The only allowed values of θ which are equivalent under this transformation are $\theta = 0$ and $\theta = \pi = -\pi \pmod{2\pi}$. The first one corresponds to trivial insulators, and the second one to topological insulators.

As mentioned earlier, the value $\theta = \pi$, which is equal within all TI media, produces the effective mass

$$m_{\text{eff}} = e^{i\pi\gamma^5}m_0 = -m_0, \qquad (2.31)$$

with an opposite sign. Thus, through Eq. (2.28) we can recover the free Dirac Lagrangian with a positive mass in exchange for the electromagnetic response $\mathcal{L}_\theta$. We will of course generally have different values for the mass and scale factors in the momentum in different TI media, but from now on we will make the strong assumption

that all of these parameters are equal to the ones of the free Dirac Lagrangian, such that the only difference between the bulk states of a TI and the vacuum is the Lagrangian $\mathcal{L}_\theta$ with $\theta = \pi$. Otherwise, we would not be able to go very far in our analysis.

2.2.3   Axion electrodynamics

The sum of the Maxwell Lagrangian and the θ-term gives the so-called axion electrodynamics (or the θ-electrodynamics) Lagrangian. That is,

$$\mathcal{L} = \mathcal{L}_{ED} + \mathcal{L}_\theta = \int d^4x \left[-\frac{1}{4} F_{\mu\nu} F^{\mu\nu} - j^\mu A_\mu - \frac{e^2}{32\pi^2} \theta(x) F_{\mu\nu} F_{\rho\sigma} \varepsilon^{\mu\nu\rho\sigma} \right]. \tag{2.32}$$

The Euler-Lagrange equations are

$$\partial_\mu \frac{\delta\mathcal{L}}{\delta(\partial_\mu A_\nu)} - \frac{\delta\mathcal{L}}{\delta A_\nu} = 0. \tag{2.33}$$

For the usual electrodynamics terms,

$$\partial_\mu \frac{\delta\mathcal{L}_{ED}}{\delta(\partial_\mu A_\nu)} = -\partial_\mu F^{\mu\nu}, \quad \frac{\delta\mathcal{L}_{ED}}{\delta A_\nu} = -j^\nu. \tag{2.34}$$

For the anomalous θ-term, we use that

$$F_{\mu\nu} F_{\rho\sigma} \varepsilon^{\mu\nu\rho\sigma} = 4(\partial_\mu A_\nu)(\partial_\rho A_\sigma) \varepsilon^{\mu\nu\rho\sigma}. \tag{2.35}$$

Thus,

$$\partial_\mu \frac{\delta\mathcal{L}_\theta}{\delta(\partial_\mu A_\nu)} = -\frac{e^2}{4\pi^2} \partial_\mu \left[\theta(x)(\partial_\rho A_\sigma) \varepsilon^{\mu\nu\rho\sigma} \right], \quad \frac{\delta\mathcal{L}_\theta}{\delta A_\nu} = 0. \tag{2.36}$$

By the anti-symmetric property of the Levy-Civita symbol, the first term reduces to

$$\partial_\mu \frac{\delta\mathcal{L}_\theta}{\delta(\partial_\mu A_\nu)} = -\frac{e^2}{8\pi^2} (\partial_\mu \theta(x)) F_{\rho\sigma} \varepsilon^{\mu\nu\rho\sigma}. \tag{2.37}$$

Thus, the only modifications to Maxwell's equations appear when $\theta(x)$ is not constant. In total,

$$\partial_\mu F^{\mu\nu} + \frac{\alpha}{2\pi} (\partial_\mu \theta(x)) F_{\rho\sigma} \varepsilon^{\mu\nu\rho\sigma} = j^\nu, \tag{2.38}$$

where we took $\alpha = e^2/4\pi$, the fine-structure constant.

Now, expressing everything in terms of the electromagnetic fields and sources,

$$\rho = j^0, \quad J^i = j^i, \quad E_i = F_{0i}, \quad B_i = -\frac{1}{2}\varepsilon_{ijk} F^{jk}, \quad F_{ij} = -\varepsilon_{ijk} B_k, \quad \varepsilon_{123} = 1, \tag{2.39}$$

then, for the $\nu = 0$ term,

$$\partial_i F^{i0} - \frac{\alpha}{2\pi} (\partial_i \theta(x)) F_{jk} \varepsilon^{0ijk} = \rho. \tag{2.40}$$

Then,

$$\nabla \cdot \mathbf{E} + \frac{\alpha}{\pi} \mathbf{B} \cdot \nabla \theta(x) = \rho. \tag{2.41}$$

For the $\nu = i$ terms,

$$\partial_0 F^{0i} + \partial_j F^{ji} + \frac{\alpha}{2\pi}(\partial_0 \theta(x)) F_{jk}\varepsilon^{0ijk} + \frac{\alpha}{\pi}(\partial_j \theta(x)) F_{0k}\varepsilon^{ji0k} = J^i. \tag{2.42}$$

Then,

$$\nabla \times \mathbf{B} - \frac{\alpha}{\pi}\frac{\partial \theta(x)}{\partial t}\mathbf{B} - \frac{\alpha}{\pi}\nabla\theta(x) \times \mathbf{E} = \mathbf{J} + \frac{\partial \mathbf{E}}{\partial t}. \tag{2.43}$$

The homogeneous parts of Maxwell's equations

$$\nabla \cdot \mathbf{B} = 0, \quad \nabla \times \mathbf{E} = -\frac{\partial \mathbf{B}}{\partial t}, \tag{2.44}$$

still hold, for they are a consequence of the general identity [28]

$$\partial_\mu \varepsilon^{\mu\nu\rho\sigma} F_{\rho\sigma} = 0. \tag{2.45}$$

Eqs. (2.41), (2.43) and (2.44) constitute the so-called axion electrodynamics equations [34]. Note that for a constant value of θ we recover the original Maxwell's equations. As we have seen in section 2.2.2, in our context we will have two cases: $\theta = \pi$ for topological insulators, and $\theta = 0$ for normal insulators. Being constant terms, we will recover the usual Maxwell's equations in the bulk of each material. The corrections will arise in the interfaces of TI with normal insulators, for there a variation of θ is present.

2.2.4 Modified boundary conditions

We now go back to SI units, recovering the vacuum permitivity ε_0, vacuum permeability μ_0 and speed of light c factors. The axion electrodynamics equations here are

$$\begin{aligned} \nabla \cdot \mathbf{E} &= \rho/\varepsilon_0 - c\frac{\alpha}{\pi}\mathbf{B} \cdot \nabla\theta(x), \\ \nabla \cdot \mathbf{B} &= 0, \\ \nabla \times \mathbf{E} &= -\frac{\partial \mathbf{B}}{\partial t}, \\ \nabla \times \mathbf{B} &= \frac{1}{c}\frac{\alpha}{\pi}\Big(\frac{\partial \theta(x)}{\partial t}\mathbf{B} + \nabla\theta(x) \times \mathbf{E}\Big) + \mu_0 \mathbf{J} + \frac{1}{c^2}\frac{\partial \mathbf{E}}{\partial t}, \end{aligned} \tag{2.46}$$
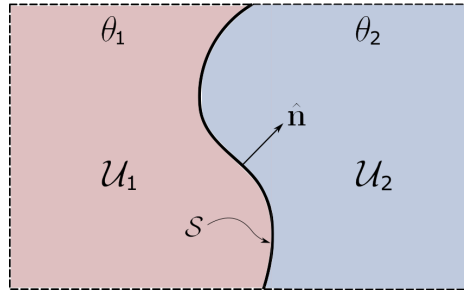
Figure 2.2: Two regions of different θ-media and the interface $\mathcal{S}$ between them.

Let us take then two regions $\mathcal{U}_1$ and $\mathcal{U}_2$ with different θ-terms, θ_1 and θ_2 respectively, such that

$$\theta(x) = \begin{cases} \theta_1, & x \in \mathcal{U}_1, \\ \theta_2, & x \in \mathcal{U}_2. \end{cases} \tag{2.47}$$

We further take the normal unit vector $\hat{\mathbf{n}}$ of the interface $\mathcal{S}$ between the materials, pointing from $\mathcal{U}_1$ to $\mathcal{U}_2$. This is depicted in Fig. 2.2. Taking $\delta(\mathcal{S})$ as the surface Dirac delta of the interface, then

$$\nabla\theta(x) = -\hat{\mathbf{n}}\delta(\mathcal{S})(\theta_1 - \theta_2), \quad \frac{\partial\theta(x)}{\partial t} = 0. \tag{2.48}$$

We further ignore any other magnetization or polarization changes in the materials, and assume that the system is static. Defining

$$\tilde{\theta} \equiv \frac{\alpha}{\pi}(\theta_1 - \theta_2), \tag{2.49}$$

then, the axion-ED equations (2.46) become

$$\begin{aligned} &\nabla \cdot \mathbf{E} = \rho/\varepsilon_0 + \delta(\mathcal{S})\tilde{\theta}c\mathbf{B} \cdot \hat{\mathbf{n}}, \\ &\nabla \cdot \mathbf{B} = 0, \\ &\nabla \times \mathbf{E} = \mathbf{0}, \\ &\nabla \times \mathbf{B} = \delta(\mathcal{S})\frac{\tilde{\theta}}{c}\mathbf{E} \times \hat{\mathbf{n}} + \mu_0\mathbf{J}. \end{aligned} \tag{2.50}$$

Thus, in absence of surface current and charge distributions in the interface[5], the boundary conditions at $\mathcal{S}$ become [33]

$$\begin{aligned} (\mathbf{E}_2 - \mathbf{E}_1)_\perp &= \tilde{\theta}c\mathbf{B}_\perp(\mathcal{S}), \\ (\mathbf{E}_2 - \mathbf{E}_1)_\| &= \mathbf{0}, \\ (\mathbf{B}_2 - \mathbf{B}_1)_\| &= -\frac{\tilde{\theta}}{c}\mathbf{E}_\|(\mathcal{S}), \\ (\mathbf{B}_2 - \mathbf{B}_1)_\perp &= \mathbf{0}. \end{aligned} \tag{2.51}$$

Here, $\perp$ and $\|$ respectively label the perpendicular and parallel components to the surface, and the sub-index denotes the region from which the field is evaluated. The evaluation of $\mathbf{B}_\perp$ and $\mathbf{E}_\|$ at the interface $\mathcal{S}$ is well defined, as these components are continuous through it.

The first of these boundary conditions implies that an external perpendicular magnetic field will induce a perpendicular polarization term. The third, that an external parallel electric field will induce a parallel magnetization term. The general phenomenon for which polarization terms arise from magnetic fields, and magnetization terms from electric fields, is called the *magnetoelectric effect*, which has been studied ever since 1888 [35]. This is an example of one such effect.

---

[5]Other than the ones responsible of for the modified boundary conditions.

3 Quantum system

On this chapter we introduce the basic quantum system from which most of the future calculations will be based on. It consists of an infinite plate of a TI with thickness L, surrounded by vacuum. By the effective electromagnetic theory seen in section 2.2, each region can be described by a θ-term with general value θ_1 for the vacuum, and θ_2 for the TI. We place a constant magnetic field B through the external vacuum medium. From the modified boundary conditions (2.51), an internal electric field $\tilde{E}$ is induced on the inner TI medium (see Fig. 3.1).
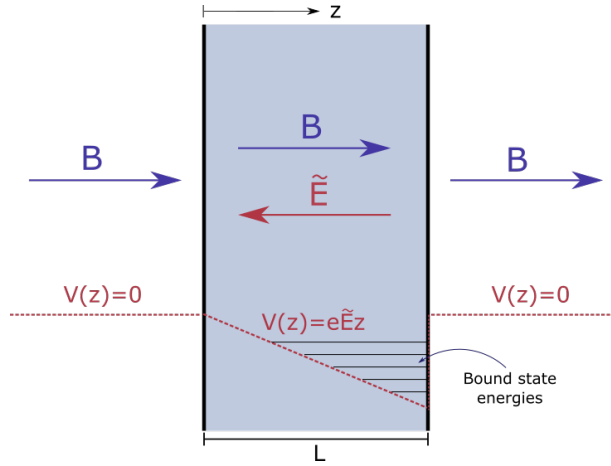
Figure 3.1: Base system: Finite plate of TI with thickness L and a perpendicular external magnetic field.

This electric field is given by

$$\tilde{E} = \tilde{\theta}cB, \quad \tilde{\theta} = \frac{\alpha}{\pi}(\theta_1 - \theta_2). \tag{3.1}$$

Recall that α is the fine-structure constant and θ is the intrinsic parameter that characterizes each medium. Particularly, for $\theta_1 = 0$ (vacuum) and $\theta_2 = \pi$ (TI), then $\tilde{\theta} = -\alpha$, and thus

$$\boxed{\tilde{E} = -\alpha cB}. \tag{3.2}$$

We suppose that the effective electromagnetic theory is sufficient to completely account for the presence of the TI, such that the quantum motion of electrons is free even inside the TI. That is, the presence of the TI is effectively described by the

induced fields such that for everything else it is treated as a vacuum. The interaction between electrons is also ignored.

With the use of Landau gauge, and the alignment of the z-axis in the field's direction, the electromagnetic potentials are

$$\mathbf{A}(\mathbf{x}) = xB\hat{e}_y, \quad \phi(\mathbf{x}) = 0, \tag{3.3}$$

for the two θ_1-media, and

$$\mathbf{A}(\mathbf{x}) = xB\hat{e}_y, \quad \phi(\mathbf{x}) = -\tilde{E}z, \tag{3.4}$$

for the θ_2-medium. Despite the potential difference from $z = 0$ to $z = L$ of the induced electric field, we take the same level of constant potential between the two θ_1-media. That is because in reality we suppose that the TI plate is a finite, but large plate in the x-y directions. This way, the two vacuum are actually connected and thus possess no potential difference.

This produces a system with a triangle potential $V(z) = q\,\phi(z)$ between $z = 0$ and $z = L$, which rises or sinks depending on the direction of the fields and charge of the particles. For a magnetic field in the positive z direction ($B > 0$ so that $\tilde{E} < 0$) and electrons ($q = -e$), this potential sinks. This gives rise to the possibility of allocating bound states inside the TI (see Fig. 3.1).

It is no coincidence that we study an infinite (thick) plate with a perpendicular magnetic field just as in the HE. The purpose of this set-up is to mimic the conditions of the HE. Despite being a 3D electron gas, the existence of bound states will allow us to treat the system as a multi-layered 2D electron gas, and thus naturally recover the QHE. Nonetheless, when we introduce the parallel electric field in chapter 5, an additional small magnetic field will be induced inside the plate. This will weakly break the usual QHE setup. Our work will consist of computing, for how much does the resulting current change. We will also make a side calculation in chapter 4 for the consequences of bound energy states dependent on the external magnetic field in this set-up. That is, we will compute the induced magnetization of this system.

We remark once again that the effects of spin are ignored for simplicity, which in turn are discussed in Appendix B.

3.1 Wave functions

It is sufficient to know the solutions of the Schrödinger equation in two cases: For a pure constant magnetic field, and for constant parallel electric and magnetic fields. For both cases the solutions to the Schrödinger equation are separable, and have the same $x - y$ components that of section 1.2.2 with the electric field in the x-direction turned off. This gives automatic continuity on those coordinates when gluing them up. The only differences are present on the z wave function, for which Airy functions appear (see Appendix C).

That is to say, the general solutions for the bound states are

$$\Psi^1_{n,k_y,\kappa}(\mathbf{x}) = e^{ik_y y}\phi_n\big(x + k_y\ell_B^2\big)\big(Ee^{-\kappa z} + Ae^{\kappa z}\big), \tag{3.5a}$$

for $z \leq 0$,
$$\Psi^2_{n,k_y,\kappa}(\mathbf{x}) = e^{ik_y y}\phi_n\big(x + k_y \ell_B^2\big)(C\,\mathrm{Ai}(\xi) + D\,\mathrm{Bi}(\xi)), \tag{3.5b}$$

for $0 \leq z \leq L$, and

$$\Psi^3_{n,k_y,\kappa}(\mathbf{x}) = e^{ik_y y}\phi_n\big(x + k_y \ell_B^2\big)(Be^{-\kappa z} + Fe^{\kappa z}), \tag{3.5c}$$

for $z \geq L$. A, B, C, D, E, F are constants to be determined, $\kappa \in \mathbb{R}^+$, $k_y \in \mathbb{R}$, $n = 0, 1, 2...$, $\phi_n(x)$ the quantum Harmonic oscillator solutions (1.36) and $\mathrm{Ai}(\xi)$, $\mathrm{Bi}(\xi)$ are the well known Airy functions [36]. Once again we took the magnetic length ℓ_B and the cyclotron frequency ω_B. We also now took the dimensionless variable

$$\xi = \left(\frac{\hbar^2}{2me\tilde{E}}\right)^{2/3}\left(\kappa^2 + \frac{2me\tilde{E}}{\hbar^2}z\right), \tag{3.6}$$

which can be put in a more compact notation,

$$\xi = \ell_{\tilde{E}}^2 \kappa^2 + \frac{z}{\ell_{\tilde{E}}} = \sigma^2 + \frac{\Gamma}{L}z, \tag{3.7}$$

where

$$\boxed{\ell_{\tilde{E}} = \left(\frac{\hbar^2}{2me\tilde{E}}\right)^{1/3}} \tag{3.8}$$

is the so-called electric length, where in this context we used the induced electric field $\tilde{E}$, and with the dimensionless constants

$$\boxed{\sigma = \left(\frac{\hbar^2}{2me\tilde{E}}\right)^{1/3}\kappa}, \quad \boxed{\Gamma = \left(\frac{2me\tilde{E}}{\hbar^2}\right)^{1/3}L}. \tag{3.9}$$

These are to be interpreted, up to a sign, as a dimensionless (bound) momentum and as a dimensionless thickness, respectively. These will be constantly used from now on. Note that, under our set-up, both σ and Γ are negative. We also have the relations

$$\xi\mid_{z=0} = \sigma^2, \quad \tau \equiv \xi\mid_{z=L} = \sigma^2 + \Gamma, \tag{3.10}$$

and

$$\frac{\partial \xi}{\partial z} = \frac{\kappa}{\sigma}. \tag{3.11}$$

The energies are given by

$$\mathcal{E}_{n,\kappa} = -\frac{\hbar^2 \kappa^2}{2m} + \hbar\omega_B\left(n + \frac{1}{2}\right). \tag{3.12}$$

The general problem reduces to solving for the boundary conditions. The $x - y$ part is of no interest, as it can be factored out in every calculation, and is already normalized[1]. From now on, when speaking about the wave function, it will be on reference to the z-dependence part.

---

[1] The wave packets $e^{ik_y y}$ cannot be properly normalized. One would take the y-direction to be finite L_y, and normalize by that length. But ignoring the y-direction altogether is equally valid.

The convergence condition of the wave function implies $E = F = 0$. Thus, defining $\omega = \kappa L$ and using Ecs. (3.10) and (3.11), the boundary conditions are

$$A = C \operatorname{Ai}(\sigma^2) + D \operatorname{Bi}(\sigma^2) \tag{3.13a}$$

$$Be^{-\omega} = C \operatorname{Ai}(\tau) + D \operatorname{Bi}(\tau) \tag{3.13b}$$

for the continuity of the wave function in $z = 0$ and $z = L$ respectively, and

$$A = \frac{1}{\sigma}(C \operatorname{Ai}'(\sigma^2) + D \operatorname{Bi}'(\sigma^2)) \tag{3.14a}$$

$$Be^{-\omega} = -\frac{1}{\sigma}(C \operatorname{Ai}'(\tau) + D \operatorname{Bi}'(\tau)) \tag{3.14b}$$

for the continuity of its derivative on the same respective points.

3.2 Energy quantization

We have 4 undetermined coefficients. With the boundary conditions and the normalization, we have 5 equations. This creates a condition equation for σ, which produces a quantization of the energies in κ. Mixing the boundary conditions we obtain

$$\begin{aligned} F(\sigma, \Gamma) \equiv\ & [\operatorname{Ai}'(\tau) + \sigma \operatorname{Ai}(\tau)][\operatorname{Bi}'(\sigma^2) - \sigma \operatorname{Bi}(\sigma^2)] \\ & - [\operatorname{Bi}'(\tau) + \sigma \operatorname{Bi}(\tau)][\operatorname{Ai}'(\sigma^2) - \sigma \operatorname{Ai}(\sigma^2)] = 0. \end{aligned} \tag{3.15}$$

For each dimensionless thickness Γ, the roots of $F(\sigma, \Gamma)$ will be the allowed values of σ. Figure 3.2a shows an example of $F(\sigma, \Gamma)$ for a representative thickness of $\Gamma = -20$. Multiple allowed values of σ are present.

(a) $F(\sigma, \Gamma)$ for $\Gamma = -20$ in log scale.

(b) Roots of F as a function of Γ.
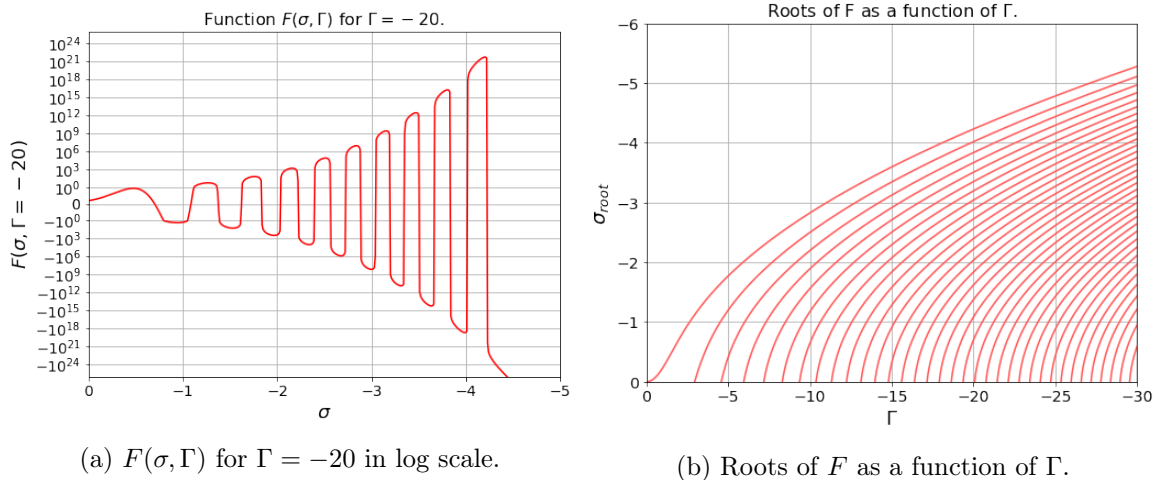
Figure 3.2: (a) Plot of the function of Eq. (3.15). The function grows exponentially fast, but with oscillations in a finite interval, which give rise to its roots. (b) The roots of F found numerically for a range of values in Γ.

We can numerically obtain the roots of $F(\sigma, \Gamma)$ for each value of Γ. With this, the result is a relationship between different energy bands described by the allowed values of σ, as a function of Γ. That is, we obtain solution curves $\sigma_k(\Gamma)$ ($k = 0, 1, 2...$). This can be seen in Figure 3.2b.

We can see that the allowed energy bands are continuous and both, the number of allowed energies, and their value, increase with $|\Gamma|$. We can also see that there exists a range of values $|\Gamma| < \Gamma_c$, with

$$\Gamma_c \approx 2.94869, \tag{3.16}$$

for which only one energy band (the ground state) is allowed. This band can be approximated for small values of Γ. That is,

$$|\sigma_0(\Gamma)| \approx \frac{1}{4}\Gamma^2. \tag{3.17}$$

for $|\Gamma| << 1$. Figure 3.3a shows the validity of this approximation, where we can see that in this scale it fits up until $|\Gamma| = 1$.

(a) Fit at quadratic order of $\sigma_0(\Gamma)$.

(b) WKB approximation for $\sigma_k(\Gamma)$.
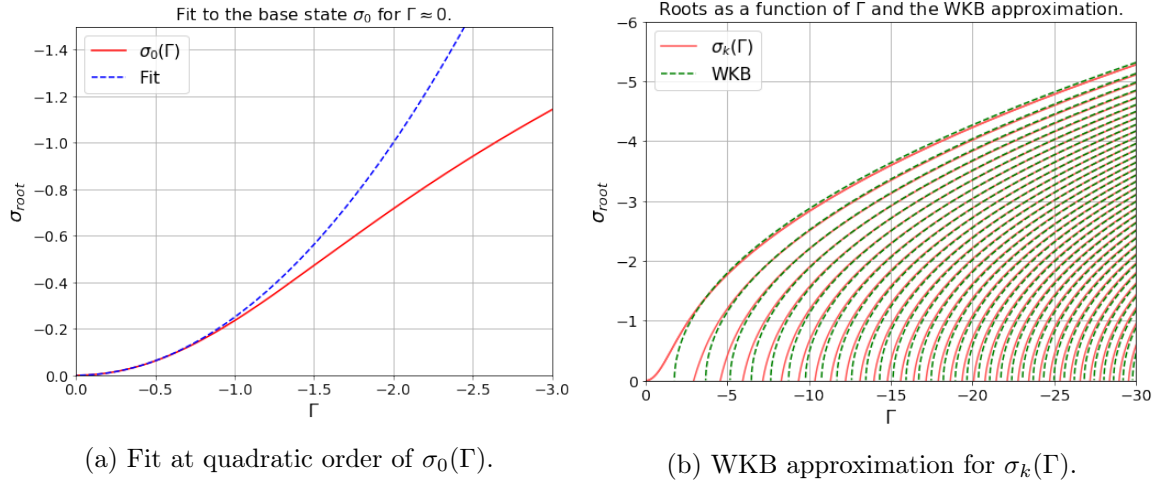
Figure 3.3: Fits (a) for the base state at low values of Γ and (b) in the WKB approximation, which best fits for bigger values of σ and Γ.

Figure 3.2b also shows that the allowed energy bands $\sigma_k(\Gamma)$ have an overall behaviour similar to $|\sigma_k(\Gamma)| \sim \sqrt{|\Gamma| - a_k}$. An analysis through the WKB approximation (see Appendix D) confirms this hypothesis. That is, under this approximation, we obtain that

$$\boxed{|\sigma_k(\Gamma)| \approx \sqrt{|\Gamma| - (3\pi/2)^{2/3}(k + 1/2)^{2/3}}}. \tag{3.18}$$

Figure 3.3b shows the comparison between this approximation and the bands obtained numerically. We can see that the WKB approximation is valid for high values of Γ and σ. The base state and first excited state, nonetheless, are the ones that fit the worst.
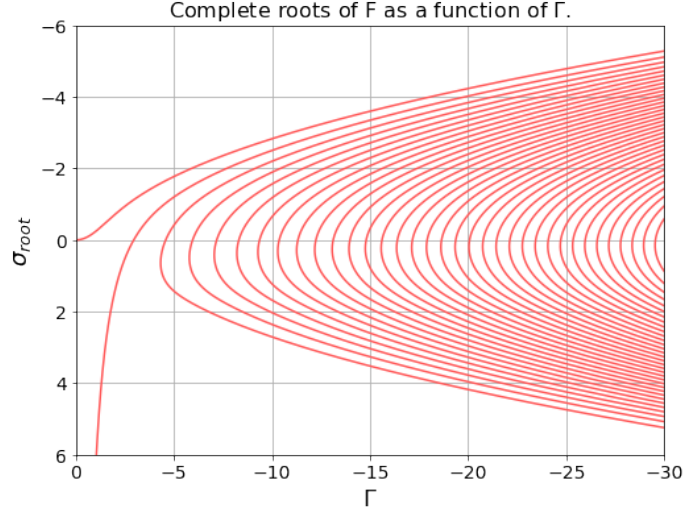
Figure 3.4: Complete bands $\sigma_k(\Gamma)$, including positive non-physical solutions.

These first bands have a peculiar behaviour, which is apparent when we also compute the positive roots of $F(\sigma, \Gamma)$, shown in Figure 3.4. Although we can have positive values of σ and Γ if we had $\tilde{E} > 0$ (i.e. $B < 0$), they must both at the end be of equal sign. Thus, the positive solutions of sigma plotted for negative values of Γ are non-physical solutions. They just allow us to visualize the complete behaviour of the mathematical solution curves. The curves for positive values of Γ are just the mirror image inverted around the Γ axis.

The solution bands σ_0 and σ_1 are special: One changes its curvature and tends to zero as Γ tends to zero, while the other one diverges to negative infinity. Meanwhile, the rest look like parabolas. That is what would be expected for bands where $\sqrt{|\Gamma| - a_k}$.

3.3   Occupation of energy states

There are three quantum numbers: (n, κ_k, k_y), where the first two are quantized (κ_k are the allowed values related to σ_k). The energies (3.12) are not dependent in k_y. That is, $\mathcal{E} = \mathcal{E}_{n,\kappa}$, so in the same way as the QHE, each (n, κ_k) level possesses the degeneracy of a Landau level,

$$g = \frac{AB}{\Phi_0}, \tag{3.19}$$

where A is still the area of the plate in the x-y direction. So, despite being a 3D system with two kinds of quantized levels n and κ_k, we can think of the combination of them as "Landau levels". For example, a system with $\mathcal{E}_{0,\kappa_0}$, $\mathcal{E}_{0,\kappa_1}$,...,$\mathcal{E}_{0,\kappa_{\nu-1}}$ filled, or one where $\mathcal{E}_{1,\kappa_0}$,...,$\mathcal{E}_{\nu-1,\kappa_0}$ are filled instead, or even one where the filling is mixed between the n-levels and the κ_k levels, can be considered as a system with ν Landau levels full, for the necessary number of electrons required to fill them is the same.

Nonetheless, there will be cases when the observables are dependent on *how* each Landau level (n, κ) is filled. From the general expressions, it is not clear whether

the filling will start first with the n levels, with the κ levels, or in a mixture. This is what we will study in this section. For clarity, we will generally use n to denote the quantum number of a *particular* Landau level, while ν will be used to denote the *number* of Landau levels filled, either for a specific κ_k level or for the total energy levels of the system.

3.3.1 Total occupied states

From Eq. (3.19), we can get that ν Landau levels will be filled when we have an electron surface density[2] n_e such that

$$\nu = n_e \frac{\Phi_0}{B}. \tag{3.20}$$

As discussed in section (1.2.3), the presence of disorder, necessary for the realisation of the QHE, will weakly break the degeneracy of each Landau level, but will be the responsible of the robustness of the Hall states. The current will change not when a Landau level starts to fill, or when is completely filled, but when the extended states of the Landau level are filled. As one can see from the density of states of Fig. 1.5, the extended levels fill whenever a Landau level is approximately *half filled*. That is, the disorder effectively produces quantized a current just as if ν_{tot} Landau levels were filled, where for an arbitrary surface density, this number is given by

$$\nu_{\text{tot}} = \left\lfloor n_e \frac{\Phi_0}{B} \right\rceil, \tag{3.21}$$

where $\lfloor x \rceil$ is the round to nearest integer function. This is the occupation number that matters to us. If we were instead interested in Landau levels with partial filling, or with complete occupation, we would need to use other kinds of rounding functions. As we will see, this would hardly matter. The degeneracy of the Landau levels is so big that the following results would also be approximately valid for these cases.

3.3.2 Filling

We take the energies (3.12), express κ in terms of σ and divide by the energy $\hbar\omega_B$ to make them dimensionless,

$$\mathcal{E}_{n,\kappa} = (n + 1/2) - \epsilon\sigma^2. \tag{3.22}$$

Here, we defined

$$\epsilon = \frac{1}{\hbar\omega_B} \frac{\hbar^2}{2m\ell_{\tilde{E}}^2} = -\alpha\ell_{\tilde{E}} \frac{mc}{\hbar}, \tag{3.23}$$

a dimensionless constant which gives us the quotient between the energy of a κ level and an energy quantum $\hbar\omega_B$. It depends only on B, is positive ($\ell_{\tilde{E}}$ is negative), and is

---

[2]Despite being a 3D system, we can still define surface density as number of electrons per unit area, as the gas is localized inside the plate and uniformly distributed in *x-y*.

of order α. For a better physical interpretation, it can be put in terms of the reduced Compton wavelength of the electron $\lambdabar \equiv \hbar/mc$. That is,

$$\epsilon = -\alpha \frac{\ell_{\tilde{E}}}{\lambdabar}. \tag{3.24}$$

As this constant only depends on the magnetic field, it is easy to visualize its order of magnitude. This is shown in Figure 3.5, for the typical range of values of B in the Hall Effect.
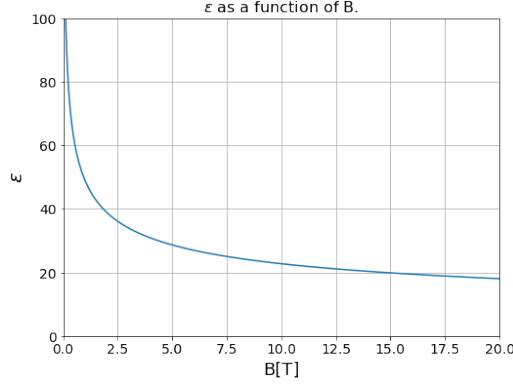
Figure 3.5: ϵ as a function of B.

Even when ϵ decreases with B, it is at least bigger than 20 for this ranges. Meanwhile, the n levels are only naturals $\{0, 1, 2, ...\}$. These numbers and the differences between different values of σ turn to be big enough for the parameters used such that the energy difference between the base state $(0, \kappa_0)$ and the first excited state in κ, $(0, \kappa_1)$, turn out to be very big. Thus, typically we wont have excited states in κ before some amount of n levels are already filled.

We can make a more systematic analysis of this. Suppose we have filled $\nu - 1$ Landau levels in the first κ level (that is, we have filled up to the $\mathcal{E}_{\nu-2,\kappa_0}$ level), and we still have more levels to be filled. For the next ν-th level to be $\mathcal{E}_{0,\kappa_1}$ instead of $\mathcal{E}_{\nu-1,\kappa_0}$, we need that

$$\mathcal{E}_{0,\kappa_1} < \mathcal{E}_{\nu-1,\kappa_0}. \tag{3.25}$$

This implies that

$$\nu - 1 > \epsilon(\sigma_0^2 - \sigma_1^2), \tag{3.26}$$

where $|\sigma_0| > |\sigma_1|$. And so, if we have an amount of at least ν Landau levels filled that is greater than $1 + \epsilon(\sigma_0^2 - \sigma_1^2)$, then there will be occupation in κ_1. As we have the ability to fill ν_{tot} Landau levels in total (as given by Eq. (3.21)), we thus find that

$$\nu_{\text{tot}} > 1 + \epsilon(\sigma_0^2 - \sigma_1^2) \tag{3.27}$$

is a sufficient condition for a system to have occupation in the κ_1 level. This a relation which depends on B, n_e and L. Although, from this last one it depends very weakly. We can see that when we use the WKB approximation (3.18), for which

$$\sigma_0^2 - \sigma_1^2 \approx \left(\frac{3\pi}{4}\right)^{2/3}(3^{2/3} - 1), \tag{3.28}$$

which gets rid of the dependence on L. Expressing ϵ in an alternative way

$$\epsilon = \left(\frac{\alpha^2}{4\pi\lambdabar^2} \frac{\Phi_0}{B} \right)^{1/3}, \tag{3.29}$$

the condition of Eq. (3.27) takes the form

$$\left\lfloor n_e \frac{\Phi_0}{B} \right\rfloor > 1 + \frac{1}{4}(3^{2/3} - 1)\left(\frac{9\pi\alpha^2}{\lambdabar^2} \frac{\Phi_0}{B} \right)^{1/3}. \tag{3.30}$$

So, defining a *superficial Compton density*

$$n_C \equiv \frac{1}{4^3}\left(\frac{9\pi\alpha^2}{\lambdabar^2} \right) \approx 1.5776 \times 10^{20}\,\mathrm{m}^{-2}, \tag{3.31}$$

this becomes

$$\left\lfloor n_e \frac{\Phi_0}{B} \right\rfloor > 1 + (3^{2/3} - 1)\left(n_C \frac{\Phi_0}{B} \right)^{1/3}, \quad (3^{2/3} - 1) \approx 1.08. \tag{3.32}$$

This is a simpler relation, dependent only on n_e and B. The numerical factor $(3^{2/3}-1)$ is left on purpose because we will generalize this formula for higher levels of κ.

One could ask himself, what is the physical interpretation of the quantity on the right hand side of this relation? As the left hand side describes the total amount of occupied Landau levels ν_{tot}, the right hand side must also be *an amount* of Landau levels. And this is true, the term

$$\nu_0 \equiv 1 + (3^{2/3} - 1)\left(n_C \frac{\Phi_0}{B} \right)^{1/3} \tag{3.33}$$

measures how many Landau levels are necessary to allocate in the κ_0 level in order to reach the κ_1 level: If $\nu_{\mathrm{tot}} < \nu_0$, we were left too short and κ_1 is not reached. If $\nu_{\mathrm{tot}} = \nu_0$ we are right on the spot from which the κ_1 level starts to be filled. If $\nu_{\mathrm{tot}} > \nu_0$ we have more than the necessary and so the levels continue to fill. Of course we ignore whether ν_0 is an integer or not, as this number was beforehand produced from approximations.
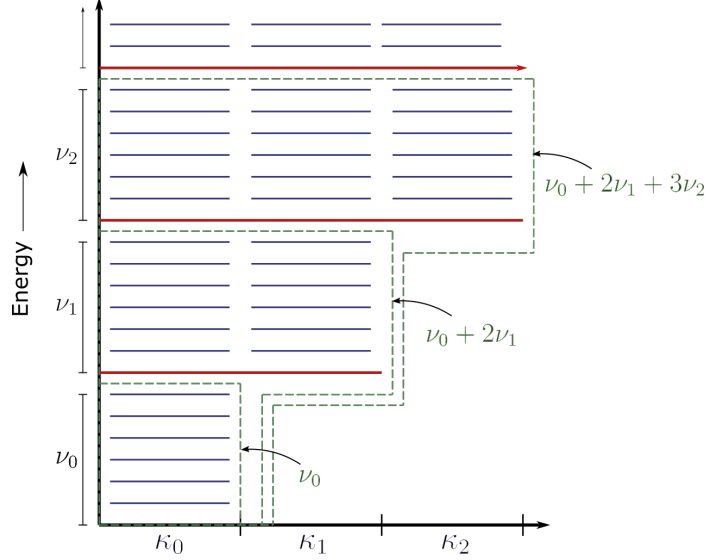
Figure 3.6: Visual representation of the filling. First, ν_0 levels need to be allocated in the κ_0 level in order to reach the κ_1 level. Next, an equal amount of ν_1 levels need to be allocated in each of the two levels: κ_0 and κ_1, leaving a total of $\nu_0 + 2\nu_1$ levels needed in order to reach the κ_2 level. In the same way, the levels needed to reach the κ_3 level are $\nu_0 + 2\nu_1 + 3\nu_2$. The process continues until all of the available levels ν_{tot} are allocated.

So, if $\nu_{\text{tot}} > \nu_0$ we can further ask ourselves whether we have enough Landau levels to reach the $\mathcal{E}_{0,\kappa_2}$ level. First note that we now have two different κ levels that have to be filled: The κ_0 level, which was left with ν_0 Landau levels occupied, and the κ_1 level, which is just now starting to fill. We assume that the energy $\mathcal{E}_{\nu_0-1,\kappa_0}$ is approximately equal to the energy $\mathcal{E}_{0,\kappa_1}$, such that the number of Landau levels needed to reach the $\mathcal{E}_{0,\kappa_2}$ level is approximately the same for both of these levels. That is, if we denote by ν_1 as the amount of Landau levels needed to allocate in the κ_1 level in order to reach the $\mathcal{E}_{0,\kappa_2}$ level, one needs a total amount of

$$\nu = \nu_0 + 2\nu_1 \tag{3.34}$$

levels to be occupied in this system: ν_0 levels are needed to first reach the $\mathcal{E}_{0,\kappa_1}$ level, ν_1 are needed to allocate in κ_1 level (filling up to the $\mathcal{E}_{\nu_1-1,\kappa_1}$ energy level) in order to reach the $\mathcal{E}_{0,\kappa_2}$ level and another ν_1 in order to account that in this process we also have to keep filling the κ_0 level, starting from where we left (and thus also filling up to the $\mathcal{E}_{\nu_0+\nu_1-1,\kappa_0}$ energy level). For a visual representation of this filling, see Fig. 3.6.

The conditions for having reached the κ_2 level are two, one for each κ level being filled:

$$\mathcal{E}_{0,\kappa_2} < \mathcal{E}_{\nu_0+\nu_1-1,\kappa_0}, \quad \mathcal{E}_{0,\kappa_2} < \mathcal{E}_{\nu_1-1,\kappa_1}. \tag{3.35}$$

These imply

$$(\nu_0 + \nu_1) - 1 > \epsilon(\sigma_0^2 - \sigma_2^2), \quad \nu_1 - 1 > \epsilon(\sigma_1^2 - \sigma_2^2). \tag{3.36}$$

Summing up both inequalities, and identifying ν from Eq. (3.34),

$$\nu > 2 + \epsilon(\sigma_0^2 + \sigma_1^2 - 2\sigma_2^2). \tag{3.37}$$

Once again using the WKB approximation, and noting that we have the ability to fill ν_{tot} Landau levels in total, given by Eq. (3.21), we now arrive at the condition

$$\left\lfloor n_e \frac{\Phi_0}{B} \right\rfloor > 2 + (2 \cdot 5^{2/3} - 3^{2/3} - 1)\left(n_C \frac{\Phi_0}{B}\right)^{1/3}, \quad (2 \cdot 5^{2/3} - 3^{2/3} - 1) \approx 2.77. \quad (3.38)$$

for the filling to reach the κ_2 level. Note that if relation (3.38) is fulfilled, so is (3.32), which is consistent with the fact that κ_0 must be filled before κ_1 is filled.

In the same way as before, the total number of Landau levels used to reach the κ_2 level is given by the right hand side of relation (3.38). That is,

$$\nu_0 + 2\nu_1 \equiv 2 + (2 \cdot 5^{2/3} - 3^{2/3} - 1)\left(n_C \frac{\Phi_0}{B}\right)^{1/3}, \quad (3.39)$$

and thus, using Eq. (3.33),

$$\nu_1 = \frac{1}{2} + (5^{2/3} - 3^{2/3})\left(n_C \frac{\Phi_0}{B}\right)^{1/3}. \quad (3.40)$$

Following the same argumentation, this process can be easily generalized. For us to reach an arbitrary level κ_m (provided of course, that Γ is such that the level exists), it is needed that

$$\left\lfloor n_e \frac{\Phi_0}{B} \right\rfloor > m + b_m \left(n_C \frac{\Phi_0}{B}\right)^{1/3}, \quad b_m \equiv m(2m+1)^{2/3} - \sum_{l=0}^{m-1}(2l+1)^{2/3}. \quad (3.41)$$

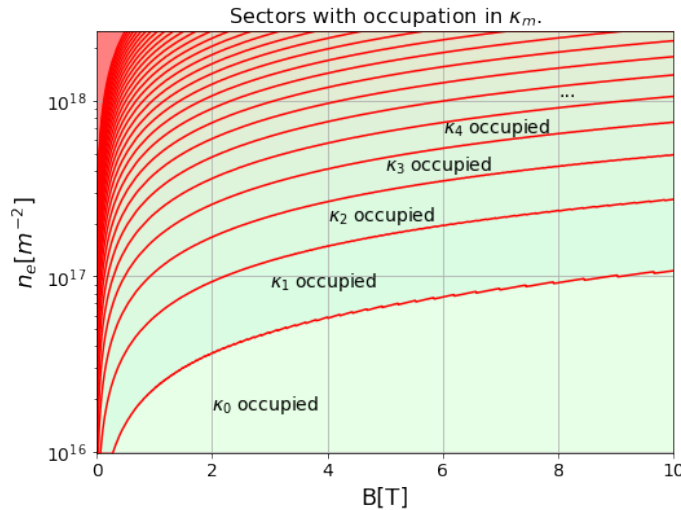

Figure 3.7: Occupation sectors in log scale for n_e.

Relation (3.41) is a sufficient condition for a system to have occupation in the κ_m level. The maximal m for which it holds, will be the maximal κ_m level filled (note that

the case $m = 0$ is always trivially fulfilled). In that way, we obtain sectors in B–n_e space for which relation (3.41) holds for a maximal occupation level κ_m. These are shown in figure 3.7. Note that the rounding function which originated from Eq. 3.21 hardly makes a difference in these scales.

The total number of Landau levels used to reach the κ_m level is once again the right hand side of the relation (3.41). That is,

$$\nu_0 + 2\nu_1 + ... + m\nu_{m-1} = m + b_m \left(n_C \frac{\Phi_0}{B} \right)^{1/3}. \tag{3.42}$$

Once again, refer to Fig. 3.6 to visualize this filling. Using this same equation to solve for ν_{m-1}:

$$m\nu_{m-1} = m + b_m \left(n_C \frac{\Phi_0}{B} \right)^{1/3} - \left(\nu_0 + 2\nu_1 + ... + (m-1)\nu_{m-2} \right)$$

$$= m + b_m \left(n_C \frac{\Phi_0}{B} \right)^{1/3} - (m-1) - b_{m-1} \left(n_C \frac{\Phi_0}{B} \right)^{1/3} \tag{3.43}$$

$$= 1 + (b_m - b_{m-1}) \left(n_C \frac{\Phi_0}{B} \right)^{1/3}.$$

As we have that

$$b_m - b_{m-1} = m(2m + 1)^{2/3} - m(2m - 1)^{2/3}, \tag{3.44}$$

then

$$\nu_{m-1} = \frac{1}{m} + c_m \left(n_C \frac{\Phi_0}{B} \right)^{1/3}, \quad c_m \equiv \frac{1}{m}(b_m - b_{m-1}) = (2m+1)^{2/3} - (2m-1)^{2/3}. \tag{3.45}$$

We recall that ν_{m-1} tells us the number of Landau levels necessary to allocate in the κ_{m-1} level in order to reach the κ_m level.

In a way, the results of this analysis do not depend on the thickness L of the plate. Nevertheless, we must emphasize that we have ignored the possibility that Γ (which is determined by L) could have a value such that a level κ_m does not even exists (see Fig 3.2b). If this were the case, the occupation would just continue to fill the n levels of all of the lower κ levels. This will be further analysed in the next section.

3.3.3 Fermi Energy

Once we know the maximal m for which relation (3.41) holds, we know what is the maximum κ level with occupation: κ_m. Now we can ask ourselves exactly how many Landau levels are allocated in each of these κ levels. We already know that we have used $\nu_0 + 2\nu_1 + ... + m\nu_{m-1}$ levels (given by Eq.(3.42)) in order to reach the κ_m

level, which have been distributed along the levels κ_0, κ_1, ..., κ_{m-1}. Namely, we have allocated $\nu_0 + \nu_1 + ... + \nu_{m-1}$ levels in κ_0, $\nu_1 + \nu_2 + ... + \nu_{m-1}$ levels in κ_1, and continued until κ_{m-1}, which has been filled with ν_{m-1} levels (see Fig 3.6), where the value of each ν_k can be obtained from Eq.(3.45). But this is not the end of the story, for we could still have some remaining Landau levels that are not sufficient to reach the next κ_{m+1} level, but need to be allocated nonetheless. These are given by

$$n_{\text{tot}} - \left(\nu_0 + 2\nu_1 + ... + m\nu_{m-1}\right) = \left\lfloor n_e \frac{\Phi_0}{B} \right\rfloor - m - b_m \left(n_C \frac{\Phi_0}{B}\right)^{1/3} \tag{3.46}$$

As we now have $m + 1$ levels to be filled (which are $\kappa_0, ..., \kappa_m$), these remaining levels must be distributed equitably in each one. Thus, if we take

$$n_m \equiv \frac{1}{m+1} \left\{ \left\lfloor n_e \frac{\Phi_0}{B} \right\rfloor - m - b_m \left(n_C \frac{\Phi_0}{B}\right)^{1/3} \right\}, \tag{3.47}$$

then, by this definition,

$$\nu_{\text{tot}} = \nu_0 + 2\nu_1 + ... + m\nu_{m-1} + (m+1)n_m. \tag{3.48}$$

With this we have exhausted all of the Landau levels available and can precisely know how many have been allocated in each κ level. That is, κ_0 has been filled with $\nu_0 + \nu_1 + ... + \nu_{m-1} + n_m$ levels, κ_1 with $\nu_1 + \nu_2 + ... + \nu_{m-1} + n_m$ levels and so on, continuing until κ_{m-1}, which has been filled with $\nu_{m-1} + n_m$ levels and finally reached κ_m, filled with n_m levels. Thus, the Fermi energy is given by

$$\mathcal{E}_F = \mathcal{E}_{n_m, \kappa_m} \approx \mathcal{E}_{\nu_{m-1}+n_m, \kappa_{m-1}} \approx ... \approx \mathcal{E}_{\nu_0 + ... + \nu_{m-1} + n_m, \kappa_0}. \tag{3.49}$$

Once again, this would be a general result if all of the κ levels were always allowed, but this is not always the case. The case for which a κ level, which in theory could be occupied but is forbidden, will now be considered. Namely, let us imagine that the level κ_{k+1} is forbidden, leaving the κ_k level as the last one available to be occupied. If $k + 1$ is greater than the maximal m previously obtained, the initial procedure is unaffected as the occupation does not even reach this forbidden level: We are done. But, if $k + 1 \leq m$, then the filling previously discussed must change. This is not so hard to correct and is in fact very similar to the procedure we have just performed. We take the levels

$$\nu_0 + \nu_1 + ... + k\nu_{k-1}, \tag{3.50}$$

which have been used in order to reach this last κ_k level. As there are no more κ levels beyond this point, we can simply distribute the remaining levels in the $k + 1$ available κ levels to be filled. That is, we take

$$n_k \equiv \frac{1}{k+1} \left\{ \left\lfloor n_e \frac{\Phi_0}{B} \right\rfloor - k - b_k \left(n_C \frac{\Phi_0}{B}\right)^{1/3} \right\}, \tag{3.51}$$

and thus the filling will be left in a similar way: κ_0 filled with $\nu_0 + \nu_1 + ... + \nu_{k-1} + n_k$ levels, κ_1 with $\nu_1 + \nu_2 + ... + \nu_{k-1} + n_k$ levels and so on, continuing until κ_{k-1}, which is filled with $\nu_{k-1} + n_k$ levels and finally reaching κ_k, filled with n_k levels. The Fermi energy will thus be

$$\mathcal{E}_F = \mathcal{E}_{n_k,\kappa_k} \approx \mathcal{E}_{\nu_{k-1}+n_k,\kappa_{k-1}} \approx ... \approx \mathcal{E}_{\nu_0+...+\nu_{k-1}+n_k,\kappa_0}. \qquad (3.52)$$

Note that is can significantly change the behaviour of the Fermi energy at points where a new κ level appears.
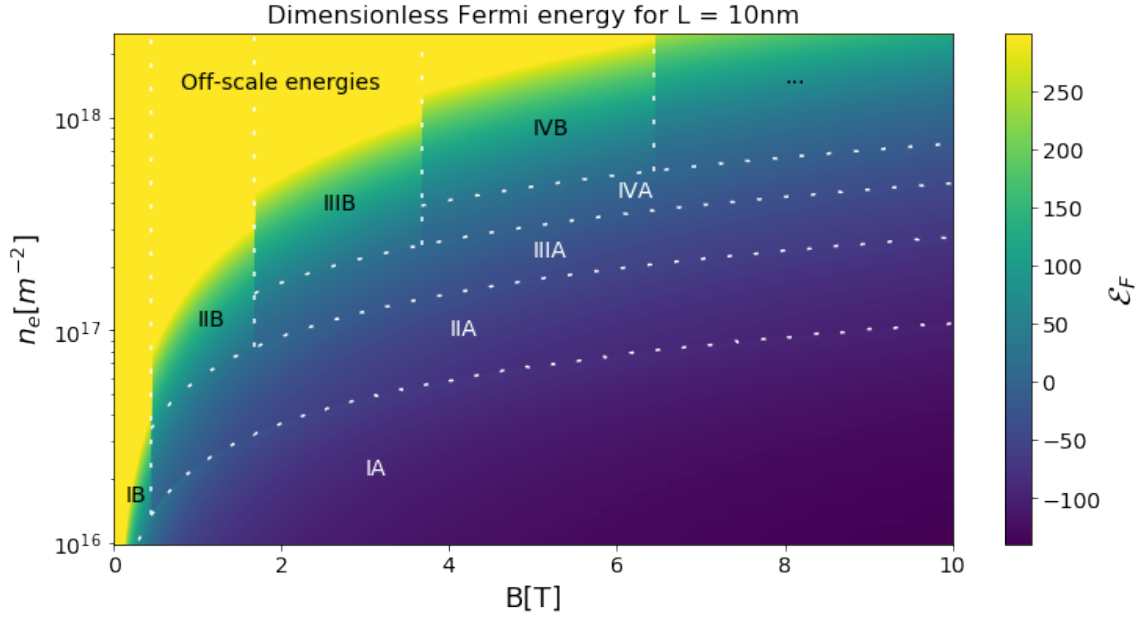
Figure 3.8: Dimensionless Fermi energy of Eq. (3.22) at a fixed thickness of $L = 10\,\text{nm}$ using the numerical roots for $\sigma(\Gamma)$, but the filling analysis with the WKB approximation of Fig. 3.7. IA: The n levels linearly increase $\mathcal{E}_F$ at the κ_0 level. IIA: The occupation reaches the κ_1 level (see Fig. 3.7), so the n levels fill half as fast as there are now two κ levels. IB: Γ is such that the κ_1 level does not exists (see Fig. 3.2b), so the κ_0 level keeps filling linearly even when the occupation sector corresponded to κ_1. IIIA: The occupation reaches the κ_2 level, so now there are three κ levels to be filled, which further reduces the speed at which the n levels are filled. IIB: Γ is such that the κ_2 level does not exists, so the κ_0 and κ_1 keep filling in a way similar to IB. An analogous process continues for IIIB, IVA, IVB and so on. Discontinuites on the Fermi energy are found on the transitions between the zones IB, IIB, IIIB, ... and the zones II, III, IV, ... (either A or B) respectively.

With the results from the previous section, and the discussion presented here we summarize the computation of the Fermi energy for arbitrary parameters in an algorithmic procedure:

1. Obtain the total amount of Landau levels ν_{tot} from Eq. (3.21).

2. Compute the maximum m for which relation (3.41) holds.

3. For this maximum m, compute n_m from Eq. (3.47).

4. The (dimensionless) Fermi energy will then be $\mathcal{E}_{n_m,\kappa_m}$.

5. If Γ is such that a κ_{k+1} level does not exists with $k+1 \leq m$ (that is, the levels could in principle reach this forbidden level), take n_k from Eq. (3.47) instead.

6. The (dimensionless) Fermi energy will instead be $\mathcal{E}_{n_k,\kappa_k}$.

7. If $k+1 > m$, the initial steps are unaffected and the Fermi energy is still the one from step 4, as the occupation does not even reach this forbidden level (this is important!).

The results from this procedure are shown in Fig. 3.8 for a convenient[3] thickness of $L = 10\,\text{nm}$. There, for the values of $\sigma(\Gamma)$ we used the exact numerical roots from Fig. 3.2b and not the WKB approximation. This is because the later breaks for small values of Γ for the σ_0 values. Apart from the transition regions expected in the filling, directly related to Fig. 3.7, we obtain other regions separated by two vertical lines, from which we can clearly see that the Fermi energy is discontinuous. These vertical lines correspond to the values of B such that Γ is at a critical point at which a σ, and thus a κ level, starts to become allowed for the particular value of $L = 10\,\text{nm}$ taken. These critical values for the magnetic field of course depend on the value of thickness and thus the location of the vertical lines Fig. 3.8 are just representative for this case.

We then obtain multiple regions. In the IA region the filling is done only on the κ_0 level, so the n levels in $\mathcal{E}_F$ make it increase linearly with n_e. From IA to IIA the filling in κ_1 starts, and so the rate at which $\mathcal{E}_F$ increases is halved according to step 4. At IB, Γ is such that κ_1 is not allowed, so the filling continues at the κ_0 level with the original rate. The same happens at IIB, where the Γ is such that κ_2 is not allowed and so the filling of the n levels maintains its halved rate for the κ_0 and the κ_1 levels. At III the κ_2 level becomes allowed, so the filling of n further reduces according to step 4. This continues for greater values of B, and changes its borders and frequency for different values of L.

The transition between the IA and IIA zones appears discontinuous, but it should in principle be smooth. The appearance of a discontinuity arises from two reasons: First, at the transition the energy of $(\nu_0 - 1, \kappa_0)$ is not exactly equal to the energy of $(0, \kappa_1)$. Second, the location of this zone is not exactly correct, as this is given by Eq. (3.41) and thus is a result from the WKB approximation. The same happens for the transition between IIA and III. The transition between IB and II (A or B), and between IIB and III is another story. As *the rate at which the energy fills changes in a discontinuous way* between these transitions, the Fermi energy **does become discontinuous** between these sectors. For example, for IB the integer n_0 is used to fill the κ_0 level, producing a Fermi energy given by $\mathcal{E}_{n_0,\kappa_0}$, but for IIA and IIB the κ_1

---

[3]For illustrative purposes it is convenient to use small values of L, as bigger values produce many more regions to appear in Fig. 3.8, cramping up the plot. On the other side, values of L smaller than $10\,\text{nm}$ are known to break the quantization of θ or the magnetoelectric effect altogether, as very small thicknesses give rise to an hybridization of the TI's edge states [37].

level is also filled, and thus the κ_0 level is filled with $\nu_0 + n_1$ levels instead, producing a Fermi energy given by $\mathcal{E}_{\nu_0 + n_1, \kappa_0}$, where n_0 is not equal to $\nu_0 + n_1$ so the energies are different, which results in a discontinuity in this variable.

This discontinuity is an important result which will reappear in many of our calculations. It is a consequence of the discontinuous appearance of new σ solutions for distinct values of Γ. From this discussion we can see that, for this transition to appear, we need two factors:

1. A new $\sigma(\Gamma)$ solution needs to appear discontinuously.

2. The occupation number must be such that the new κ level is able to be filled.

3.3.4 Dispersion states

In general, dispersion states will appear when the occupation is big enough such that $\mathcal{E}_F > 0$. As seen by Fig. 3.8, this does happens frequently for the parameters taken. These dispersion states will correspond to taking $\kappa \longrightarrow \pm ik$ in the energies and wave functions. Physically, as these states are not bound to the plate, they will wander off it. Thus, if we have $\mathcal{E}_F > 0$, we expect the positive energy bound states to decay into dispersion states and escape the system. This is undesired for our purposes as this condition is exactly what we need to obtain discontinuities of the macroscopic variables (such as the Fermi energy of the last section). The reason for this is that, when a new κ_m allowed state appears, its energy is approximately zero (as σ is small). As stated in the last section, for the discontinuities to arise we need an occupation number big enough such that this new state can be filled. Thus, we must necessarily have $\mathcal{E}_F > 0$ if we want to study these discontinuities.

We can come around this problem by embedding the system in a box with a gas of the electrons. This is in fact what is usually done in most of the thermodynamic treatments: Take a finite volume V of the system by surrounding it with an impenetrable box, such that the system is closed. In our context we do that by placing an infinite potential at $z < -L_z/2$ and at $z > L_z/2$ and assuming that $L_z \gg L$ so that our bound solutions and energies are not affected by this potential. The extra gas of electrons will maintain the dispersion states occupied, and thus preclude the positive energy bound states from decaying. The presence of this gas will nonetheless modify the electronic properties studied later, but these modifications will be ignored as the free electron gas is a very basic and well known system.

In conclusion, from now on when we talk about positive Fermi energy we assume that the system is in such finite volume set-up, but nevertheless ignore the modifications induced by the presence of the free electron gas. When we talk about the number of particles N, we will still refer solely to the bound states, ignoring the number of particles in the dispersion states. Finally, we assume that the system is in thermodynamic equilibrium, such that the Fermi energy in both systems is equal. Although this implies that there will be an interchange of particles between bound and dispersion states when a new κ level appears (the Fermi Energy changes, just like in Fig. 3.8), we will ignore this phenomenon for simplicity, but therefore expect that our results for the discontinuities of the macroscopic variables will not be exact.

Nevertheless, the important factor is that the discontinuities will still be present, as this interchange will also discontinuously change the corresponding macroscopic variables of the electron gas when changing it's particle number. The exact contribution of this phenomenon is left as a possible direction for future research.
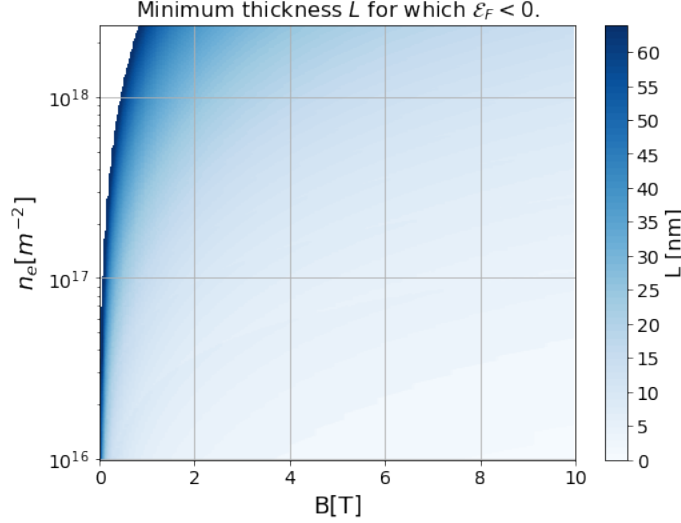
Figure 3.9: Minimum thickness L for which $\mathcal{E}_F < 0$.

Finally, and for completeness, we include a plot of the minimum thickness L for which $\mathcal{E}_F < 0$ and thus no dispersion states exist. For thicknesses greater than those it is not necessary to enclose the system in a box with an electron gas, but also won't present discontinuities in the macroscopic variables. On the other side, the smaller ones will be the ones fit for the discontinuities to arise (provided we have our finite box set-up). This plot is shown in Fig. 3.9.

3.4 Normalization condition

We explicitly write the normalization condition, as it will be needed in the future. It is convenient to define the functions

$$A(\xi) = C \, \mathrm{Ai}(\xi) + D \, \mathrm{Bi}(\xi), \tag{3.53}$$

and

$$B(\xi) = C^* \, \mathrm{Ai}(\xi) + D^* \, \mathrm{Bi}(\xi). \tag{3.54}$$

These are not to be confused with the constants A and B of the amplitudes of the wave functions, nor with the original Airy functions $\mathrm{Ai}(\xi)$ and $\mathrm{Bi}(\xi)$. These general linear combinations of Airy functions have a closed form for various useful integrals (see Appendix C) and will be used throughout this work.

By the boundary conditions (3.13a), (3.13b), (3.14a) and (3.14b), the functions $A(\xi)$ and $B(\xi)$ satisfy

$$A(\sigma^2) = \frac{1}{\sigma} A'(\sigma^2) = A \tag{3.55}$$

and

$$A(\tau) = \frac{-1}{\sigma} A'(\tau) = B e^{-w}. \tag{3.56}$$

The expressions are analogous for $B(\xi) = A^*(\xi)$. In general, we will express the constants A and B in terms of $A(\xi)$ and $B(\xi)$ by means of these equations, for it is more practical.

Thus, the norm of the wave function is

$$\langle \Psi | \Psi \rangle = \int \mathrm{d}y \int_{-\infty}^{\infty} \phi_n \left(x + k_y l_B^2 \right)^2 \mathrm{d}x \left[|A|^2 \int_{-\infty}^{0} e^{2\kappa z} \, \mathrm{d}z \right.$$
$$\left. + \int_{0}^{L} A(\xi) B(\xi) \, \mathrm{d}z + |B|^2 \int_{L}^{\infty} e^{-2\kappa z} \, \mathrm{d}z \right]. \tag{3.57}$$

As usual, the divergent integral in y is regularized by means of a finite length L_y. The Hermite functions are already normalized. With this, and using the relations (3.55), (3.56) and (C.6), we get the normalization condition

$$\langle \Psi | \Psi \rangle = L_y \ell_{\tilde{E}} \left[\frac{1}{2\sigma} A(\sigma^2) B(\sigma^2) + \left(\frac{1}{2\sigma} + \Gamma \right) A(\tau) B(\tau) \right] = 1, \tag{3.58}$$

which puts the final constraints on the constants of the wave function. Nonetheless, we wont solve for them until we need them later in chapter 5.

3.4.1 Orthogonality

Having obtained the normalization condition, in this section, the non-trivial orthogonality relation

$$\left\langle \Psi^{(0)}_{n',k_y,\kappa'} \middle| \Psi^{(0)}_{n,k_y,\kappa} \right\rangle = \delta_{n,n'} \delta_{\kappa,\kappa'} \tag{3.59}$$

will be explicitly derived. The y part is ignored, as before. The x part is the well known orthogonal Hermite function. It is sufficient to prove the non-trivial relation in the z part. Thus, we are to prove that

$$P_{\kappa,\kappa'} \equiv A'^* A \int_{-\infty}^{0} e^{(\kappa+\kappa')z} \, \mathrm{d}z + \int_{0}^{L} A(\xi) B(\xi') \, \mathrm{d}z + B'^* B \int_{L}^{\infty} e^{-(\kappa+\kappa')z} \, \mathrm{d}z \tag{3.60}$$

is zero for $\kappa \neq \kappa'$.

Making the proper change of variables, the second integral ends up proportional to (C.7). Identifying the constants A and B with the functions $A(\xi)$ and $B(\xi)$ by means of (3.55) and (3.56), then

$$P_{\kappa,\kappa'} = \ell_{\tilde{E}} \left[A(\sigma^2) B(\sigma'^2) \frac{1}{\sigma + \sigma'} + I_1 \Big|_{\sigma^2}^{\sigma^2+\Gamma} + A(\tau) B(\tau) \frac{1}{\sigma + \sigma'} \right]. \tag{3.61}$$

Substituting I_1 and imposing the boundary conditions, we are left with

$$I_1 \Big|_{\sigma^2}^{\sigma^2+\Gamma} = -\frac{1}{\sigma + \sigma'} [A(\tau) B(\tau') + A(\sigma^2) B(\sigma'^2)] \tag{3.62}$$

which cancels the other terms of (3.60). Thus,

$$P_{\kappa,\kappa'} = 0 \tag{3.63}$$

for $\kappa \neq \kappa'$. This proves the orthogonality of the solutions.

4 Magnetization in TI

Take the bound states in a finite TI plate with an external magnetic field B analyzed in chapter 3. For this chapter, it is useful to work better with the H field. We have an induced electric field $\tilde{E} = -\alpha c B$ coming from the magnetoelectric effect of the effective theory. At first instance, there is no magnetization and the H field is

$$H = B/\mu_0. \tag{4.1}$$

With this consideration, we will arrive in this chapter that nevertheless, the nature of the bound-state system does induce a magnetization. By the formal definition of the magnetization, we must work with the H field nonetheless. And so, we could not take the magnetization term in the H field before calculating it. In some way, we could think of this as a first order correction.

In this approximation, the cyclotron energy is

$$\omega_B = \frac{eB}{m} \approx \frac{e\mu_0 H}{m}. \tag{4.2}$$

The expression of σ in Eq. (3.9) allows us to re-express the energies of Eq. (3.12) as

$$\mathcal{E}_{n,k} = -\frac{\hbar^2}{2m\ell_{\tilde{E}}^2}\sigma_k^2(\Gamma) + \hbar\omega_B(n + 1/2), \quad n = 0, 1, ..., \quad k = 0, 1, ..., \tag{4.3}$$

where $\sigma_k(\Gamma)$ is the number k band of Fig. 3.2b, which is a function of Γ. $k = 0$ is the upper band, and the level with the lowest energy (that is, the ground state).

As before, for simplicity we completely ignore spin in the following calculations. The results with spin taken into account are presented in Appendix B.

4.1 Thin-plate magnetization

For $|\Gamma| < |\Gamma_c|$ of Eq. (3.16), all of the electrons can only occupy the ground state in κ, no matter the temperature, for this is the only allowed energy. They still respect the Pauli exclusion principle, as there is an infinite number of Landau levels (n) to occupy.

In this case, for a constant volume (constant L), we have a system given by the Landau levels plus a constant dependent on the H field. That is, we have

$$\epsilon_n \equiv \mathcal{E}_{n,0} = -\mathcal{E}_0(H) + \hbar\omega_B(n + 1/2), \tag{4.4}$$

with

$$\mathcal{E}_0(H) = \frac{\hbar^2}{2m\ell_{\tilde{E}}^2}\sigma_0^2(\Gamma),\tag{4.5}$$

where

$$\tilde{E} \approx -\sqrt{\frac{\mu_0}{\epsilon_0}}\alpha H.\tag{4.6}$$

This induces a magnetization identical to the well known Landau magnetization [38,39] with the addition of a correction given by $\mathcal{E}_0(H)$. This treatment is thus very similar to the computation of the Landau magnetization with some corrections[1]. We take then the partition function with the Fermi-Dirac statistics [39]

$$\ln Q = g\sum_{n=0}^{\infty}\ln[1 + e^{\beta(\mu-\epsilon_n)}],\tag{4.7}$$

where $\beta = 1/k_BT$ and g is the degeneracy of each Landau level, which was calculated previously in section 1.2.1. That is,

$$g = \frac{V^{2/3}}{2\pi\ell_B^2}\tag{4.8}$$

with ℓ_B the magnetic length. This is related to the $2D$ free (spinless) electron's gas degeneracy

$$g_0 = \frac{mV^{2/3}}{2\pi\hbar^2}\tag{4.9}$$

by $g = g_0\hbar\omega_B$. Furthermore, because the energies are of the form $\epsilon_n = \hbar\omega_B(n+1/2) - \mathcal{E}_0(H)$, then $\Delta\epsilon_n = \hbar\omega_B \equiv \Delta x$.

Defining

$$S(\epsilon) \equiv \ln[1 + e^{\beta\epsilon}],\tag{4.10}$$

and

$$\mu_{\mathcal{E}} \equiv \mu - \frac{1}{2}\hbar\omega_B + \mathcal{E}_0(H),\tag{4.11}$$

then

$$\ln Q = g_0\Delta x\sum_{n=0}^{\infty}S(\mu_{\mathcal{E}} - n\hbar\omega_B).\tag{4.12}$$

Thus, for $\Delta x \ll k_bT$, we can use the Euler-Maclaurin formula [40]

$$\Delta x\sum_{n=0}^{\infty}f(a_n) \approx \int_{a_0}^{\infty}f(x)\,\mathrm{d}x + \frac{\Delta x}{2}[f(a_\infty) + f(a_0)] + \frac{(\Delta x)^2}{12}[f'(a_\infty) - f'(a_0)] + O(\Delta x)^4.\tag{4.13}$$

---

[1]There are also some peculiarities, as this is an electron gas bounded into a 2D system, while the usual Landau magnetization is given for a 3D electron gas system [38,39]

In the case of S we assume that $\hbar\omega_B << k_B T$. That is, H is sufficiently small. Now, all of the terms with a_∞ are zero. Taking into account that $a_n = \mu_\mathcal{E} - n\hbar\omega_B$ decreases with n, some changes of sign are made. Thus,

$$\ln Q = g_0 \left[\int_{-\infty}^{\mu_\mathcal{E}} S(\epsilon)\, d\epsilon + \frac{\hbar\omega_B}{2} S(\mu_\mathcal{E}) + \frac{(\hbar\omega_B)^2}{12} S'(\mu_\mathcal{E}) + O(H^4) \right] \qquad (4.14)$$

Expanding all of the terms as a Taylor series around $\mu = \mu_\mathcal{E} + \frac{1}{2}\hbar\omega_B - \mathcal{E}_0(H)$, (which is valid for $|\frac{1}{2}\hbar\omega_B - \mathcal{E}_0(H)| \ll k_B T$), and leaving everything in terms of $S(\mu)$, we then have

$$\ln Q = g_0 \left[\int_{-\infty}^{\mu} S(\epsilon)\, d\epsilon + \mathcal{E}_0(H)S(\mu) - \frac{(\hbar\omega_B)^2}{24} S'(\mu) + O(H^3) \right]. \qquad (4.15)$$

We are allowed to take $\mathcal{E}_0(H)$ as small as $\hbar\omega_B$ because we are in the $\Gamma \longrightarrow 0$ limit, where we can take $\sigma_0(\Gamma)$ as arbitrarily small. We have ignored some terms of $\mathcal{E}_0(H)$ by generally assuming that its behaviour is like

$$\mathcal{E}_0(H) \sim H^p, \quad 2 \leq p < 3. \qquad (4.16)$$

Were it the case that $p = 3$ or more, then this correction would be of the order of all of the H^3 terms that we ignored. If we had p less than 2, then higher order terms in $\mathcal{E}_0(H)$ would also have to be taken into account. Fortunately, in our case where $\Gamma \longrightarrow 0$, we have that the order is exactly $p = 2$ and thus this result also applies here.

On the other hand, the partition function of the free (2D) system is approximately

$$\ln Q(H = 0) \approx g_0 \int_0^\infty \ln[1 + e^{\beta(\mu - \epsilon)}]\, d\epsilon = \int_{-\infty}^{\mu} g_0 S(\epsilon)\, d\epsilon \qquad (4.17)$$

where $S(\epsilon)$ is the function of Eq. (4.10). Thus, we have that for our partition function

$$\ln Q \approx \left[1 + \mathcal{E}_0(H)\frac{\partial}{\partial \mu} - \frac{(\hbar\omega_B)^2}{24}\frac{\partial^2}{\partial \mu^2} + O(H^3) \right] \ln Q(H = 0). \qquad (4.18)$$

Taking the Grand potential [41] (or Landau potential) $\Omega = -k_B T \ln Q$, with $F = \Omega + \mu N$ for N (number of particles) constant, for which $\frac{\partial F}{\partial \mu} = 0$, then

$$\Omega(T, V, \mu, H) \approx \left[1 + \mathcal{E}_0(H)\frac{\partial}{\partial \mu} - \frac{(\hbar\omega_B)^2}{24}\frac{\partial^2}{\partial \mu^2} + O(H^3) \right] \Omega(T, V, \mu, H = 0), \quad (4.19)$$

where $\Omega_0 = \Omega(H = 0)$. At low temperatures $\mu \approx \mathcal{E}_F$ and $S'(\mu - \mathcal{E}) \approx \beta h(\mathcal{E}_F - \mathcal{E})$, where

$$h(\epsilon) = \begin{cases} 1, & \epsilon > 0, \\ 0, & \epsilon < 0, \end{cases} \qquad (4.20)$$

is the Heaviside step function. Therefore, using Eq. (4.17), we obtain that

$$\frac{\partial \Omega_0}{\partial \mu} \approx -\frac{1}{\beta}\frac{\partial}{\partial \mu}\int_0^\infty g_0(\varepsilon)S(\mu - \epsilon)\, d\epsilon = -\int_0^{\mathcal{E}_F} g_0(\mathcal{E})\, d\mathcal{E} = -N. \qquad (4.21)$$

where N is the particle number. Furthermore,

$$\frac{\partial^2 \Omega_0}{\partial \mu^2} \approx -g_0(\mathcal{E}_F) = -g_0. \tag{4.22}$$

The density of states generally depends on the energy, but in the free 2D electron gas case it is constant. The magnetization (in SI) is defined as [38, 41]

$$M \equiv -\frac{1}{\mu_0 V}\frac{\partial F}{\partial H} = -\frac{1}{\mu_0 V}\frac{\partial \Omega}{\partial H} \tag{4.23}$$

for constant N. So

$$M = \frac{1}{\mu_0 V}\frac{\partial \mathcal{E}_0(H)}{\partial H}N - \frac{\mu_0}{3V}\mu_B^2 H g_0. \tag{4.24}$$

We used that $\hbar \omega_B = 2\mu_B \mu_0 H$, where $\mu_B = e\hbar/(2m)$ is the Bohr magneton. The second term is similar to the Landau magnetization, which is produced from the energy levels $\hbar \omega_B(n+1/2)$. Nonetheless, it is not exactly the same as the one obtained usually in an 3D electron gas with a constant magnetic field. This is because in 3D, the gas is allowed to take the continuum of wave vectors in z between $-k_F$ and k_F (where k_F is the Fermi wave vector), while here the bound states have only one value allowed. So, we have a susceptibility

$$\chi = \frac{\partial M}{\partial H}, \tag{4.25}$$

that results in

$$\chi_{\text{tot}} = \chi_{\tilde{\theta}} + \tilde{\chi}_{\text{Landau}}. \tag{4.26}$$

The magneto-electric contribution is

$$\chi_{\tilde{\theta}} = \frac{N}{\mu_0 V}\frac{\partial^2 \mathcal{E}_0(H)}{\partial H^2} = \frac{n_e^{3D}}{\mu_0}\frac{\partial^2 \mathcal{E}_0(H)}{\partial H^2}, \tag{4.27}$$

with $n_e^{3D} = N/V$ the electronic volume density.

To relate our Landau-like contribution to the original one, we relate the density of states of the 2D free electron gas (4.9) with the density of states of the 3D free (spinless) electron gas $g_{3D}(\mathcal{E}_F) = \frac{mk_F}{2\pi^2\hbar^2}$. That is,

$$\frac{g_0(\mathcal{E}_F)}{V} = \frac{m}{\pi\hbar^2 L} = \frac{\pi}{Lk_F}g_{3D}(\mathcal{E}_F). \tag{4.28}$$

So, in comparison with the Landau diamagnetism of a 3D electron gas [41] (in SI)

$$\chi_{\text{Landau}} = -\frac{\mu_0}{3}\mu_B^2 g_{3D}(\mathcal{E}_F), \tag{4.29}$$

we obtain that

$$\boxed{\tilde{\chi}_{\text{Landau}} = -\frac{m\mu_0\mu_B^2}{6\pi\hbar^2 L} = \frac{\pi}{Lk_F}\chi_{\text{Landau}}}. \tag{4.30}$$

The extra factor of this susceptibility corresponds to the difference between taking only localized states with one allowed value of k_z, and of having an unlocalized gas of electrons with free k_z. That is, if we apply the integration

$$\int_{-k_F}^{k_F} \frac{L \, \mathrm{d}k_z}{2\pi},$$

to Eq. (4.30), we recover the Landau diamagnetism.

Now we analyze the $\chi_{\tilde{\theta}}$ term. If we take $\Gamma \longrightarrow 0$ such that, following the approximation (3.17), we have $|\sigma_0(\Gamma)| \approx \frac{1}{4}\Gamma^2$,

$$\mathcal{E}_0(H) \approx \frac{m}{8\hbar^2} e^2 E^2 L^4 \approx \frac{m\mu_0}{8\hbar^2\epsilon_0} e^2 \alpha^2 H^2 L^4. \tag{4.31}$$

This is of order H^2, as desired, so the previous hypothesis taken holds. With this,

$$\boxed{\chi_{\tilde{\theta}} = \frac{m}{4\hbar^2\epsilon_0} e^2 L^4 \alpha^2 n_e^{3D}}, \tag{4.32}$$

which results in a paramagnetic term.

4.2 Phase transitions

We saw in section 3.2 that there are special values of Γ for which a new σ allowed band appears. As discussed in section 3.3.3, these appearances affect the filling of the states, and thus can produce discontinuities of macroscopic quantities such as the Fermi energy when varying the magnetic field at these special points and as long as the electronic density is large enough. Furthermore, this will clearly affect the partition function of the material, as it will discontinuously change from one value of Γ to another, potentially producing a phase transition. In this section we analyze this effect by means of the magnetization as an order parameter.

We first study the simplest of these cases, which is the appearance of the $\sigma_1(\Gamma)$ band at $|\Gamma| = \Gamma_c$ of Eq. (3.16). Thus, for $|\Gamma| < \Gamma_c$, only the base state κ_0 is allowed, but for $|\Gamma| > \Gamma_c$, the κ_1 starts to be allowed. In the last section we generalize the results for an arbitrary band at a critical point.

4.2.1 Before the critical point

We start with the case $|\Gamma| < \Gamma_c$, where only the $\sigma_0(\Gamma)$ band is present. For this case the partition function is, like in the last section,

$$\ln Q^- \equiv \ln Q(|\Gamma| < \Gamma_c) = g \sum_{n=0}^{\infty} \ln[1 + e^{\beta(\mu - \epsilon_{n,0})}], \tag{4.33}$$

with energies

$$\epsilon_{n,0} \equiv -\mathcal{E}_0(H) + \hbar\omega_B(n + 1/2), \quad \mathcal{E}_0(H) = \frac{\hbar^2}{2m\ell_{\tilde{E}}^2}\sigma_0^2(\Gamma). \tag{4.34}$$

We once again express it as

$$\ln Q^- = g_0 \Delta x \sum_{n=0}^{\infty} S(\mu_{\mathcal{E}_0} - n\hbar\omega_B), \quad \mu_{\mathcal{E}_0} \equiv \mu - \frac{1}{2}\hbar\omega_B + \mathcal{E}_0(H), \tag{4.35}$$

and make use of the Euler-Maclaurin formula so that

$$\ln Q^- = g_0 \left[\int_{-\infty}^{\mu_{\mathcal{E}_0}} S(\epsilon) \, d\epsilon + \frac{\hbar\omega_B}{2} S(\mu_{\mathcal{E}_0}) + \frac{(\hbar\omega_B)^2}{12} S'(\mu_{\mathcal{E}_0}) + O(H^4) \right]. \tag{4.36}$$

Following the same procedure as before, we would next expand this expression as a Taylor series around $\mu = \mu_{\mathcal{E}_0} + \frac{1}{2}\hbar\omega_B - \mathcal{E}_0(H)$. Nevertheless, we can no longer assume that $|\frac{1}{2}\hbar\omega_B - \mathcal{E}_0(H)| \ll k_B T$, as $\mathcal{E}_0(H)$ is no longer small in the regime $\Gamma \approx \Gamma_c$. In fact, as we saw in section 3.3.2, this energy is much greater than the energy of a normal Landau level $\hbar\omega_B$. The most we can do is expand around $\mu + \mathcal{E}_0(H)$. Here we only need that $\frac{1}{2}\hbar\omega_B \ll k_B T$.

Furthermore, as $|\Gamma| > 1$, the behaviour of $\sigma_0(\Gamma)$ is best described by the WKB approximation (3.18). That is,

$$|\sigma_0(\Gamma)| \approx \sqrt{|\Gamma| - a_0}, \quad a_0 = (3\pi/4)^{2/3}. \tag{4.37}$$

And thus

$$\mathcal{E}_0(H) \approx \frac{\hbar^2}{2m\ell_{\tilde{E}}^2} \left(L/|\ell_{\tilde{E}}| - a_0 \right) = e|\tilde{E}|L - a_0 \left(\frac{\hbar^2 e^2 \tilde{E}^2}{2m} \right)^{1/3}. \tag{4.38}$$

This contains terms of order H and $H^{2/3}$. Either way, this compels us to take into account higher order powers of $\mathcal{E}_0(H)$ (which still appear in this expansion). These will correspond to third order derivatives of Ω_0 with respect to the chemical potential. But, from Eq. (4.22), as g_0 is constant with respect to the energy/chemical potential, then

$$\frac{\partial^3}{\partial\mu^3} \Omega_0 \approx \frac{\partial}{\partial\mu} g_0 = 0 \tag{4.39}$$

as well as all of the higher-order derivatives.

Taking all of this into account, the Taylor expansion of (4.36) yields

$$\ln Q^- \approx g_0 \left[\int_{-\infty}^{\mu + \mathcal{E}_0(H)} S(\epsilon) \, d\epsilon - \frac{(\hbar\omega_B)^2}{24} S'[\mu + \mathcal{E}_0(H)] + O(H^3) \right]. \tag{4.40}$$

Ignoring once again the third order derivatives of the potential,

$$\frac{\partial}{\partial H} \ln Q^- \approx g_0 \frac{\partial \mathcal{E}_0(H)}{\partial H} S[\mu + \mathcal{E}_0(H)] - \frac{1}{24} g_0 \left[\frac{\partial}{\partial H} (\hbar\omega_B)^2 \right] S'[\mu + \mathcal{E}_0(H)] \tag{4.41}$$

and

$$\frac{\partial^2}{\partial H^2} \ln Q^- \approx g_0 \frac{\partial^2 \mathcal{E}_0(H)}{\partial H^2} S[\mu + \mathcal{E}_0(H)]$$
$$+ g_0 \left(\left[\frac{\partial \mathcal{E}_0(H)}{\partial H} \right]^2 - \frac{1}{24} \left[\frac{\partial^2}{\partial H^2} (\hbar\omega_B)^2 \right] \right) S'[\mu + \mathcal{E}_0(H)]. \tag{4.42}$$

In terms of the Grand potential $\Omega^- = -k_B T \ln Q^-$,

$$\frac{\partial}{\partial H}\Omega^-(T, V, \mu, H) \approx \left[\frac{\partial\mathcal{E}_0(H)}{\partial H}\frac{\partial}{\partial\mu} - \frac{1}{24}\left[\frac{\partial}{\partial H}(\hbar\omega_B)^2\right]\frac{\partial^2}{\partial\mu^2}\right]\Omega_0[\mu + \mathcal{E}_0(H)], \quad (4.43)$$

and

$$\frac{\partial^2}{\partial H^2}\Omega^-(T, V, \mu, H) \approx \left[\frac{\partial^2\mathcal{E}_0(H)}{\partial H^2}\frac{\partial}{\partial\mu} + \left[\frac{\partial\mathcal{E}_0(H)}{\partial H}\right]^2\frac{\partial^2}{\partial\mu^2}\right.$$
$$\left. - \frac{1}{24}\left[\frac{\partial^2}{\partial H^2}(\hbar\omega_B)^2\right]\frac{\partial^2}{\partial\mu^2}\right]\Omega_0[\mu + \mathcal{E}_0(H)].$$
$$(4.44)$$

Note how now we have taken $\Omega_0[\mu+\mathcal{E}_0(H)] \equiv \Omega(T, V, \mu+\mathcal{E}_0(H), H = 0)$ with the non-negligible energy $\mathcal{E}_0(H)$ added to the chemical potential. This has a very important consequence. Namely,

$$\frac{\partial\Omega_0[\mu + \mathcal{E}_0(H)]}{\partial\mu} = -\int_0^{\mathcal{E}_F+\mathcal{E}_0(H)} g_0(\mathcal{E})\,\mathrm{d}\mathcal{E} = -\int_{-\mathcal{E}_0(H)}^{\mathcal{E}_F} g_0(\mathcal{E})\,\mathrm{d}\mathcal{E} = -N. \quad (4.45)$$

Thus, for a given chemical potential, the number of particles given here is now increased. This should be expected, as with the base state energy reduction given by $-\mathcal{E}_0(H)$, the number of Landau levels necessary to reach a given energy increases. Still, for $|\Gamma| < \Gamma_c$, Eq. (4.45) recovers the total number of particles N, as κ_0 is the only allowed value in κ.

On the other hand, the second order derivative

$$\frac{\partial^2\Omega_0}{\partial\mu^2}[\mu + \mathcal{E}_0(H)] = -g_0 \quad (4.46)$$

still recovers the density of states of the free 2D electron gas.

In total, the magnetization and susceptibility for $|\Gamma| < \Gamma_c$ are

$$M^- = M_{\tilde{\theta}}^- + H\tilde{\chi}_{\text{Landau}}, \quad \chi^- = \chi_{\tilde{\theta}}^- + \tilde{\chi}_{\text{Landau}}, \quad (4.47)$$

where

$$M_{\tilde{\theta}}^- = \frac{1}{\mu_0 V}\frac{\partial\mathcal{E}_0(H)}{\partial H}N, \quad (4.48)$$

$$\chi_{\tilde{\theta}}^- = \frac{1}{\mu_0 V}\frac{\partial^2\mathcal{E}_0(H)}{\partial H^2}N + \frac{1}{\mu_0 V}\left[\frac{\partial\mathcal{E}_0(H)}{\partial H}\right]^2 g_0 \quad (4.49)$$

and $\tilde{\chi}_{\text{Landau}}$ is given by Eq. (4.30). Notice how to obtain $\chi_{\tilde{\theta}}^-$ as the derivative with respect of H of $M_{\tilde{\theta}}^-$ we must use the implicit H dependence of N given by Eq. (4.45).

Using the resulting expression of $\mathcal{E}_0(H)$ from the WKB approximation (4.38),

$$\frac{\partial\mathcal{E}_0(H)}{\partial H} = e\sqrt{\frac{\mu_0}{\epsilon_0}}\alpha L - \frac{2}{3}a_0\left(\frac{\hbar^2 e^2\mu_0}{2m\epsilon_0}\alpha^2\right)^{1/3}H^{-1/3}$$
$$= \left(1 - \frac{2}{3}\frac{a_0}{|\Gamma|}\right)e\sqrt{\frac{\mu_0}{\epsilon_0}}\alpha L$$
$$(4.50)$$

and

$$\frac{\partial^2 \mathcal{E}_0(H)}{\partial H^2} = \frac{2}{9} a_0 \left(\frac{\hbar^2 e^2 \mu_0}{2m\epsilon_0} \alpha^2 \right)^{1/3} H^{-4/3}$$
$$= \frac{2}{9} \frac{a_0}{|\Gamma|} \frac{2m}{\hbar^2} \frac{\mu_0}{\epsilon_0} e^2 \alpha^2 L^4$$

(4.51)

In the last steps of these two equations, we used that H can be expressed in terms of $|\Gamma|$ as

$$H = \frac{\hbar^2}{2m} \sqrt{\frac{\epsilon_0}{\mu_0}} \frac{1}{e\alpha} \frac{|\Gamma|^3}{L^3}.$$

(4.52)

Combining those two equations in Eqs. (4.48) and (4.49) we obtain

$$\boxed{M_{\tilde{\theta}}^- = \left(1 - \frac{2}{3} \frac{a_0}{|\Gamma|} \right) ce\alpha L n_e^{3D}}$$

(4.53)

and

$$\boxed{\chi_{\tilde{\theta}}^- = \frac{2m}{\hbar^2 \epsilon_0} e^2 \alpha^2 L \left[\frac{2}{9} \frac{a_0}{\Gamma^4} L^3 n_e^{3D} + \frac{1}{4\pi} \left(1 - \frac{2}{3} \frac{a_0}{|\Gamma|} \right)^2 \right]},$$

(4.54)

which is once again a paramagnetic term[2].

4.2.2 After the critical point

Now we take $|\Gamma| > \Gamma_c$. For this case the new κ_1 level is now also allowed. We must be careful to note the partition function is not the only relevant object that discontinuously changes. If we wish to work at a constant total particle number N, then the chemical potential must also change. This can be seen in Fig. 3.8 by looking at how the Fermi energy discontinuously diminishes from the IB to the IIA and IIB regions. Nevertheless, this only happens when the occupation number is such that the κ_1 level can be reached. That is, when $\mathcal{E}_F > 0$ in our context. Thus,

$$\ln Q^+ \equiv \ln Q(|\Gamma| > \Gamma_c) = g \sum_{n=0}^{\infty} \left[\ln[1 + e^{\beta(\mu' - \epsilon_{n,0})}] + \ln[1 + e^{\beta(\mu' - \epsilon_{n,1})}] \right], \quad (4.55)$$

where

$$\mu' \approx \begin{cases} \mu - n_1 \hbar \omega_B, & \mathcal{E}_F > 0, \\ \mu, & \mathcal{E}_F < 0, \end{cases}$$

(4.56)

where n_1 is the remaining amount of n Levels filled in κ_1 **after this level appears** (consistent within our notation in section 3.3.2). A way to convince oneself that the change in the chemical potential (Fermi energy) is given by this expression is by looking at the filling visualization of Fig.3.6. Close to the critical point the zeroth energy is the first red line where the κ_1 level is reached. Thus, when only κ_0 is allowed,

---

[2]Substituting the numerical values of $a_0 = (3\pi/4)^{2/3}$ and $|\Gamma| \approx \Gamma_c = 2.95$ we obtain that $1 - 2a_0/(3|\Gamma|) \approx 0.6$ so that the magnetization is positive, *i.e.* in the direction of the H field.

but the Fermi energy is positive, half of the Landau levels above the first red line are passed onto the κ_1 level. This amount of Landau levels is in fact the n_1 constant from Eq. (3.47). Note that in both cases the chemical potential maintains its original sign. The energy $\epsilon_{n,0}$ is the same one as in Eq. (4.34) and the new energy is given similarly by

$$\epsilon_{n,1} \equiv -\mathcal{E}_1(H) + \omega_B \hbar (n + 1/2), \quad \mathcal{E}_1(H) = \frac{\hbar^2}{2m\ell_{\tilde{E}}^2}\sigma_1^2(\Gamma). \tag{4.57}$$

Once again we express the partition function as

$$\ln Q^+ = g_0 \Delta x \sum_{n=0}^{\infty} \left[S(\mu'_{\mathcal{E}_0} - n\hbar\omega_B) + S(\mu'_{\mathcal{E}_1} - n\hbar\omega_B) \right], \tag{4.58}$$

with

$$\mu'_{\mathcal{E}_0} \equiv \mu' - \frac{1}{2}\hbar\omega_B + \mathcal{E}_0(H), \quad \mu'_{\mathcal{E}_1} \equiv \mu' - \frac{1}{2}\hbar\omega_B + \mathcal{E}_1(H). \tag{4.59}$$

Using the Euler-Maclaurin formula and performing the same Taylor expansion as in Eq. (4.40) for the first term, and as in Eq. (4.18) for the second term ($\mathcal{E}_1(H) \approx 0$ for $|\Gamma| \gtrsim \Gamma_c$), then

$$\ln Q^+ \approx g_0 \left[\int_{-\infty}^{\mu'+\mathcal{E}_0(H)} S(\epsilon)\,d\epsilon - \frac{(\hbar\omega_B)^2}{24}S'[\mu' + \mathcal{E}_0(H)] + O(H^3) \right]$$
$$+ g_0 \left[\int_{-\infty}^{\mu'} S(\epsilon)\,d\epsilon + \mathcal{E}_1(H)S(\mu') - \frac{(\hbar\omega_B)^2}{24}S'(\mu') + O(H^3) \right]. \tag{4.60}$$

Now, as $\nu_1 \sim \nu_{tot} \sim 1/B$ and $\hbar\omega_B \sim B$, then the modified chemical potential μ' does not depend on H, and thus is not affected by the derivatives with respect to H. Therefore, the result from differentiating and expressing everything in terms of the Grand potential $\Omega^+ = -k_B T \ln Q^+$ is

$$\frac{\partial}{\partial H}\Omega^+(T, V, \mu', H) \approx \left[\frac{\partial\mathcal{E}_0(H)}{\partial H}\frac{\partial}{\partial\mu'} - \frac{1}{24}\left[\frac{\partial}{\partial H}(\hbar\omega_B)^2 \right]\frac{\partial^2}{\partial\mu'^2} \right]\Omega_0[\mu' + \mathcal{E}_0(H)]$$
$$+ \left[\frac{\partial\mathcal{E}_1(H)}{\partial H}\frac{\partial}{\partial\mu'} - \frac{1}{24}\left[\frac{\partial}{\partial H}(\hbar\omega_B)^2 \right]\frac{\partial^2}{\partial\mu'^2} \right]\Omega_0[\mu'], \tag{4.61}$$

and

$$\frac{\partial^2}{\partial H^2}\Omega^+(T, V, \mu', H) \approx \left[\frac{\partial^2\mathcal{E}_0(H)}{\partial H^2}\frac{\partial}{\partial\mu'} + \left[\frac{\partial\mathcal{E}_0(H)}{\partial H} \right]^2\frac{\partial^2}{\partial\mu'^2} \right.$$
$$\left. - \frac{1}{24}\left[\frac{\partial^2}{\partial H^2}(\hbar\omega_B)^2 \right]\frac{\partial^2}{\partial\mu'^2} \right]\Omega_0[\mu' + \mathcal{E}_0(H)]$$
$$+ \left[\frac{\partial^2\mathcal{E}_1(H)}{\partial H^2}\frac{\partial}{\partial\mu'} - \frac{1}{24}\left[\frac{\partial^2}{\partial H^2}(\hbar\omega_B)^2 \right]\frac{\partial^2}{\partial\mu'^2} \right]\Omega_0[\mu']. \tag{4.62}$$

Now, by construction,

$$\frac{\partial\Omega_0}{\partial\mu'}[\mu' + \mathcal{E}_0(H)] = -\int_{-\mathcal{E}_0(H)}^{\mathcal{E}_F - n_1\hbar\omega_B} g_0(\mathcal{E})\,d\mathcal{E} = -(N - n_1 g), \tag{4.63}$$

and

$$\frac{\partial \Omega_0}{\partial \mu'}[\mu'] = -\int_0^{\mathcal{E}_F - n_1 \hbar \omega_B} g_0(\mathcal{E}) \, \mathrm{d}\mathcal{E} = -n_1 g, \tag{4.64}$$

where we used that $g_0 \hbar \omega_B = g$. For $\mathcal{E}_F > 0$, $n_1 \neq 0$, whereas for $\mathcal{E}_F < 0$, $n_1 = 0$. We also implicitly used that

$$N = (\nu_0 + 2n_1)g, \tag{4.65}$$

where ν_0 are the necessary n levels to go from $\mathcal{E} = -\mathcal{E}_0(H)$ to $\mathcal{E} = -\mathcal{E}_1(H) \approx 0$.

For the second derivatives,

$$\frac{\partial^2 \Omega_0}{\partial \mu'^2}[\mu' + \mathcal{E}_0(H)] = -g_0, \tag{4.66}$$

and

$$\frac{\partial^2 \Omega_0}{\partial \mu'^2}[\mu'] = -g_0 h(\mathcal{E}_F), \tag{4.67}$$

where $h(x)$ is the Heaviside function (4.20). This function appears because Eq. (4.64) is zero for $\mathcal{E}_F < 0$.

In total, the magnetization and susceptibility for $|\Gamma| > \Gamma_c$ are

$$M^+ = M_{\tilde{\theta}}^+ + H \tilde{\chi}_{\text{Landau}}(1 + h(\mathcal{E}_F)), \quad \chi^+ = \chi_{\tilde{\theta}}^+ + \tilde{\chi}_{\text{Landau}}(1 + h(\mathcal{E}_F)), \tag{4.68}$$

where

$$M_{\tilde{\theta}}^+ = \frac{1}{\mu_0 V} \frac{\partial \mathcal{E}_0(H)}{\partial H}(N - n_1 g) + \frac{1}{\mu_0 V} \frac{\partial \mathcal{E}_1(H)}{\partial H} n_1 g, \tag{4.69}$$

$$\chi_{\tilde{\theta}}^+ = \frac{1}{\mu_0 V} \frac{\partial^2 \mathcal{E}_0(H)}{\partial H^2}(N - n_1 g) + \frac{1}{\mu_0 V} \frac{\partial^2 \mathcal{E}_1(H)}{\partial H^2} n_1 g + \frac{1}{\mu_0 V} \left[\frac{\partial \mathcal{E}_0(H)}{\partial H}\right]^2 g_0, \tag{4.70}$$

and $\tilde{\chi}_{\text{Landau}}$ is given by Eq. (4.30).

For $\mathcal{E}_0(H)$ we once again use the WKB approximation and thus the derivatives given in Eqs. (4.50) and (4.51). For $\mathcal{E}_1(H)$ we cannot do the same, as the WKB approximation results in specially poor results for small values of sigma (that is, near $|\Gamma| = \Gamma_c$). Instead, according to our initial supposition that $|\Gamma| \gtrsim \Gamma_c$ so that $\mathcal{E}_1(H)$ is small, we use a direct linear fit for $\sigma_1(\Gamma)$ around $|\Gamma| \approx \Gamma_c$. Numerically, we obtain that

$$|\sigma_1(\Gamma)| \approx m_1(|\Gamma| - \Gamma_c), \quad m_1 \approx 0.0975, \tag{4.71}$$

for $|\Gamma| \gtrsim \Gamma_c$. With this

$$\mathcal{E}_1(H) \approx \frac{\hbar^2}{2m\ell_{\tilde{E}}^2} m_1^2 \left(L/|\ell_{\tilde{E}}| - \Gamma_c\right)^2, \tag{4.72}$$

and thus

$$\frac{\partial \mathcal{E}_1(H)}{\partial H} = \frac{\hbar^2}{3m\ell_{\tilde{E}}^2} \frac{m_1^2}{H}(|\Gamma| - \Gamma_c)(2|\Gamma| - \Gamma_c) \approx 0 \tag{4.73}$$

and

$$
\frac{\partial^2 \mathcal{E}_1(H)}{\partial H^2} = \frac{\hbar^2}{9m\ell_{\tilde{E}}^2} \frac{m_1^2}{H^2} \left(2|\Gamma|^2 - \Gamma_c^2 \right)
$$

$$
\approx \frac{2}{9} \frac{m_1^2}{\Gamma_c^3} \frac{2m}{\hbar^2} \frac{\mu_0}{\epsilon_0} e^2 \alpha^2 L^4
$$

(4.74)

Thus, Eqs. (4.69) and (4.70) become

$$
\boxed{M_{\tilde{\theta}}^+ = \left(1 - \frac{2}{3} \frac{a_0}{\Gamma_c} \right) ce\alpha L \left(n_e^{3D} - n_1 g/V \right)}
$$

(4.75)

and

$$
\boxed{\chi_{\tilde{\theta}}^+ = \frac{2m}{\hbar^2 \epsilon_0} e^2 \alpha^2 L \left[\frac{2}{9} \frac{L^3}{\Gamma_c^4} \left(a_0(n_e^{3D} - n_1 g/V) + \Gamma_c m_1^2 n_1 g/V \right) + \frac{1}{4\pi} \left(1 - \frac{2}{3} \frac{a_0}{\Gamma_c} \right)^2 \right]}.
$$

(4.76)

Because $n_e^{3D} = N/V$, where $N > n_1 g$, we once again obtain a paramagnetic term.

4.2.3   Order parameter

From Eqs. (4.47), (4.48), (4.68) and (4.69) we see that the magnetization is discontinuous at the transition point $|\Gamma| = \Gamma_c$. The discontinuity is given by

$$
\Delta M \equiv \left(M^+ - M^- \right) \big|_{|\Gamma| = \Gamma_c}
$$

$$
= \left(M_{\tilde{\theta}}^+ - M_{\tilde{\theta}}^- + H \tilde{\chi}_{\text{Landau}} h(\mathcal{E}_F) \right) \big|_{|\Gamma| = \Gamma_c}
$$

(4.77)

$$
= \left[\frac{1}{\mu_0 V} \left(\frac{\partial \mathcal{E}_1(H)}{\partial H} - \frac{\partial \mathcal{E}_0(H)}{\partial H} \right) n_1 g + H \tilde{\chi}_{\text{Landau}} h(\mathcal{E}_F) \right] \bigg|_{|\Gamma| = \Gamma_c}.
$$

If $\mathcal{E}_F < 0$, then $n_1 = 0$ and thus the magnetization (as well as the susceptibility) becomes continuous once again. This is the same thing that happened in the Fermi energy when considering the filling. That is, for $\mathcal{E}_F < 0$ the κ_1 level is not occupied, so its presence doesn't affects the system.

Substituting the derivatives (4.50) and (4.73), as well as the modified Landau susceptibility (4.30), and evaluating H at $|\Gamma| = \Gamma_c$ by means of Eq. (4.52), we explicitly obtain that

$$
\Delta M = -\left(1 - \frac{2}{3} \frac{a_0}{\Gamma_c} \right) ce\alpha L n_1 g/V - \frac{\mu_B \lambdabar}{24\pi\alpha} \frac{\Gamma_c^3}{L^4} h(\mathcal{E}_F),
$$

(4.78)

where we used the reduced Compton wavelength of the electron $\lambdabar = \hbar/mc$. Substituting the value of g in terms of H (and thus in terms of Γ_c), then

$$
\boxed{\Delta M = -\frac{\mu_B}{2\pi} \frac{\Gamma_c^3}{L^3} \left[\left(1 - \frac{2}{3} \frac{a_0}{\Gamma_c} \right) n_1 + \frac{\lambdabar}{12\alpha L} h(\mathcal{E}_F) \right]}.
$$

(4.79)

This corresponds to a discontinuity of a first derivative of the partition function, proper of a phase transition of first order, being the magnetization the order parameter. This phase transition is not related at all with thermal fluctuations, but instead to a discontinuous transition in the energy spectrum of the Hamiltonian. Furthermore, this approximation is valid in the zero temperature limit, and its only dependence on the thermodynamic variables lies in the value of L and of H (defined implicitly by the value of Γ_c). What we have obtained then is a so-called **quantum phase transition of first order** [42].

4.2.4 General case

This phenomenon happens infinitely often as $|\Gamma|$ increases, as more σ_k bands appear, and at a rate given (through the WKB approximation) by $\Delta\Gamma = a_0\left[(2k+3)^{2/3} - (2k+1)^{2/3}\right]$, which becomes smaller at greater values of k.

From Eqs. (4.48) and (4.69) and our knowledge of how the filling is done we can infer the general expression for the magnetization when $m+1$ bands are allowed. That is,

$$M_{\tilde{\theta}}^{(m)} = \frac{1}{\mu_0 V}\frac{\partial \mathcal{E}_0(H)}{\partial H}n_0^{(m)}g + \frac{1}{\mu_0 V}\frac{\partial \mathcal{E}_1(H)}{\partial H}n_1^{(m)}g + ... + \frac{1}{\mu_0 V}\frac{\partial \mathcal{E}_m(H)}{\partial H}n_m^{(m)}g, \quad (4.80)$$

where $N = (\nu_0 + 2\nu_1 + ... + m\nu_{m-1} + (m+1)n_m)g$ such that

$$n_k^{(m)} = \nu_k + \nu_{k+1} + ... + \nu_{m-1} + n_m \quad (4.81)$$

give the total number of n levels occupied in each κ_k level. Each κ level with occupation also contributes with an equal term of the Landau magnetization, just like in Eq. (4.68). Therefore, taking $\mathcal{E}_m(H) \approx 0$, the discontinuity in the magnetization produced by the appearance of a $\sigma_m(\Gamma)$ band at a critical point $|\Gamma| = \Gamma_c^{(m)}$ is

$$\Delta M^{(m)} \equiv \left(M^{(m)} - M^{(m-1)}\right)\big|_{|\Gamma|=\Gamma_c^{(m)}}$$
$$= \left(M_{\tilde{\theta}}^{(m)} - M_{\tilde{\theta}}^{(m-1)} + H\tilde{\chi}_{\text{Landau}}h(\mathcal{E}_F)\right)\big|_{|\Gamma|=\Gamma_c^{(m)}}$$
$$= \left[\frac{1}{\mu_0 V}\left(\frac{\partial \mathcal{E}_m(H)}{\partial H} - \frac{\partial \mathcal{E}_0(H)}{\partial H} - ... - \frac{\partial \mathcal{E}_{m-1}(H)}{\partial H}\right)n_m g \right.$$
$$\left. + H\tilde{\chi}_{\text{Landau}}h(\mathcal{E}_F)\right]\bigg|_{|\Gamma|=\Gamma_c^{(m)}}, \quad (4.82)$$

where once again the derivative of $\mathcal{E}_m(H)$ at the critical point is zero. For the other ones we use the general values $a_k = (3\pi/2)^{2/3}(k+1/2)^{2/3}$ in Eq. (4.50) to finally obtain

$$\boxed{\Delta M^{(m)} = -\frac{\mu_B}{2\pi}\frac{\Gamma_c^{(m)3}}{L^3}\left[\left(m - \frac{2}{3}\frac{1}{\Gamma_c^{(m)}}(a_0 + ... + a_{m-1})\right)n_m + \frac{\lambda}{12\alpha L}h(\mathcal{E}_F)\right].} \quad (4.83)$$

The first term changes only on the numerical factor and is always dependent on the number of occupied Landau levels of the new κ band. The second term remains unchanged, where once again it only counts when there is occupation on this new band.

The change on the magnetization ends up being negative every time, decreasing the magnetization at each critical point. Nevertheless, like in Eqs. (4.53) and (4.75), the magnetization $M_{\tilde{\theta}}$ always increases with L, and thus with $|\Gamma|$. The associated Landau diamagnetism decreases with L, but also its corresponding (negative) increment. Therefore, in general we expect a *see-saw* behaviour of the magnetization, where it gradually increases but suddenly drops at each critical point. As the critical points grow closer, the phase transition eventually becomes immeasurable in accordance to the classical limit.

5 Quantum Hall effect in TI

We consider the system of chapter 3 once again, where an external magnetic field induces an internal electric field that creates bound energy states. Furthermore, we now take an external electric field E in the x direction just as in chapter 1 of the HE. By the modified boundary conditions (2.51) with $\tilde{\theta} = -\alpha$ we now also obtain an induced magnetic field

$$\boxed{\tilde{B} = \alpha \frac{E}{c}}. \tag{5.1}$$

The system described with the electromagnetic fields outside and inside the material is shown in Fig. 5.1.
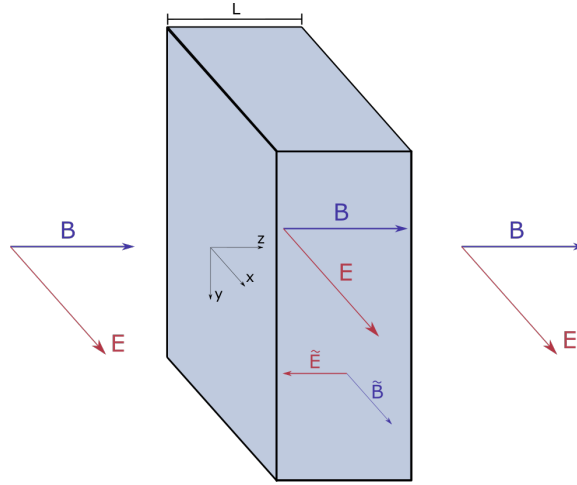
Figure 5.1: Quantum Hall effect system in TI. We have external fields E and B, and induced internal fields $\tilde{E}$ and $\tilde{B}$ such that on the interior the magnetic field is $\mathbf{B} = (\tilde{B}, 0, B)$ and the electric field is $\mathbf{E} = (E, 0, -\tilde{E})$. For clarity, note that E and B are not the same as the magnitude of the fields $|\mathbf{E}|$ and $|\mathbf{B}|$.

The purpose of this chapter is to compute the quantum Hall current produced by the bulk states in the same way as in section 1.2.2 by exploiting the existence of bound states inside the plate, and to obtain the corrections originated from the induced electromagnetic fields $\tilde{E}$ and $\tilde{B}$. Note nonetheless that this is an additional contribution to the one described by the θ-term. The magnetoelectric effect produced by the θ-term is a consequence of the HE present in the **edge states** of the TI [43].

Here, we are studying the HE of the **bulk states** which are effectively bound to the material through the magnetoelectric effect.

Having noted the context in which we are working, we now analyse the wave function solutions of this system. The presence of the induced magnetic field of Eq. (5.1) inside the TI now prevents us from separating the wave-functions such that they can fulfill the boundary conditions at the x, y directions. Furthermore, solving directly for the total Hamiltonian results very troublesome, as the energy spectrum differs from inside and outside the plate. This means that the quantum numbers (n, k_y, κ) cannot be taken as equal both inside and outside, so one needs to expand one set of solutions in terms of the other with the constriction that the expanded parameters are such that the energies are equal in both sides. Doing so solves both the boundary conditions and energy continuity difficulties, but at the cost of expressing the first ones by means of an infinite matrix. Thus, the quantization condition (3.15) becomes an infinite determinant and the wave-functions themselves end up being infinite series of the free eigenfunctions, which results very troublesome when trying to compute the allowed values of σ. Fortunately we can avoid these complications by separating the terms arising from the induced magnetic field $\tilde{B}$ and treating them as a perturbation potential. This naturally recovers both the same energy spectrum and the boundary conditions at the x, y directions. This is also appropriate, as the small α factor lends itself perfectly to be treated as a perturbation parameter. Note nevertheless that we do not take the term from $\tilde{E}$ as a perturbation potential, even when it is also proportional to α, as it is necessary to produce the original bound state solutions. This is consistent, because $\tilde{E}$ is also proportional to the magnetic field B, which for the QHE is very big, this variable is not considered as a small parameter. We remark thus that the perturbation variable will be taken as $\tilde{B}$. This will result in non-integer powers of α in the final perturbation expansion of the current.

As before, spin is ignored in our calculations. Its corrections are discussed in Appendix B.

5.1   Hamiltonian

5.1.1   Total Hamiltonian

Outside

The electromagnetic potentials outside are

$$\phi(\mathbf{x}) = -xE, \quad \mathbf{A}(\mathbf{x}) = xB\hat{e}_y. \tag{5.2}$$

Thus, the Hamiltonian outside is given by

$$\hat{H} = \frac{1}{2m}\left[\hat{p}_x^2 + \hat{p}_z^2 + \left(\hat{p}_y + eB\hat{x}\right)^2\right] + eE\hat{x} \tag{5.3}$$

Inside

The electromagnetic potentials inside are

$$\phi(\mathbf{x}) = -xE + z\alpha cB, \quad \mathbf{A}(\mathbf{x}) = \left(xB - \frac{\alpha}{c}Ez\right)\hat{e}_y \tag{5.4}$$

Thus, the Hamiltonian inside is given by

$$\hat{H} = \frac{1}{2m}\left[\hat{p}_x^2 + \hat{p}_z^2 + \left(\hat{p}_y + eB\hat{x} - e\frac{\alpha}{c}E\hat{z}\right)^2\right] + eE\hat{x} - e\alpha cB\hat{z} \tag{5.5}$$

5.1.2 Perturbation Hamiltonian

As noted previously, we treat the problem by means of perturbation theory. We then take

$$\hat{H} = \hat{H}_0 + \hat{H}', \tag{5.6}$$

with

$$\hat{H}_0 = \begin{cases} \frac{1}{2m}\left[\hat{p}_x^2 + \hat{p}_z^2 + \left(\hat{p}_y + eB\hat{x}\right)^2\right] + eE\hat{x}, & z \leq 0 \ \vee \ z \geq L. \\ \frac{1}{2m}\left[\hat{p}_x^2 + \hat{p}_z^2 + \left(\hat{p}_y + eB\hat{x}\right)^2\right] + eE\hat{x} + e\tilde{E}\hat{z}, & 0 \leq z \leq L. \end{cases} \tag{5.7}$$

and

$$\hat{H}' = \begin{cases} 0, & z \leq 0 \ \vee \ z \geq L. \\ \frac{1}{2}m\omega_{\tilde{B}}^2\hat{z}^2 - \omega_{\tilde{B}}\hat{z}\left(\hat{p}_y + eB\hat{x}\right), & 0 \leq z \leq L. \end{cases} \tag{5.8}$$

$\omega_{\tilde{B}}$ is of the order of the small parameter α. With that in mind, the first term of $\hat{H}'$ is of quadratic order, so this will be ignored at first order. To be clear, let us define

$$\hat{H}'_1 = \begin{cases} 0, & z \leq 0 \ \vee \ z \geq L. \\ -\omega_{\tilde{B}}\hat{z}\left(\hat{p}_y + eB\hat{x}\right), & 0 \leq z \leq L, \end{cases} \tag{5.9}$$

a first order correction, and

$$\hat{H}'_2 = \begin{cases} 0, & z \leq 0 \ \vee \ z \geq L. \\ \frac{1}{2}m\omega_{\tilde{B}}^2\hat{z}^2, & 0 \leq z \leq L, \end{cases} \tag{5.10}$$

a second order correction. In that way,

$$\hat{H}' = \hat{H}'_1 + \hat{H}'_2. \tag{5.11}$$

5.2 Zero order solutions

The free Hamiltonian of Eq. (5.7) is a mixture of the ones in sections 1.2.2 and 3.1. It is equally separable and we can easily deduce the solutions (just add the term of the x-Electric field to the Hermite functions). Thus, the boundary conditions,

quantization and spectrum are the ones previously studied. We recall some of the important results.

The wave functions are

$$\Psi^1_{n,k_y,\kappa} = e^{ik_y y}\phi_n\left(x + k_y\ell_B^2 + \frac{mE}{eB^2}\right)Ae^{\kappa z}, \qquad z \leq 0, \tag{5.12}$$

$$\Psi^2_{n,k_y,\kappa} = e^{ik_y y}\phi_n\left(x + k_y\ell_B^2 + \frac{mE}{eB^2}\right)\big(C\,\mathrm{Ai}(\xi) + D\,\mathrm{Bi}(\xi)\big), \qquad 0 \leq z \leq L, \tag{5.13}$$

$$\Psi^2_{n,k_y,\kappa} = e^{ik_y y}\phi_n\left(x + k_y\ell_B^2 + \frac{mE}{eB^2}\right)Be^{-\kappa z}, \qquad z \geq L, \tag{5.14}$$

with

$$\phi_n(x) = \frac{1}{\sqrt{2^n n!\ell_B}}\frac{1}{\pi^{1/4}}e^{-x^2/2\ell_B^2}H_n(x/\ell_B), \tag{5.15}$$

the Hermite functions [14], being H_n the Hermite polynomials. Their energies are

$$\mathcal{E}_{n,k_y,\kappa} = \hbar\omega_B\left(n + \frac{1}{2}\right) - eE\left(k_y\ell_B^2 + \frac{mE}{2eB^2}\right) - \frac{\hbar^2\kappa^2}{2m} \tag{5.16}$$

As before, the boundary conditions in x-y are automatically satisfied. Once again the boundary conditions in z imply

$$A = C\,\mathrm{Ai}(\sigma^2) + D\,\mathrm{Bi}(\sigma^2), \tag{5.17a}$$

$$\sigma A = C\,\mathrm{Ai}'(\sigma^2) + D\,\mathrm{Bi}'(\sigma^2), \tag{5.17b}$$

and

$$Be^{-\omega} = C\,\mathrm{Ai}(\sigma^2 + \Gamma) + D\,\mathrm{Bi}(\sigma^2 + \Gamma), \tag{5.18a}$$

$$-\sigma Be^{-\omega} = C\,\mathrm{Ai}'(\sigma^2 + \Gamma) + D\,\mathrm{Bi}'(\sigma^2 + \Gamma), \tag{5.18b}$$

which give the quantization condition

$$\begin{aligned} F(\sigma, \Gamma) &\equiv [\mathrm{Ai}'(\tau) + \sigma\,\mathrm{Ai}(\tau)][\mathrm{Bi}'(\sigma^2) - \sigma\,\mathrm{Bi}(\sigma^2)] \\ &\quad - [\mathrm{Bi}'(\tau) + \sigma\,\mathrm{Bi}(\tau)][\mathrm{Ai}'(\sigma^2) - \sigma\,\mathrm{Ai}(\sigma^2)] = 0, \end{aligned} \tag{5.19}$$

with $\tau = \sigma^2 + \Gamma$. This is the same one as section 3.1, so we once again obtain the same κ energy curves defined by the allowed $\sigma_k(\Gamma)$ bands of Fig. 3.2b. We will also work once again with the functions

$$A(\xi) = C\,\mathrm{Ai}(\xi) + D\,\mathrm{Bi}(\xi), \tag{5.20}$$

and

$$B(\xi) = C^*\,\mathrm{Ai}(\xi) + D^*\,\mathrm{Bi}(\xi). \tag{5.21}$$

Not to be confused with the constants A and B of the amplitudes of the wave functions, nor with the original Airy functions $\mathrm{Ai}(\xi)$ and $\mathrm{Bi}(\xi)$.

By the boundary conditions (5.17a), (5.17b), (5.18a) y (5.18b), the functions $A(\xi)$ and $B(\xi)$ satisfy

$$A(\sigma^2) = \frac{1}{\sigma}A'(\sigma^2) = A \tag{5.22}$$

and

$$A(\tau) = \frac{-1}{\sigma}A'(\tau) = Be^{-w}. \tag{5.23}$$

The expressions are analogous for $B(\xi) = A^*(\xi)$. In general, we will express the constants A and B in terms of $A(\xi)$ and $B(\xi)$ by means of these equations, for it is more practical.

Also, using the boundary conditions, it is possible to obtain that

$$A(\tau) = \pi A(\sigma^2)G(\sigma,\Gamma) \tag{5.24}$$

and

$$B(\tau) = \pi B(\sigma^2)G(\sigma,\Gamma), \tag{5.25}$$

where

$$G(\sigma,\Gamma) = \mathrm{Bi}(\tau)(\mathrm{Ai}'(\sigma^2) - \sigma\,\mathrm{Ai}(\sigma^2)) + \mathrm{Ai}(\tau)(\sigma\,\mathrm{Bi}(\sigma^2) - \mathrm{Bi}'(\sigma^2)). \tag{5.26}$$

For simplicity, C and D will now be assumed reals, such that $A(\xi)$ and $B(\xi)$ coincide[1]. Thus, by means of Eqs. (3.58), (5.24) and (5.25), we get

$$A(\sigma^2) = B(\sigma^2) = \frac{1}{\sqrt{L_y l_{\tilde{E}}}}\frac{1}{\sqrt{\frac{1}{2\sigma} + \left(\frac{1}{2\sigma} + \Gamma\right)\pi^2 G^2(\sigma,\Gamma)}}, \tag{5.27}$$

$$A(\tau) = B(\tau) = \frac{1}{\sqrt{L_y l_{\tilde{E}}}}\frac{\pi G(\sigma,\Gamma)}{\sqrt{\frac{1}{2\sigma} + \left(\frac{1}{2\sigma} + \Gamma\right)\pi^2 G^2(\sigma,\Gamma)}}. \tag{5.28}$$

Nonetheless, it is useful to keep using the distinction between each function $A(\xi)$ and $B(\xi)$, for inner products of different wave functions will appear later. These will result in products such as $A(\sigma^2)B(\sigma'^2)$, $A(\tau)B(\tau')$, where each function corresponds to a different wave function, and therefore is defined as a linear combination of different constants.

5.3 Perturbation matrix elements

As usual, the perturbation corrections are given in terms of the matrix element of the perturbation Hamiltonian

$$\left\langle \Psi^{(0)}_{n',k'_y,\kappa'} \middle| \hat{H}' \middle| \Psi^{(0)}_{n,k_y,\kappa} \right\rangle. \tag{5.29}$$

When computing this, $\hat{p}_y$ is substituted by $\hbar k_y$, and thus the wave functions in y induce a $\delta(k_y - k'_y)$ (equivalent to L_y when $k_y = k'_y$). At the moment this will be obviated.

---

[1]Without this, they would in general differ by an arbitrary and unimportant phase, so this assumption can be done without loss of generality.

5.3.1 First Order

The first order Hamiltonian can be expressed as

$$H'^{\,\kappa,\kappa'}_{1n,n'} \equiv \left\langle \Psi^{(0)}_{n',k_y,\kappa'} \right| \hat{H}'_1 \left| \Psi^{(0)}_{n,k_y,\kappa} \right\rangle = \omega_{\tilde{B}}\, V^{n',\kappa'}_{n,\kappa}, \tag{5.30}$$

where

$$V^{n',\kappa'}_{n,\kappa} = -\int_{-\infty}^{\infty} \int_0^L \mathrm{d}x\, \mathrm{d}z\, \phi_{n'}\left(x + k_y \ell_B^2 + \frac{mE}{eB^2}\right) B(\xi') z(\hbar k_y + eBx)$$

$$\times\, \phi_n\left(x + k_y \ell_B^2 + \frac{mE}{eB^2}\right) A(\xi), \tag{5.31}$$

where $\xi = \sigma^2 + \frac{\Gamma}{L}z$ and $\xi' = \sigma'^2 + \frac{\Gamma}{L}z$. Because the Hermite functions are orthonormal, and because [12]

$$\int_{-\infty}^{\infty} \phi_{n'}(x) x \phi_n(x)\, \mathrm{d}x = \ell_B \sqrt{\frac{n+1}{2}} \delta_{n',n+1} + \ell_B \sqrt{\frac{n}{2}} \delta_{n',n-1}, \tag{5.32}$$

then

$$V^{n',\kappa'}_{n,\kappa} = \left[\delta_{n,n'} \frac{mE}{B} - eB\ell_B \sqrt{\frac{n+1}{2}} \delta_{n',n+1} - eB\ell_B \sqrt{\frac{n}{2}} \delta_{n',n-1} \right] \int_0^L A(\xi) z B(\xi')\, \mathrm{d}z$$

$$\equiv \Upsilon_{n,n'}\, I_{\kappa,\kappa'}, \tag{5.33}$$

with

$$\Upsilon_{n,n'} = \delta_{n,n'} \frac{mE}{B} - eB\ell_B \sqrt{\frac{n+1}{2}} \delta_{n',n+1} - eB\ell_B \sqrt{\frac{n}{2}} \delta_{n',n-1} \tag{5.34}$$

and

$$I_{\kappa,\kappa'} = \int_0^L A(\xi) z B(\xi')\, \mathrm{d}z. \tag{5.35}$$

With the change of variables $\xi = \sigma^2 + \frac{\Gamma}{L}z$ and $\xi' = \xi + \Delta$ with $\Delta = \sigma'^2 - \sigma^2$, then

$$I_{\kappa,\kappa'} = \frac{L^2}{\Gamma^2} \int_{\sigma^2}^{\sigma^2+\Gamma} A(\xi)(\xi - \sigma^2) B(\xi + \Delta)\, \mathrm{d}\xi. \tag{5.36}$$

So, in general

$$I_{\kappa,\kappa'} = l_{\tilde{E}}^2 [I_2 - \sigma^2 I_1] \Big|_{\sigma^2}^{\sigma^2+\Gamma}, \tag{5.37}$$

where, depending of whether κ is equal to κ' or not, will be the case that the I_1 and I_2 of this expression correspond to the ones in Eqs. (C.7) and (C.9), or to the ones in Eqs. (C.6) and (C.8).

Case $\kappa \neq \kappa'$:

Here we have $\Delta \neq 0$, so Eqs. (C.7) and (C.9) are used. Furthermore, with Eqs. (5.22) and (5.23), we obtain that

$$\left[I_2 - \sigma^2 I_1\right]\Big|_{\sigma^2} = \left[\frac{2}{(\sigma - \sigma')^2(\sigma + \sigma')^3} - \frac{1}{(\sigma + \sigma')^2}\right] A(\sigma^2) B(\sigma'^2), \tag{5.38}$$

and

$$\left[I_2 - \sigma^2 I_1\right]\Big|^{\sigma^2 + \Gamma} = -\left[\frac{2}{(\sigma - \sigma')^2(\sigma + \sigma')^3} + \frac{1}{(\sigma + \sigma')^2}\right.$$
$$\left. + \Gamma\left(\frac{1}{\sigma + \sigma'} + \frac{2}{(\sigma'^2 - \sigma^2)^2}\right)\right] A(\tau) B(\tau'). \tag{5.39}$$

Case $\kappa = \kappa'$:

Here we have $\Delta = 0$, so Eqs. (C.6) and (C.8) are used. Again, by means of Eqs. (5.22) and (5.23) we get

$$\left[\bar{I}_2 - \sigma^2 \bar{I}_1\right]\Big|_{\sigma^2} = \frac{\sigma}{3} A(\sigma^2) B(\sigma^2), \tag{5.40}$$

and

$$\left[\bar{I}_2 - \sigma^2 \bar{I}_1\right]\Big|^{\sigma^2 + \Gamma} = \left[\frac{\Gamma}{3}(\Gamma - 2\sigma^2) - \frac{\sigma}{3}\right] A(\tau) B(\tau). \tag{5.41}$$

Final form of $I_{\kappa,\kappa'}$

With these results, along with Eqs. (5.27) and (5.28) applied respectively to σ and σ', we have completely determined $I_{\kappa,\kappa'}$ in terms of Airy functions. That is,

$$I_{\kappa,\kappa} = -\ell_{\tilde{E}} \left\{ \left[\frac{\Gamma}{3}(2\sigma^2 - \Gamma) + \frac{\sigma}{3}\right] \pi^2 G^2(\sigma, \Gamma) + \frac{\sigma}{3} \right\} \frac{1}{\frac{1}{2\sigma} + \left(\frac{1}{2\sigma} + \Gamma\right)\pi^2 G^2(\sigma, \Gamma)} \tag{5.42}$$

if $\kappa = \kappa'$, and

$$I_{\kappa,\kappa'} = -\ell_{\tilde{E}} \left\{ \left[\frac{2}{(\sigma - \sigma')^2(\sigma + \sigma')^3} + \frac{1}{(\sigma + \sigma')^2} + \Gamma\left(\frac{1}{\sigma + \sigma'} + \frac{2}{(\sigma'^2 - \sigma^2)^2}\right)\right] \right.$$
$$\times \pi^2 G(\sigma', \Gamma) G(\sigma, \Gamma) + \left[\frac{2}{(\sigma - \sigma')^2(\sigma + \sigma')^3} - \frac{1}{(\sigma + \sigma')^2}\right] \right\}$$
$$\times \frac{1}{\sqrt{\frac{1}{2\sigma} + \left(\frac{1}{2\sigma} + \Gamma\right)\pi^2 G^2(\sigma, \Gamma)} \sqrt{\frac{1}{2\sigma'} + \left(\frac{1}{2\sigma'} + \Gamma\right)\pi^2 G^2(\sigma', \Gamma)}} \tag{5.43}$$

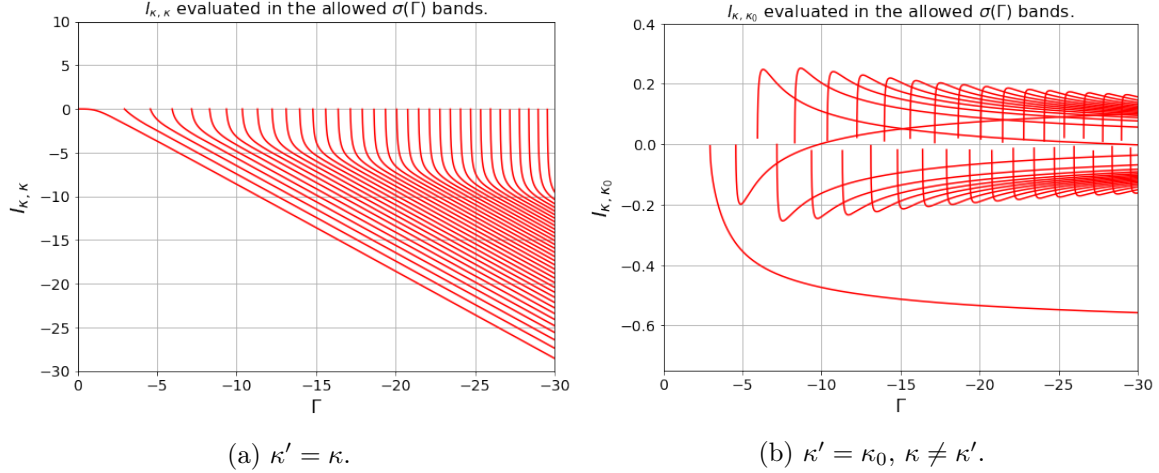(a) $\kappa' = \kappa$.   (b) $\kappa' = \kappa_0$, $\kappa \neq \kappa'$.

Figure 5.2: Plots of the matrix element $I_{\kappa,\kappa'}$ evaluated in the allowed $\sigma(\Gamma)$ bands of Fig. 3.2b.

if $\kappa \neq \kappa'$. The L_y previously ignored at the beginning was recovered here to be canceled with the $1/L_y$ involved in Eqs. (5.27) and (5.28). It can be seen that the limit $\kappa' \longrightarrow \kappa$ in (5.43) does not recover (5.42) and in fact results in a pole. This is discussed in Appendix E.

Fig. 5.2a shows a plot of $I_{\kappa,\kappa}$ (ignoring the $\ell_{\tilde{E}}$ factor), where it has been evaluated on the different allowed values of $\sigma(\Gamma)$. This gives different curves of $I_{\kappa,\kappa}$ which only depend on Γ. The base state (the level with the highest allowed value of σ) corresponds to the lower curve. The next levels subsequently follow it from above.

Fig. 5.2b shows in an analogous way the plot of I_{κ,κ_0}. That is, $I_{\kappa,\kappa'}$ with the different levels of $\sigma = \sigma(\Gamma)$ and with $\sigma' = \sigma_0(\Gamma)$, the base state. The first excited state σ_1 corresponds to the lower curve. The next levels follow it, alternating in positive/negative curves.

Approximations for $I_{\kappa,\kappa}$

Eqs. (5.42) and (5.43) are cumbersome expressions. Specially with the term $G(\sigma, \Gamma)$ of Eq. (5.26), which includes Airy functions[2]. Nonetheless, it is useful to look at the graph of $G(\sigma, \Gamma)$ (such as in Fig. 5.3), focusing on the allowed values of σ, for which it will be evaluated at the end. We then see that these allowed values are positioned in points close to where $G(\sigma, \Gamma)$ takes a maximum amplitude. That is, at many of the allowed values, the assumption

$$|G(\sigma_{\text{root}}, \Gamma)| \gg 1 \tag{5.44}$$

holds.

---

[2]This term not only is algebraically cumbersome. The main problem is that the Airy functions involved quickly diverge (causing overflow issues with numerical computations). This is exactly in correspondence with the approximation made in this section.
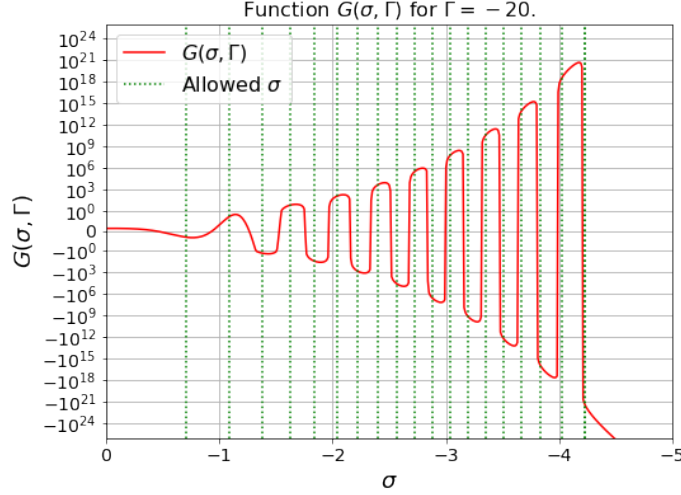
Figure 5.3: Plot of $G(\sigma, \Gamma)$ in log scale for $\Gamma = -20$, with the position of the respective allowed values of σ. The values of G at these positions tend to be at maximum amplitudes.

That allows us to take an approximation with $G^2(\sigma, \Gamma) \longrightarrow \infty$. With this limit, Eq. (5.42) results in

$$I_{\kappa,\kappa} \approx -\ell_{\tilde{E}}\left[\frac{\Gamma}{3}(2\sigma^2 - \Gamma) + \frac{\sigma}{3}\right]\frac{2\sigma}{1 + 2\sigma\Gamma}. \tag{5.45}$$

This is more manageable, and in fact reproduces the original behaviour at most cases. This can be seen in Fig. 5.4a, where both expressions are compared.

(a) Approximation $G^2(\sigma, \Gamma) \longrightarrow \infty$.

(b) Approximation $\sigma\Gamma \gg 1$.

Figure 5.4: Comparison between the two approximations (5.45) and (5.46) with the exact expression, evaluated in the allowed values of σ, which depend on Γ..

A further approximation can be made, where we focus on the regime $\sigma\Gamma \gg 1$. In this case, we get

$$I_{\kappa,\kappa} \approx \ell_{\tilde{E}}\frac{1}{3}(\Gamma - 2\sigma^2). \tag{5.46}$$

Fig. 5.4b shows a comparison between this approximation and the exact one.

To have a more intuitive idea of the general order of magnitude of $I_{\kappa,\kappa}$, we can take $\sigma \sim \sqrt{|\Gamma|}$ (such as in WKB), so that

$$I_{\kappa,\kappa} \sim -\ell_{\tilde{E}}\frac{\Gamma}{3} = -\frac{L}{3}. \tag{5.47}$$

That is, it is mostly linearly dependent on Γ (as it could be seen in Fig. 5.2a). Cancelling the electric length we obtain that this function approximately of order zero in terms of the perturbation parameter α, and in fact goes like the thickness of the plate L.

Approximations for $I_{\kappa,\kappa'}$.

The approximation methods for $I_{\kappa,\kappa'}$ are the same that the ones for $I_{\kappa,\kappa}$. The only detail is that now the limit has the behaviour $G(\sigma,\Gamma)G(\sigma',\Gamma) \longrightarrow \pm\infty$. That is, there is an undefined sign. That is of no greater importance, because the corrections are quadratic in $I_{\kappa,\kappa'}$. Thus, up to a sign, the first approximation is

$$I_{\kappa,\kappa'} \approx -\ell_{\tilde{E}}\left(\Gamma + \frac{1}{\sigma+\sigma'}\right)\left(\frac{1}{\sigma+\sigma'} + \frac{2}{(\sigma'^2-\sigma^2)^2}\right)\frac{2\sqrt{\sigma\sigma'}}{\sqrt{1+2\sigma\Gamma}\sqrt{1+2\sigma'\Gamma}}. \tag{5.48}$$

Fig. 5.5a shows the comparison between this approximation and the exact expression, where we manually placed the correct sign for each curve.

(a) Approximation $G^2(\sigma,\Gamma) \longrightarrow \infty$.　　　(b) Approximation $\sigma\Gamma \gg 1$.
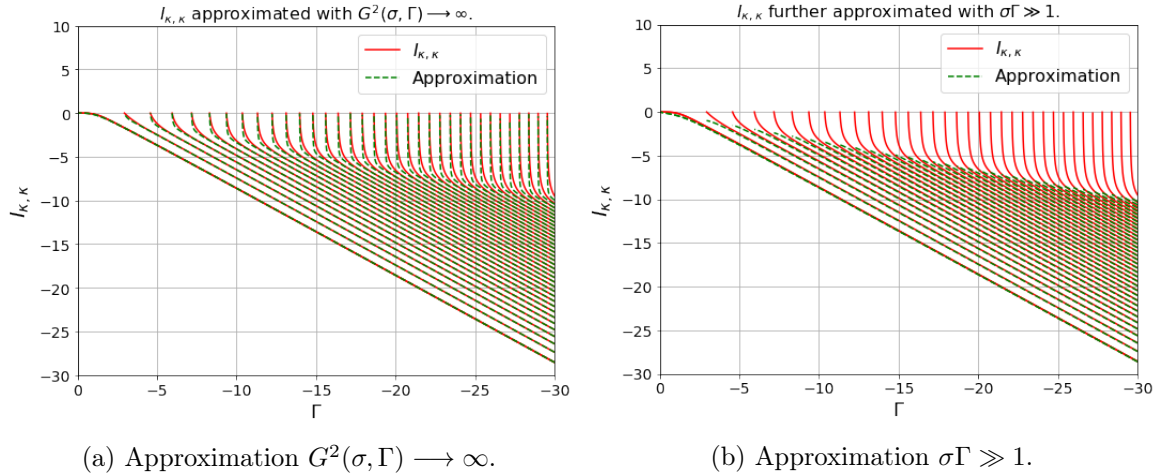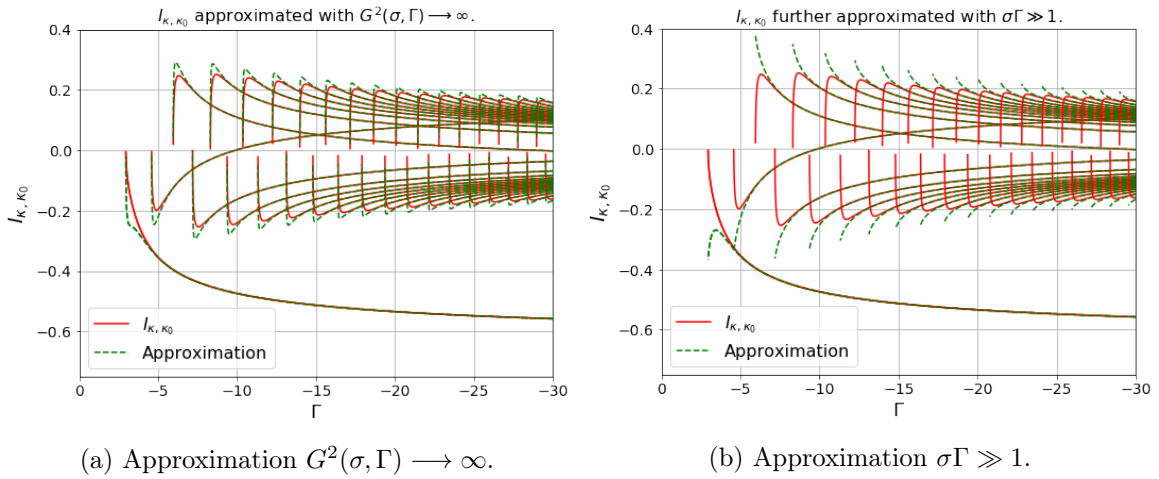
Figure 5.5: Comparison between the two approximations (5.48) and (5.49) with the exact expression, evaluated in the allowed values of σ, which depend on Γ.

If we further suppose that $\sigma\Gamma \gg 1$ and $\sigma'\Gamma \gg 1$, then

$$\boxed{I_{\kappa,\kappa'} \approx -\ell_{\tilde{E}}\left(\frac{1}{\sigma+\sigma'} + \frac{2}{(\sigma'^2-\sigma^2)^2}\right).} \tag{5.49}$$

Fig. 5.5b shows the comparison between this approximation and the exact expression.

To obtain the order of magnitude of $I_{\kappa,\kappa'}$, we can note that for big values of Γ (which is generally the case), the second term dominates over the first one. This is because $\sigma + \sigma' \sim \sqrt{|\Gamma|}$, which can be big, while $(\sigma'^2 - \sigma^2)^2$ tends to a constant. For example, by means of the WKB approximation (3.18), we have that

$$\sigma_0^2 - \sigma_1^2 \approx \left(\frac{3\pi}{4}\right)^{2/3}(3^{2/3} - 1) \approx 1.91. \tag{5.50}$$

So, the order of $I_{\kappa,\kappa'}$ goes like

$$I_{\kappa,\kappa'} \sim -\ell_{\tilde{E}}\frac{2}{(\sigma'^2 - \sigma^2)^2} \tag{5.51}$$

This can be seen in Fig. 5.2b, where $I_{\kappa,\kappa'}$ tend to constants as Γ increases. In particular I_{κ_0,κ_1}, the biggest one, tends to

$$I_{\kappa_0,\kappa_1} \sim -\ell_{\tilde{E}}\frac{2}{(1.91)^2} = -0.55\ell_{\tilde{E}}. \tag{5.52}$$

That coincides with the plot. So $I_{\kappa,\kappa'}$ can be seen in the order of magnitude of the electric length of the induced field.

5.3.2   Second Order

The matrix element of second order in α is

$$H'^{\,\kappa,\kappa'}_{2n,n'} \equiv \left\langle \Psi^{(0)}_{n',k_y,\kappa'}\,\middle|\,\hat{H}'_2\,\middle|\,\Psi^{(0)}_{n,k_y,\kappa}\right\rangle = \frac{1}{2}m\omega_{\tilde{B}}^2\delta_{n,n'}\,J_{\kappa,\kappa'}, \tag{5.53}$$

with

$$J_{\kappa,\kappa'} \equiv \int_0^L A(\xi)z^2 B(\xi')\,\mathrm{d}z. \tag{5.54}$$

A similar, but more extensive[3], calculation as the one in the previous section results in

$$J_{\kappa,\kappa} = -\frac{1}{15}\ell_{\tilde{E}}^2\left\{\left[\Gamma^2(4\sigma^2 - 3\Gamma) - (1 + 2\Gamma\sigma)(4\sigma^3 - 3)\right]\pi^2 G^2(\sigma,\Gamma) + (4\sigma^3 + 3)\right\}$$
$$\times \frac{1}{\frac{1}{2\sigma} + \left(\frac{1}{2\sigma} + \Gamma\right)\pi^2 G^2(\sigma,\Gamma)} \tag{5.55}$$

---

[3]One must use an integral formula for the linear combination of Airy functions multiplied by a quadratic term in ξ, also found in Ref. [36].

if $\kappa = \kappa'$, and

$$J_{\kappa,\kappa'} = -\ell_{\tilde{E}}^2 \left\{ \left[\left(\frac{2}{(\sigma + \sigma')^3} + \frac{12}{(\sigma - \sigma')^2(\sigma + \sigma')^4} + \frac{24}{(\sigma - \sigma')^4(\sigma + \sigma')^5} \right) (1 + (\sigma + \sigma')\Gamma) \right. \right.$$
$$\left. + \Gamma^2 \left(\frac{1}{\sigma + \sigma'} + \frac{4}{(\sigma'^2 - \sigma^2)^2} \right) \right] \pi^2 G(\sigma', \Gamma) G(\sigma, \Gamma)$$
$$- \left[\frac{2}{(\sigma + \sigma')^3} - \frac{12}{(\sigma - \sigma')^2(\sigma + \sigma')^4} + \frac{24}{(\sigma - \sigma')^4(\sigma + \sigma')^5} \right] \right\}$$
$$\times \frac{1}{\sqrt{\frac{1}{2\sigma} + \left(\frac{1}{2\sigma} + \Gamma \right) \pi^2 G^2(\sigma, \Gamma)}} \frac{1}{\sqrt{\frac{1}{2\sigma'} + \left(\frac{1}{2\sigma'} + \Gamma \right) \pi^2 G^2(\sigma', \Gamma)}} \tag{5.56}$$

if $\kappa \neq \kappa'$. No further treatments will be made, as it will be seen that these integrals actually cancel out.

5.4   Perturbative corrections

5.4.1   Wave Function

The perturbation matrix element is

$$H''^{\kappa,\kappa'}_{n,n'} = H'^{\,\kappa,\kappa'}_{1\,n,n'} + H'^{\,\kappa,\kappa'}_{2\,n,n'}, \tag{5.57}$$

with

$$H'^{\,\kappa,\kappa'}_{1\,n,n'} = \omega_{\tilde{B}} \Upsilon_{n,n'} I_{\kappa,\kappa'} \tag{5.58}$$

of first order in α, and

$$H'^{\,\kappa,\kappa'}_{2\,n,n'} = \frac{1}{2} m \omega_{\tilde{B}}^2 \delta_{n,n'} J_{\kappa,\kappa'}. \tag{5.59}$$

of second order in α. If we define the energy difference

$$\Delta \mathcal{E}^{\kappa,\kappa'}_{n,n'} = \mathcal{E}^{(0)}_{n,k_y,\kappa} - \mathcal{E}^{(0)}_{n',k_y,\kappa'} = \hbar \omega_B (n - n') - \frac{\hbar^2}{2m}(\kappa^2 - \kappa'^2), \tag{5.60}$$

then the perturbation series of the wave function (without normalization) is [11]

$$\left| \Psi_{n,\kappa} \right\rangle = \left| \Psi^{(0)}_{n,\kappa} \right\rangle + \omega_{\tilde{B}} \sum_{M' \neq M} \frac{\Upsilon_{n,n'} I_{\kappa,\kappa'}}{\Delta \mathcal{E}^{\kappa,\kappa'}_{n,n'}} \left| \Psi^{(0)}_{n',\kappa'} \right\rangle + \omega_{\tilde{B}}^2 \left(\frac{m}{2} \sum_{\kappa' \neq \kappa} \frac{J_{\kappa,\kappa'}}{\Delta \mathcal{E}^{\kappa,\kappa'}_{n,n}} \left| \Psi^{(0)}_{n,\kappa'} \right\rangle \right.$$
$$+ \sum_{M'' \neq M} \sum_{M' \neq M} \frac{\Upsilon_{n'',n'} \Upsilon_{n',n} I_{\kappa'',\kappa'} I_{\kappa',\kappa}}{\Delta \mathcal{E}^{\kappa,\kappa''}_{n,n''} \Delta \mathcal{E}^{\kappa,\kappa'}_{n,n'}} \left| \Psi^{(0)}_{n'',\kappa''} \right\rangle - \sum_{M' \neq M} \frac{\Upsilon_{n,n} \Upsilon_{n',n} I_{\kappa,\kappa} I_{\kappa',\kappa}}{(\Delta \mathcal{E}^{\kappa,\kappa'}_{n,n'})^2} \left| \Psi^{(0)}_{n',\kappa'} \right\rangle \right)$$
$$+ O(\alpha^3) \tag{5.61}$$

where $M = \{n, \kappa\}$ is taken to simplify the notation, with the convention that a sum with $M' \neq M$ implies that at least one of the quantum numbers is different (that is, one could still be equal). The k_y term is obviated, as it involves no corrections. The first row corresponds to the usual terms which are linear in the perturbation series. Nevertheless, the linear term correspondent to H'_2 is of second order in α. For this it is attached with a parenthesis to the quadratic terms, which lie on the second row. This second row doesn't includes the quadratic term of H'_2, nor the product of H'_1 with H'_2, for they are of fourth and third order, respectively.

The normalized wave function is defined by

$$\big|\Psi_{n,\kappa}\big\rangle_N = (Z_{n,\kappa})^{1/2}\big|\Psi_{n,\kappa}\big\rangle, \tag{5.62}$$

where up to second order,

$$Z_{n,\kappa} = 1 - \omega_{\tilde{B}}^2 \sum_{M' \neq M} \frac{|\Upsilon_{n,n'} I_{\kappa,\kappa'}|^2}{(\Delta \mathcal{E}_{n,n'}^{\kappa,\kappa'})^2} + O(\alpha^3). \tag{5.63}$$

5.4.2   Current

Once again we consider the system as an electron gas. So, in its most simplified form, and just like the one presented in section 1.2.2, the average current is

$$\mathbf{I} = -\frac{e}{m} \sum_{\text{O.S.}} \langle \Psi_{n,k_y,\kappa}| - i\hbar \nabla + e\mathbf{A}(\hat{\mathbf{x}})|\Psi_{n,k_y,\kappa}\rangle, \tag{5.64}$$

where the sum is made over the occupied states. We take each Landau level as completely full (no matter if in reality the levels are half filled), in the same way that it was taken for this same calculation in section 1.2.2. Thus, we are implicitly assuming that the perturbations from the induced fields do not disturb at zeroth order the quantization of the current. That is, we assume that the perturbation is small enough such that the property that the current behaves as if the Landau levels were full even when they are only partially full is maintained.

In our case, the total vector potential is

$$\mathbf{A}(\mathbf{x}) = \begin{cases} xB\hat{e}_y, & z \leq 0 \ \lor \ z \geq L. \\ (xB - \frac{\alpha}{c}Ez)\hat{e}_y, & 0 \leq z \leq L. \end{cases} \tag{5.65}$$

To simplify the notation, we define the operator

$$\tilde{z} = \begin{cases} 0, & z \leq 0 \ \lor \ z \geq L. \\ z, & 0 \leq z \leq L. \end{cases} \tag{5.66}$$

Thus, the current is

$$\mathbf{I} = -\frac{e}{m} \sum_{(n,k_y,\kappa)} \big\langle \Psi_{n,k_y,\kappa}\big| - i\hbar \nabla + e(Bx - \frac{\alpha}{c}E\tilde{z})\hat{e}_y\big|\Psi_{n,k_y,\kappa}\big\rangle \tag{5.67}$$

with (n, k_y, κ) the values of the occupied states. The associated Hall current is given by the y-component

$$I_y = -\frac{e}{m} \sum_{(n,k_y,\kappa)} \left\langle \Psi_{n,k_y,\kappa} \middle| \hbar k_y + eBx - e\frac{\alpha}{c}E\tilde{z} \middle| \Psi_{n,k_y,\kappa} \right\rangle \qquad (5.68)$$

When substituting the perturbation series, we only have to consider the matrix elements (where we obviate the Dirac delta of k_y)

$$\left\langle \Psi^{(0)}_{n',k_y,\kappa'} \middle| \Psi^{(0)}_{n,k_y,\kappa} \right\rangle = \delta_{n,n'}\delta_{\kappa',\kappa'}, \qquad (5.69)$$

$$\langle x \rangle^{\kappa,\kappa'}_{n,n'} \equiv \left\langle \Psi^{(0)}_{n',k_y,\kappa'} \middle| x \middle| \Psi^{(0)}_{n,k_y,\kappa} \right\rangle$$
$$= \delta_{\kappa,\kappa'} \left[\ell_B\sqrt{\frac{n+1}{2}}\delta_{n',n+1} + \ell_B\sqrt{\frac{n}{2}}\delta_{n',n-1} - (k_y\ell_B^2 + \frac{mE}{eB^2})\delta_{n,n'} \right], \qquad (5.70)$$

and

$$\langle \tilde{z} \rangle^{\kappa,\kappa'}_{n,n'} \equiv \left\langle \Psi^{(0)}_{n',k_y,\kappa'} \middle| \tilde{z} \middle| \Psi^{(0)}_{n,k_y,\kappa} \right\rangle = \delta_{n,n'}\, I_{\kappa,\kappa'}. \qquad (5.71)$$

The first equation is the orthogonality relation of the unperturbed states, calculated in section 3.4.1. The second term is analogous to $\Upsilon_{n,n'}$ of Eq. (5.34). The third one is exactly given by $I_{\kappa,\kappa'}$, calculated in section 5.3.1.

Current at first order

At first order, the wave function is

$$\left| \Psi_{n,k_y,\kappa} \right\rangle = \left| \Psi^{(0)}_{n,k_y,\kappa} \right\rangle + \omega_{\tilde{B}} \sum_{M' \neq M} \frac{\Upsilon_{n,n'}\, I_{\kappa,\kappa'}}{\Delta\mathcal{E}^{\kappa,\kappa'}_{n,n'}} \left| \Psi^{(0)}_{n',k_y,\kappa'} \right\rangle \qquad (5.72)$$

and the normalization constant is $Z_{n,\kappa} = 1$. The current in y is then

$$I_y = -\frac{e}{m} \sum_{(n,k_y,\kappa)} \left[\left\langle \Psi^{(0)}_{n,k_y,\kappa} \middle| + \omega_{\tilde{B}} \sum_{M'' \neq M} \frac{\Upsilon_{n,n''}\, I_{\kappa,\kappa''}}{\Delta\mathcal{E}^{\kappa,\kappa''}_{n,n''}} \left\langle \Psi^{(0)}_{n'',k_y,\kappa''} \middle| \right] (\hbar k_y + eBx - e\frac{\alpha}{c}E\tilde{z}) \right.$$
$$\left. \times \left[\left| \Psi^{(0)}_{n,k_y,\kappa} \right\rangle + \omega_{\tilde{B}} \sum_{M' \neq M} \frac{\Upsilon_{n,n'}\, I_{\kappa,\kappa'}}{\Delta\mathcal{E}^{\kappa,\kappa'}_{n,n'}} \left| \Psi^{(0)}_{n',k_y,\kappa'} \right\rangle \right] \right] \qquad (5.73)$$

In terms of the matrix elements (5.69), (5.70) and (5.71), and ignoring quadratic terms in α, we have

$$I_y = -\frac{e}{m} \sum_{(n,k_y,\kappa)} \left[\hbar k_y - eB(k_y\ell_B^2 + \frac{mE}{eB^2}) - e\frac{\alpha}{c}E\langle \tilde{z}\rangle^{\kappa,\kappa}_{n,n} + \omega_{\tilde{B}}eB \sum_{M''\neq M} \langle x\rangle^{\kappa,\kappa''}_{n,n''}\frac{\Upsilon_{n,n''}\, I_{\kappa,\kappa''}}{\Delta\mathcal{E}^{\kappa,\kappa''}_{n,n''}} \right.$$
$$\left. + \omega_{\tilde{B}}eB \sum_{M'\neq M} \langle x\rangle^{\kappa',\kappa}_{n',n}\frac{\Upsilon_{n',n}\, I_{\kappa',\kappa}}{\Delta\mathcal{E}^{\kappa,\kappa'}_{n,n'}} \right] \qquad (5.74)$$

Taking $M'' \longrightarrow M'$ (mute indexes), inserting the value of the matrix element of $\tilde{z}$, and noting that all elements are symmetric,

$$I_y = -\frac{e}{m} \sum_{(n,k_y,\kappa)} \left[-\frac{mE}{B} - e\frac{\alpha}{c} E\,\mathrm{I}_{\kappa,\kappa} + 2\omega_{\tilde{B}} eB \sum_{M' \neq M} \langle x \rangle_{n,n'}^{\kappa,\kappa'} \frac{\Upsilon_{n,n'}\,\mathrm{I}_{\kappa,\kappa'}}{\Delta\mathcal{E}_{n,n'}^{\kappa,\kappa'}} \right]. \tag{5.75}$$

Now, $\langle x \rangle_{n,n'}^{\kappa,\kappa'} \sim \delta_{\kappa,\kappa'}$, so in the sum, $\kappa' = \kappa$. That forces $n' \neq n$ and $\Delta\mathcal{E}_{n,n'}^{\kappa,\kappa} = \hbar\omega_B(n - n')$. Thus

$$I_y = \frac{e}{m} \sum_{(n,k_y,\kappa)} \left[\frac{mE}{B} + e\frac{\alpha}{c} E\,\mathrm{I}_{\kappa,\kappa} - 2\frac{\omega_{\tilde{B}} eB}{\hbar\omega_B}\,\mathrm{I}_{\kappa,\kappa} \sum_{n' \neq n} \frac{\langle x \rangle_{n,n'}^{\kappa,\kappa}\Upsilon_{n,n'}}{n - n'} \right] \tag{5.76}$$

In the last term, the only non-zero terms are the ones where[4] $n' = n+1$ and $n' = n-1$, for which

$$\frac{\langle x \rangle_{n,n+1}^{\kappa,\kappa}\Upsilon_{n,n+1}}{-1} + \frac{\langle x \rangle_{n,n-1}^{\kappa,\kappa}\Upsilon_{n,n-1}}{1} = eB\ell_B^2 \left(\frac{n+1}{2}\right) - eB\ell_B^2 \left(\frac{n}{2}\right) = \frac{1}{2} eB\ell_B^2. \tag{5.77}$$

Simplifying the factor

$$\frac{\omega_{\tilde{B}} e^2 B^2 \ell_B^2}{\hbar\omega_B} = e\frac{\alpha}{c} E, \tag{5.78}$$

we then have

$$\begin{aligned} I_y &= \frac{e}{m} \sum_{(n,k_y,\kappa)} \left[\frac{mE}{B} + e\frac{\alpha}{c} E(\mathrm{I}_{\kappa,\kappa} - \mathrm{I}_{\kappa,\kappa}) \right] \\ &= e \sum_{n,k_y,\kappa} \frac{E}{B} \end{aligned} \tag{5.79}$$

The first order correction nullifies itself exactly, and so we recover the original expression of equation (1.45). Despite having an extra sum over the κ levels, the final result will be the same because a filled κ level possesses exactly the same degeneracy (given by the sum in k_y) with respect to a n level and because the current presents no dependency on the quantum numbers. That is, it matters not how each Landau level is filled and how the quantum energies are structured. The only difference is the interpretation of the integer that defined each plateau. Originally it corresponded to the number of filled Landau (n) levels. Now we must think of it as a mixture between the discrete n and κ Levels, which in turn allow us to generally consider them as Landau levels again (just as how it was taken in section 3.3). A second order calculation is needed.

Current at second order

Now it is crucial to take into account what was mentioned in section 1.2.2. That is, we must be careful to take the complete limits a, b on the integration of k_y, which

---

[4]This is still valid for the case $n = 0$, because that term is null either way.

are given in Eq. (1.40). This is important, because now, apart from the trivial sum

$$\sum_{k_y} \longrightarrow \frac{L_y}{2\pi} \int_a^b dk_y = \frac{L_y}{2\pi}(b-a) = \frac{L_x L_y}{2\pi \ell_B^2} \equiv N, \qquad (5.80)$$

which gives the number of states of each Landau level, there will appear linear integrals in k_y. In those ones,

$$\sum_{k_y} k_y \longrightarrow \frac{L_y}{2\pi} \int_a^b k_y \, dk_y = \frac{L_y}{2\pi}\frac{1}{2}(b^2-a^2) = \frac{L_y}{2\pi}\frac{1}{2}(b-a)(b+a) = -N\frac{1}{\ell_B^2}\frac{mE}{eB^2}. \quad (5.81)$$

where we can factorize the number of states N of each Landau level.

Now, at second order, the wave function is given completely by (5.61), and the normalization constant by (5.63). Explicitly, the current in y is

$$I_y = -\frac{e}{m}\sum_{(n,k_y,\kappa)} Z_{n,\kappa}\left[\langle\Psi_{n,\kappa}^{(0)}| + \omega_{\tilde{B}}\sum_{M''\neq M}\frac{\Upsilon_{n,n''}\,\mathrm{I}_{\kappa,\kappa''}}{\Delta\mathcal{E}_{n,n''}^{\kappa,\kappa''}}\langle\Psi_{n'',\kappa''}^{(0)}| + \omega_{\tilde{B}}^2\left(\frac{m}{2}\sum_{\kappa'\neq\kappa}\frac{\mathrm{J}_{\kappa,\kappa'}}{\Delta\mathcal{E}_{n,n}^{\kappa,\kappa'}}\langle\Psi_{n,\kappa'}^{(0)}|\right.\right.$$

$$+ \sum_{M''\neq M}\sum_{M'\neq M}\frac{\Upsilon_{n'',n'}\Upsilon_{n',n}\,\mathrm{I}_{\kappa'',\kappa'}\,\mathrm{I}_{\kappa',\kappa}}{\Delta\mathcal{E}_{n,n''}^{\kappa,\kappa''}\Delta\mathcal{E}_{n,n'}^{\kappa,\kappa'}}\langle\Psi_{n'',\kappa''}^{(0)}| - \sum_{M'\neq M}\frac{\Upsilon_{n,n}\Upsilon_{n',n}\,\mathrm{I}_{\kappa,\kappa}\,\mathrm{I}_{\kappa',\kappa}}{(\Delta\mathcal{E}_{n,n'}^{\kappa,\kappa'})^2}\langle\Psi_{n',\kappa'}^{(0)}|\right)\right]$$

$$\times \left(\hbar k_y + eBx - e\frac{\alpha}{c}E\tilde{z}\right)$$

$$\times \left[|\Psi_{n,\kappa}^{(0)}\rangle + \omega_{\tilde{B}}\sum_{M'\neq M}\frac{\Upsilon_{n,n'}\,\mathrm{I}_{\kappa,\kappa'}}{\Delta\mathcal{E}_{n,n'}^{\kappa,\kappa'}}|\Psi_{n',\kappa'}^{(0)}\rangle + \omega_{\tilde{B}}^2\left(\frac{m}{2}\sum_{\kappa'\neq\kappa}\frac{\mathrm{J}_{\kappa,\kappa'}}{\Delta\mathcal{E}_{n,n}^{\kappa,\kappa'}}|\Psi_{n,\kappa'}^{(0)}\rangle\right.\right.$$

$$+ \sum_{M''\neq M}\sum_{M'\neq M}\frac{\Upsilon_{n'',n'}\Upsilon_{n',n}\,\mathrm{I}_{\kappa'',\kappa'}\,\mathrm{I}_{\kappa',\kappa}}{\Delta\mathcal{E}_{n,n''}^{\kappa,\kappa''}\Delta\mathcal{E}_{n,n'}^{\kappa,\kappa'}}|\Psi_{n'',\kappa''}^{(0)}\rangle - \sum_{M'\neq M}\frac{\Upsilon_{n,n}\Upsilon_{n',n}\,\mathrm{I}_{\kappa,\kappa}\,\mathrm{I}_{\kappa',\kappa}}{(\Delta\mathcal{E}_{n,n'}^{\kappa,\kappa'})^2}|\Psi_{n',\kappa'}^{(0)}\rangle\right)\right]$$

$$(5.82)$$

In terms of the matrix elements (5.69), (5.70) and (5.71), at second order in α we

have

$$
\begin{aligned}
I_y = {}& -\frac{e}{m}\sum_{n,k_y,\kappa} Z_{n,\kappa}\Bigg[\hbar k_y - eB(k_y\ell_B^2 + \frac{mE}{eB^2}) - e\frac{\alpha}{c}E\langle\tilde z\rangle^{\kappa,\kappa}_{n,n} \\
& + \omega_{\tilde B}\sum_{M'\neq M}\left(eB\langle x\rangle^{\kappa,\kappa'}_{n,n'} - \frac{\alpha}{c}eE\langle\tilde z\rangle^{\kappa,\kappa'}_{n,n'}\right)\frac{\Upsilon_{n,n'}\,\mathrm{I}_{\kappa,\kappa'}}{\Delta\mathcal{E}^{\kappa,\kappa'}_{n,n'}} + \omega_{\tilde B}^2 eB\left(\frac{m}{2}\sum_{\kappa'\neq\kappa}\langle x\rangle^{\kappa,\kappa'}_{n,n}\frac{\mathrm{J}_{\kappa,\kappa'}}{\Delta\mathcal{E}^{\kappa,\kappa'}_{n,n}}\right. \\
& + \sum_{M''\neq M}\sum_{M'\neq M}\langle x\rangle^{\kappa,\kappa''}_{n,n''}\frac{\Upsilon_{n'',n'}\Upsilon_{n',n}\,\mathrm{I}_{\kappa'',\kappa'}\,\mathrm{I}_{\kappa',\kappa}}{\Delta\mathcal{E}^{\kappa,\kappa''}_{n,n''}\Delta\mathcal{E}^{\kappa,\kappa'}_{n,n'}} - \sum_{M'\neq M}\langle x\rangle^{\kappa,\kappa'}_{n,n'}\frac{\Upsilon_{n,n}\Upsilon_{n',n}\,\mathrm{I}_{\kappa,\kappa}\,\mathrm{I}_{\kappa',\kappa}}{(\Delta\mathcal{E}^{\kappa,\kappa'}_{n,n'})^2}\Bigg) \\
& + \omega_{\tilde B}\sum_{M''\neq M}\left(eB\langle x\rangle^{\kappa'',\kappa}_{n'',n} - e\frac{\alpha}{c}E\langle\tilde z\rangle^{\kappa'',\kappa}_{n'',n}\right)\frac{\Upsilon_{n'',n}\,\mathrm{I}_{\kappa'',\kappa}}{\Delta\mathcal{E}^{\kappa,\kappa''}_{n,n''}} \\
& + \omega_{\tilde B}^2\sum_{M''\neq M}\sum_{M'\neq M}\left(\hbar k_y\delta_{n'',n'}\delta_{\kappa'',\kappa'} + eB\langle x\rangle^{\kappa'',\kappa'}_{n'',n'}\right)\frac{\Upsilon_{n,n''}\,\mathrm{I}_{\kappa,\kappa''}\,\Upsilon_{n,n'}\,\mathrm{I}_{\kappa,\kappa'}}{\Delta\mathcal{E}^{\kappa,\kappa''}_{n,n''}\Delta\mathcal{E}^{\kappa,\kappa'}_{n,n'}} \\
& + \omega_{\tilde B}^2 eB\left(\frac{m}{2}\sum_{\kappa'\neq\kappa}\langle x\rangle^{\kappa',\kappa}_{n,n}\frac{\mathrm{J}_{\kappa,\kappa'}}{\Delta\mathcal{E}^{\kappa,\kappa'}_{n,n}} + \sum_{M''\neq M}\sum_{M'\neq M}\langle x\rangle^{\kappa'',\kappa}_{n'',n}\frac{\Upsilon_{n'',n'}\Upsilon_{n',n}\,\mathrm{I}_{\kappa'',\kappa'}\,\mathrm{I}_{\kappa',\kappa}}{\Delta\mathcal{E}^{\kappa,\kappa''}_{n,n''}\Delta\mathcal{E}^{\kappa,\kappa'}_{n,n'}}\right. \\
& \left.\left. - \sum_{M'\neq M}\langle x\rangle^{\kappa',\kappa}_{n',n}\frac{\Upsilon_{n,n}\Upsilon_{n',n}\,\mathrm{I}_{\kappa,\kappa}\,\mathrm{I}_{\kappa',\kappa}}{(\Delta\mathcal{E}^{\kappa,\kappa'}_{n,n'})^2}\right)\right]
\end{aligned}
\tag{5.83}
$$

The order of expansion was this: First, all of the terms that multiply the term of zero order on the left of Eq. (5.82), which gives the first three rows. Then, the terms which multiply the one of first order at the left, which gives the fourth and fifth rows. Finally, the ones that multiply the term of second order, which give the sixth and seventh rows.

The $\mathrm{J}_{\kappa,\kappa'}$ elements include a $\langle x\rangle^{\kappa,\kappa'}_{n,n}\sim\delta_{\kappa,\kappa'}$. Because the sum over them is made over $\kappa\neq\kappa'$, these sums are zero. We then use the symmetry properties of each matrix element and also substitute the value of $\tilde z$,

$$
\begin{aligned}
I_y = {}& -\frac{e}{m}\sum_{n,k_y,\kappa} Z_{n,\kappa}\Bigg[-\frac{mE}{B} - e\frac{\alpha}{c}E\,\mathrm{I}_{\kappa,\kappa} \\
& + 2\omega_{\tilde B}\sum_{M'\neq M}\left(eB\langle x\rangle^{\kappa,\kappa'}_{n,n'} - e\frac{\alpha}{c}E\delta_{n,n'}\,\mathrm{I}_{\kappa,\kappa'}\right)\frac{\Upsilon_{n,n'}\,\mathrm{I}_{\kappa,\kappa'}}{\Delta\mathcal{E}^{\kappa,\kappa'}_{n,n'}} \\
& + 2\omega_{\tilde B}^2 eB\left(\sum_{M''\neq M}\sum_{M'\neq M}\langle x\rangle^{\kappa,\kappa''}_{n,n''}\frac{\Upsilon_{n'',n'}\Upsilon_{n',n}\,\mathrm{I}_{\kappa'',\kappa'}\,\mathrm{I}_{\kappa',\kappa}}{\Delta\mathcal{E}^{\kappa,\kappa''}_{n,n''}\Delta\mathcal{E}^{\kappa,\kappa'}_{n,n'}}\right. \\
& \left. - \sum_{M'\neq M}\langle x\rangle^{\kappa,\kappa'}_{n,n'}\frac{\Upsilon_{n,n}\Upsilon_{n',n}\,\mathrm{I}_{\kappa,\kappa}\,\mathrm{I}_{\kappa',\kappa}}{(\Delta\mathcal{E}^{\kappa,\kappa'}_{n,n'})^2}\right) \\
& + \omega_{\tilde B}^2\sum_{M''\neq M}\sum_{M'\neq M}\left(\hbar k_y\delta_{n'',n'}\delta_{\kappa'',\kappa'} + eB\langle x\rangle^{\kappa'',\kappa'}_{n'',n'}\right)\frac{\Upsilon_{n,n''}\,\mathrm{I}_{\kappa,\kappa''}\,\Upsilon_{n,n'}\,\mathrm{I}_{\kappa,\kappa'}}{\Delta\mathcal{E}^{\kappa,\kappa''}_{n,n''}\Delta\mathcal{E}^{\kappa,\kappa'}_{n,n'}}\Bigg]
\end{aligned}
\tag{5.84}
$$

We have already obtained that the linear terms cancel each other, so we automatically suppress them now. We then expand the sums with the respective Kronecker deltas that restrict them. For that we use $\langle x \rangle_{n,n'}^{\kappa,\kappa'} \sim \delta_{\kappa,\kappa'}$, which makes $\kappa' = \kappa$, and so $n' \neq n$, $\Delta\mathcal{E}_{n,n'}^{\kappa,\kappa} = \hbar\omega_B(n - n')$. Thus,

$$
\begin{aligned}
I_y = \frac{e}{m} \sum_{n,k_y,\kappa} Z_{n,\kappa} \Bigg[& \frac{mE}{B} + 2\omega_{\tilde{B}} e\alpha \frac{E}{c} \Upsilon_{n,n} \sum_{\kappa' \neq \kappa} \frac{(\mathrm{I}_{\kappa,\kappa'})^2}{\Delta\mathcal{E}_{n,n}^{\kappa,\kappa'}} \\
& - 2\frac{\omega_{\tilde{B}}^2 eB}{\hbar\omega_B} \sum_{n'' \neq n} \sum_{M' \neq M} \frac{\langle x \rangle_{n,n''}^{\kappa,\kappa} \Upsilon_{n'',n'} \Upsilon_{n',n} \mathrm{I}_{\kappa,\kappa'} \mathrm{I}_{\kappa',\kappa}}{(n - n'')\Delta\mathcal{E}_{n,n'}^{\kappa,\kappa'}} \\
& + 2\frac{\omega_{\tilde{B}}^2 eB}{\hbar^2 \omega_B^2} \sum_{n' \neq n} \frac{\langle x \rangle_{n,n'}^{\kappa,\kappa} \Upsilon_{n,n} \Upsilon_{n',n} \mathrm{I}_{\kappa,\kappa} \mathrm{I}_{\kappa,\kappa}}{(n - n')^2} - \omega_{\tilde{B}}^2 \hbar k_y \sum_{M' \neq M} \frac{\Upsilon_{n,n'} \mathrm{I}_{\kappa,\kappa'} \Upsilon_{n,n'} \mathrm{I}_{\kappa,\kappa'}}{(\Delta\mathcal{E}_{n,n'}^{\kappa,\kappa'})^2} \\
& - \omega_{\tilde{B}}^2 eB \sum_{n'' \neq n} \sum_{M' \neq M} \frac{\langle x \rangle_{n'',n'}^{\kappa',\kappa'} \Upsilon_{n,n''} \mathrm{I}_{\kappa,\kappa'} \Upsilon_{n,n'} \mathrm{I}_{\kappa,\kappa'}}{\Delta\mathcal{E}_{n,n''}^{\kappa,\kappa'} \Delta\mathcal{E}_{n,n'}^{\kappa,\kappa'}} \Bigg].
\end{aligned}
$$

$$(5.85)$$

From the way we take the sums over M', we have

$$
\sum_{M' \neq M} (...) = \sum_{\substack{n' \neq n \\ \kappa' = \kappa}} (...) + \sum_{\substack{\kappa' \neq \kappa \\ n' = n}} (...).
\tag{5.86}
$$

We also take

$$
\frac{1}{\hbar\omega_B}\Delta\mathcal{E}_{n,n}^{\kappa,\kappa'} = \frac{1}{\hbar\omega_B}\frac{\hbar^2}{2m\ell_{\tilde{E}}^2}(\sigma'^2 - \sigma^2) = \epsilon\Delta,
\tag{5.87}
$$

with the same $\Delta = \sigma'^2 - \sigma^2$ that we previously defined, and with ϵ, the quotient of between a κ energy level and the energy quantum of an n level $\hbar\omega_B$, which was already defined in Eq. (3.23).

With that in mind, we have

$$
\begin{aligned}
I_y = \frac{e}{m} \sum_{n,k_y,\kappa} Z_{n,\kappa} \Bigg[& \frac{mE}{B} + 2\frac{\omega_{\tilde{B}} e\alpha E/c}{\hbar\omega_B}\frac{mE}{B}\sum_{\kappa'\neq\kappa}\frac{(\mathrm{I}_{\kappa,\kappa'})^2}{\epsilon\Delta} \\
& - 2\frac{\omega_{\tilde{B}}^2 eB}{\hbar^2\omega_B^2}(\mathrm{I}_{\kappa,\kappa})^2 \sum_{n''\neq n}\sum_{n'\neq n}\frac{\langle x\rangle_{n,n''}^{\kappa,\kappa}\Upsilon_{n'',n'}\Upsilon_{n',n}}{(n-n'')(n-n')} \\
& - 2\frac{\omega_{\tilde{B}}^2 eB}{\hbar^2\omega_B^2}\frac{mE}{B}\sum_{\kappa'\neq\kappa}\frac{(\mathrm{I}_{\kappa,\kappa'})^2}{\epsilon\Delta}\sum_{n''\neq n}\frac{\langle x\rangle_{n,n''}^{\kappa,\kappa}\Upsilon_{n'',n}}{(n-n'')} \\
& + 2\frac{\omega_{\tilde{B}}^2 eB}{\hbar^2\omega_B^2}\frac{mE}{B}(\mathrm{I}_{\kappa,\kappa})^2\sum_{n'\neq n}\frac{\langle x\rangle_{n,n'}^{\kappa,\kappa}\Upsilon_{n',n}}{(n-n')^2} - \omega_{\tilde{B}}^2\hbar k_y\sum_{M'\neq M}\frac{\Upsilon_{n,n'}\,\mathrm{I}_{\kappa,\kappa'}\Upsilon_{n,n'}\,\mathrm{I}_{\kappa,\kappa'}}{(\Delta\mathcal{E}_{n,n'}^{\kappa,\kappa'})^2} \\
& - \frac{\omega_{\tilde{B}}^2 eB}{\hbar^2\omega_B^2}(\mathrm{I}_{\kappa,\kappa})^2\sum_{n''\neq n}\sum_{n'\neq n}\frac{\langle x\rangle_{n'',n'}^{\kappa',\kappa'}\Upsilon_{n,n''}\Upsilon_{n,n'}}{(n-n'')(n-n')} \\
& - \frac{\omega_{\tilde{B}}^2 eB}{\hbar^2\omega_B^2}\frac{mE}{B}\sum_{\kappa'\neq\kappa}\frac{(\mathrm{I}_{\kappa,\kappa'})^2}{\epsilon\Delta}\sum_{n''\neq n}\frac{\langle x\rangle_{n,n''}^{\kappa',\kappa'}\Upsilon_{n,n''}}{\epsilon\Delta+(n-n'')} \Bigg].
\end{aligned}
$$

$$(5.88)$$

We didn't expand the second sum in the fourth row, which involves a linear k_y term, for it cancels exactly later. Now, explicitly performing the sums

$$
\sum_{n''\neq n}\sum_{n'\neq n}\frac{\langle x\rangle_{n,n''}^{\kappa,\kappa}\Upsilon_{n'',n'}\Upsilon_{n',n}}{(n-n'')(n-n')} = -\frac{1}{2}eB\ell_B^2\frac{mE}{B}(2n+1)
$$
$$
+ \frac{1}{4}e^2 B^2\ell_B^3\left[(n+1)\sqrt{\frac{n+2}{2}} + n\sqrt{\frac{n-1}{2}}\right],
$$

$$(5.89)$$

$$
\sum_{n''\neq n}\frac{\langle x\rangle_{n,n''}^{\kappa,\kappa}\Upsilon_{n'',n}}{(n-n'')} = \frac{1}{2}eB\ell_B^2,
$$

$$(5.90)$$

$$
\sum_{n'\neq n}\frac{\langle x\rangle_{n,n'}^{\kappa,\kappa}\Upsilon_{n',n}}{(n-n')^2} = -\frac{1}{2}eB\ell_B^2(2n+1),
$$

$$(5.91)$$

$$
\sum_{n''\neq n}\sum_{n'\neq n}\frac{\langle x\rangle_{n'',n'}^{\kappa',\kappa'}\Upsilon_{n,n''}\Upsilon_{n,n'}}{(n-n'')(n-n')} = -\frac{1}{2}e^2 B^2\ell_B^2\left(k_y\ell_B^2 + \frac{mE}{eB^2}\right)(2n+1).
$$

$$(5.92)$$

This last one, when performing the linear sum over k_y of Eq. (5.81), ends up being zero (the cumbersome limits on k_y were very important!). Finally,

$$
\sum_{n''\neq n}\frac{\langle x\rangle_{n,n''}^{\kappa',\kappa'}\Upsilon_{n,n''}}{\epsilon\Delta+(n-n'')} = -\frac{1}{2}eB\ell_B^2\left[\frac{n}{\epsilon\Delta+1} + \frac{n+1}{\epsilon\Delta-1}\right].
$$

$$(5.93)$$

In this one we note that there exists a pole at $|\epsilon\Delta| = 1$. This is nothing more than the case where

$$\frac{\hbar}{2m}|\kappa'^2 - \kappa^2| = \hbar\omega_B. \tag{5.94}$$

That is, this is the case where the energy difference between two κ levels is equal to $\hbar\omega_B$, and so $\mathcal{E}_{1,\kappa}$ and $\mathcal{E}_{0,\kappa'}$ (or vice-versa) are degenerate. In that case, we would have to use degenerate perturbation theory instead. Expressing ϵ in terms of the magnetic field and other constants we obtain that for that to happen we would need a magnetic field such that

$$B = \pm\Delta^3 \frac{\alpha^2 \Phi_0}{4\pi \lambdabar^2} \approx \pm\Delta^3 (1.18 \times 10^5 \, \text{T}). \tag{5.95}$$

As Δ is at the least of order 1, this condition will never happen at a typical QHE experiment, so this very particular case does not occur.

Now we perform some factor simplifications,

$$\frac{\omega_{\tilde{B}}^2 e^2 B^2 \ell_B^2}{\hbar^2 \omega_B^2} = \alpha^2 \frac{e}{\hbar B}\left(\frac{E}{c}\right)^2, \quad eB\ell_B \frac{B}{mE} = 2\frac{\ell_E^3}{\ell_B^3}. \tag{5.96}$$

So, with these sums (leaving out once again the previously mentioned k_y factor which cancels at the end), we have

$$I_y = \frac{e}{m}\sum_{n,k_y,\kappa}\frac{mE}{B}Z_{n,\kappa}\left[1 + \alpha^2\frac{e}{\hbar B}\left(\frac{E}{c}\right)^2\left(2\sum_{\kappa'\neq\kappa}\frac{(\mathrm{I}_{\kappa,\kappa'})^2}{\epsilon\Delta} + (\mathrm{I}_{\kappa,\kappa})^2(2n+1)\right.\right.$$

$$- (\mathrm{I}_{\kappa,\kappa})^2\frac{\ell_E^3}{\ell_B^3}\left[(n+1)\sqrt{\frac{n+2}{2}} + n\sqrt{\frac{n-1}{2}}\right] - \sum_{\kappa'\neq\kappa}\frac{(\mathrm{I}_{\kappa,\kappa'})^2}{\epsilon\Delta}$$

$$- (\mathrm{I}_{\kappa,\kappa})^2(2n+1) + \frac{1}{2}\sum_{\kappa'\neq\kappa}\frac{(\mathrm{I}_{\kappa,\kappa'})^2}{\epsilon\Delta}\left[\frac{n}{\epsilon\Delta+1} + \frac{n+1}{\epsilon\Delta-1}\right]\right)$$

$$\left. - \omega_{\tilde{B}}^2\hbar k_y\frac{B}{mE}\sum_{M'\neq M}\frac{\Upsilon_{n,n'}\,\mathrm{I}_{\kappa,\kappa'}\,\Upsilon_{n,n'}\,\mathrm{I}_{\kappa,\kappa'}}{(\Delta\mathcal{E}_{n,n'}^{\kappa,\kappa'})^2}\right]. \tag{5.97}$$

Grouping terms together, and performing the sum over k_y by means of Eqs. (5.80) and (5.81), where

$$\sum_{k_y} -\hbar k_y\frac{B}{mE} \longrightarrow N\frac{\hbar}{eB}\frac{1}{\ell_B^2} = N, \tag{5.98}$$

we have that

$$
I_y = \frac{eE}{B} N \sum_{n,\kappa} Z_{n,\kappa} \left[1 + \alpha^2 \frac{e}{\hbar B} \left(\frac{E}{c} \right)^2 \left(\frac{1}{2} \sum_{\kappa' \neq \kappa} \frac{(I_{\kappa,\kappa'})^2}{\epsilon \Delta} \left[\frac{n}{\epsilon \Delta + 1} + \frac{n+1}{\epsilon \Delta - 1} + 2 \right] \right.\right.
$$

$$
\left. - (I_{\kappa,\kappa})^2 \frac{\ell_E^3}{\ell_B^3} \left[(n+1)\sqrt{\frac{n+2}{2}} + n\sqrt{\frac{n-1}{2}} \right] \right)
$$

$$
+ \omega_{\tilde{B}}^2 \sum_{M' \neq M} \frac{\Upsilon_{n,n'} I_{\kappa,\kappa'} \Upsilon_{n,n'} I_{\kappa,\kappa'}}{(\Delta \mathcal{E}_{n,n'}^{\kappa,\kappa'})^2} \right]
\tag{5.99}
$$

Thus, the last term cancels out exactly when doing the multiplication with $Z_{n,\kappa}$ of Eq. (5.63) at second order. Once again, we emphasize that the correct, but cumbersome limits of k_y, give useful cancellations. We are left with

$$
I_y = \frac{eE}{B} N \sum_{n,\kappa} \left[1 + \alpha^2 \frac{e}{\hbar B} \left(\frac{E}{c} \right)^2 \left(\frac{1}{2} \sum_{\kappa' \neq \kappa} \frac{(I_{\kappa,\kappa'})^2}{\epsilon \Delta} \left[\frac{n}{\epsilon \Delta + 1} + \frac{n+1}{\epsilon \Delta - 1} + 2 \right] \right.\right.
$$

$$
\left.\left. - (I_{\kappa,\kappa})^2 \frac{\ell_E^3}{\ell_B^3} \left[(n+1)\sqrt{\frac{n+2}{2}} + n\sqrt{\frac{n-1}{2}} \right] \right) \right].
\tag{5.100}
$$

Now, we must remember that the expression of $I_{\kappa,\kappa'}$ in Eqs. (5.42) and (5.43) possesses a factor given by the electric length $\ell_{\tilde{E}}$. Thus, we can factor it from both terms, implicitly redefining $I_{\kappa,\kappa'}$ without this factor (so that it becomes dimensionless). Thus we express the overall factor of the quadratic correction as

$$
\alpha^2 \frac{e}{\hbar B} \left(\frac{E}{c} \right)^2 \ell_{\tilde{E}}^2 = \frac{\ell_B^2 \ell_{\tilde{E}}^2}{\ell_{\tilde{B}}^4},
\tag{5.101}
$$

which is a dimensionless variable.

The sum $\sum_{(n,\kappa)}$ over the first term gives the total amount of occupied energy levels (denoted by ν_{tot}), which are independent of whether they are n levels or κ levels. The sum over the rest of the terms must be done depending on the way the energy levels are filled (it does matters here). So this will be implicitly left as $\sum_{(n,\kappa)}$. Thus

$$
I_y = \frac{eE}{B} N \left[\nu_{\text{tot}} + \frac{\ell_B^2 \ell_{\tilde{E}}^2}{\ell_{\tilde{B}}^4} \sum_{(n,\kappa)} \left(\frac{1}{2} \sum_{\kappa' \neq \kappa} \frac{(I_{\kappa,\kappa'})^2}{\epsilon \Delta} \left[\frac{n}{\epsilon \Delta + 1} + \frac{n+1}{\epsilon \Delta - 1} + 2 \right] \right.\right.
$$

$$
\left.\left. - (I_{\kappa,\kappa})^2 \frac{\ell_E^3}{\ell_B^3} \left[(n+1)\sqrt{\frac{n+2}{2}} + n\sqrt{\frac{n-1}{2}} \right] \right) \right].
\tag{5.102}
$$

We define the dimensionless functions of E, B and L,

$$
\boxed{ f(E, B, L) \equiv \frac{\ell_E^3 \ell_{\tilde{E}}^2}{\ell_B \ell_{\tilde{B}}^4} \frac{1}{\nu_{\text{tot}}} \sum_{(n,\kappa)} (I_{\kappa,\kappa})^2 \left[(n+1)\sqrt{\frac{n+2}{2}} + n\sqrt{\frac{n-1}{2}} \right] \right) }, \tag{5.103}
$$

and

$$g(E, B, L) \equiv \frac{\ell_B^2 \ell_{\tilde{E}}^2}{\ell_{\tilde{B}}^4} \frac{1}{\nu_{\text{tot}}} \sum_{(n,\kappa)} \frac{1}{2} \sum_{\kappa' \neq \kappa} \frac{(\mathrm{I}_{\kappa,\kappa'})^2}{\epsilon \Delta} \left[\frac{n}{\epsilon \Delta + 1} + \frac{n+1}{\epsilon \Delta - 1} + 2 \right], \tag{5.104}$$

so that

$$I_y = I_y^{(0)} (1 + g - f), \tag{5.105}$$

where $I_y^{(0)}$ is the original Hall current with ν_{tot} Landau levels filled. So there are two corrections, and in fact we can give a physical interpretation to each one.

If only one κ level is allowed, the filling is done over the usual n Landau levels. So $\nu_{\text{tot}} = \nu$, and we in fact recover the same bi-dimensional system that the one in the original QHE (In fact, a single allowed κ level is obtained when the thickness of the plate is very small). Because there is only one level in κ, then the function g is zero, and the only correction is given by f. Thus, f can be interpreted as the pure correction from the θ electrodynamics.

Increasing the thickness of the plate, multiple κ levels will be allowed, which is equivalent to a multitude of layered bi-dimensional systems. The term of zeroth order corresponds to the total amount of Landau levels filled in each subsystem, which in turn corresponds to the amount of Hall currents given by the sum of the stacked plates with filled Landau levels. Like before, f gives the summed θ-electrodynamics corrections of each layer. Thus, g can be interpreted as the correction given by the thickness of the material, and the interaction between the superposed layers in it (which at the end emerge also from the θ corrections).

While both of these corrections are of quadratic order in α, their behaviour still allows their values to significantly differ. We can analyze the order of magnitude of the first function with the approximation for $\mathrm{I}_{\kappa,\kappa}$ of Eq. (5.47) (taking into account that we have already taken out the electric length). With this,

$$f(E, B, L) \sim \frac{\ell_E^3 \ell_{\tilde{E}}^2}{\ell_B \ell_{\tilde{B}}^4} \frac{\Gamma^2}{9} \approx 2.25 \times 10^{-4} \left(\frac{\sqrt{B}}{\mathrm{T}^{1/2}} \right) \left(\frac{E}{\mathrm{V/m}} \right) \left(\frac{L^2}{\mathrm{m}^2} \right). \tag{5.106}$$

From this we can see that this correction does not satisfy Ohm's law $J = \sigma E$. It is instead a quadratic correction on the electric field (dividing by $I_y^{(0)}$ we had already taken out an electric field factor). Nevertheless, we can in the same way define a conductivity or resistivity just like in Ohm's law, but it will now instead depend on the electric field (linearly in this case).

For g, we can see that the I_{κ_0,κ_1} term dominates, so we can take the approximation (5.52). We can also note that in

$$\left[\frac{n}{\epsilon \Delta + 1} + \frac{n+1}{\epsilon \Delta - 1} + 2 \right] \tag{5.107}$$

the 2 dominates, for $\epsilon \gg 1$ (see Fig. 3.5). And so, with $\Delta = \Delta_{1,0} \approx -1.91$, we have

$$g(E, B, L) \sim \frac{\ell_B^2 \ell_{\tilde{E}}^2}{\ell_B^4} \frac{4}{\epsilon \Delta_{1,0}^5} \approx -1.53 \times 10^{-26} \left(\frac{E^2}{\mathrm{V}^2/\mathrm{m}^2} \right) \left(\frac{\mathrm{T}^{4/3}}{B^{4/3}} \right) \tag{5.108}$$

The fact that this expression does not depend on L is no contradiction to our interpretation of g as a correction due to the thickness of the plate. This is just because the approximation is very brute. In reality Δ and $I_{\kappa,\kappa'}$ do carry an L-dependence. Another interesting fact is that this is a cubic correction of Ohm's law, but far smaller than f. So f is the one that dominates between the two. This comes from the fact that $|I_{\kappa,\kappa}|$ is not bound from above, while $|I_{\kappa,\kappa'}|$ is. Nevertheless, in general f is small. This can be an advantage if one does wants to recover the Hall effect, for this system possesses the advantage of automatically confining the electrons in a bi-dimensional plate, no matter its thickness.

5.4.3 Total conductivity

To obtain the resistivity, it is necessary to make a complete analysis of the conductivity in 3 dimensions. That is, we must obtain the matrix equation

$$\mathbf{J} = \sigma_e \mathbf{E}, \tag{5.109}$$

with

$$\sigma_e = \begin{pmatrix} \sigma_{xx} & \sigma_{xy} & \sigma_{xz} \\ \sigma_{yx} & \sigma_{yy} & \sigma_{yz} \\ \sigma_{zx} & \sigma_{zy} & \sigma_{zz} \end{pmatrix} \tag{5.110}$$

at the same order in the perturbation series. Note that, as we have seen in the last section, this conductivity depends on the electric field. We have obtained that, for $\mathbf{E} = (E_x, 0, 0)$, we produce $\mathbf{J} = (J_x, J_y, J_z)$ with

$$J_y = \frac{e\nu_{\text{tot}}}{\Phi_0}\big(1 - f + g\big)E. \tag{5.111}$$

For the current in x and z, the current is only given by

$$I_{x,y} = -\frac{e}{m} \sum_{(n,k_y,\kappa)} \big\langle \Psi_{n,k_y,\kappa} \big| - i\hbar\partial_{x,y} \big| \Psi_{n,k_y,\kappa} \big\rangle. \tag{5.112}$$

In both cases the complex factor $e^{ik_y y}$ can pass through the derivative and cancel with its conjugate, leaving us with only real functions. Multiplied by the $-i\hbar$ factor, the matrix element at the end will be purely imaginary. As the expectation value of an Hermitian operator (such as the momentum operator) is always real, this result must then be zero. So in the end $\sigma_{xx} = \sigma_{zx} = 0$.

Now, by symmetry $\sigma_{yy} = \sigma_{zy} = 0$, and also

$$\sigma_{yx} = -\sigma_{xy} = \sigma_{yx}^{(0)}(1 - f + g) \tag{5.113}$$

with

$$\sigma_{yx}^{(0)} = \frac{e^2}{2\pi\hbar}\nu_{\text{tot}}, \tag{5.114}$$

the total conductivity of the usual QHE. Furthermore, a test electric field in z will not produce any electromagnetic field through the action of the TI. Thus in this case

we would have only a magnetic and electric field (external and induced) in z. These fields do not produce currents in the x or y directions, and thus $\sigma_{xz} = \sigma_{yz} = 0$. In total we have

$$\sigma_e = \begin{pmatrix} 0 & \sigma_{xy} & 0 \\ -\sigma_{xy} & 0 & 0 \\ 0 & 0 & \sigma_{zz} \end{pmatrix} \tag{5.115}$$

It will not be necessary to compute the current in z, for we can directly obtain the inverse matrix as

$$\rho = \sigma_e^{-1} = \begin{pmatrix} 0 & -1/\sigma_{xy} & 0 \\ 1/\sigma_{xy} & 0 & 0 \\ 0 & 0 & 1/\sigma_{zz} \end{pmatrix}. \tag{5.116}$$

In this way, even when we have a 3-dimensional system, the relation between the transverse resistivity and conductivity is the same as the one in the original bi-dimensional Hall effect.

The final expression for the resistivity of the Hall effect with second order corrections is then

$$\boxed{\rho_{xy} = \rho_{xy}^{(0)}(1 - f + g)^{-1} \approx \rho_{xy}^{(0)}(1 + f - g)}, \tag{5.117}$$

with

$$\rho_{xy}^{(0)} = \frac{2\pi\hbar}{e^2} \frac{1}{\nu_{\text{tot}}}. \tag{5.118}$$

5.4.4 The occupation in the correction functions

The functions $f(E, B, L)$ and $g(E, B, L)$ of Eqs. (5.103) and (5.104) also have an implicit dependency on the electron's density, as the sums over (n, κ) are performed over the occupied states. To this end we remember the discussion of section 3.3, where in section 3.3.2 we discussed how a certain number of Landau n levels must be filled before reaching higher levels of κ, and in section 3.3.3 we further developed this discussion by taking into account the appearance of κ bands at certain Γ values, which caused the occupation in the n levels of each κ level to discontinuously change at certain values of B for a fixed thickness L, giving rise to discontinuities in macroscopic variables. In that section we exemplified this phenomenon with the Fermi energy. Furthermore, in chapter 4 we also obtained that this discontinuities also appear in the induced magnetization. By the exact same principle, the correction functions f and g will now possess the same kind of discontinuities, making the current (or conductivity) the macroscopic discontinuous variable.

The sums over (n, κ) are not so simple to perform, but can calculated with an algorithm very similar to the one presented in section 3.3.3. That is, we can compute the number of n levels occupied in each κ level allowed and perform the sums of Eqs. (5.103) and (5.104) with these numbers, together with the corresponding values of σ and Γ. We show this result in Figs. 5.6a for the function f and 5.6b for the function g at the same values used in section 3.3.3 so that the discontinuities appear at the same values. We further use a representative experimental value for the QHE of the electric field given by [4] $E = 12\,\text{mV}/130\,\mu\text{m} \approx 100\,\text{V/m}$. By how it is defined, the function g is zero at the region where only the κ_0 level is allowed.
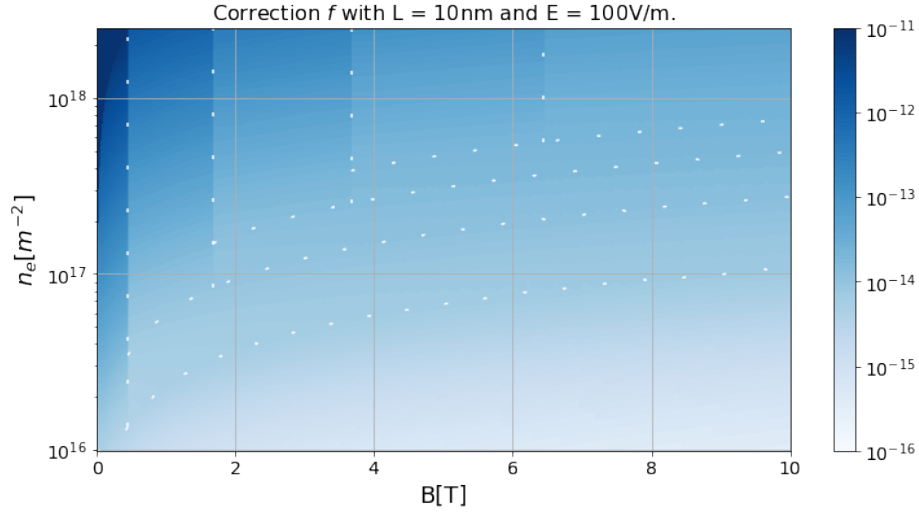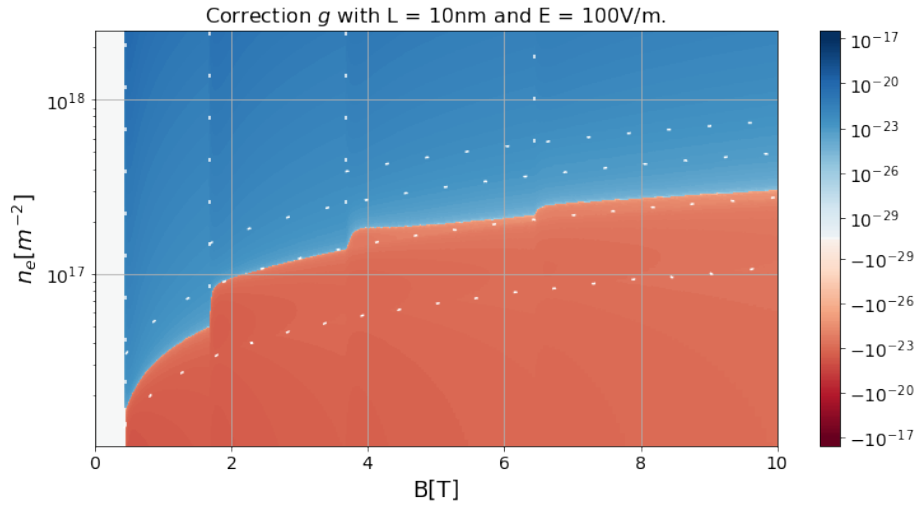
(a) Plot of f(E,B,L).

(b) Plot of g(E,B,L).

Figure 5.6: Correction functions for $L = 10\,\mathrm{nm}$ and $E = 100\,\mathrm{V/m}$. Just like in Fig. 3.8 they present discontinuities at certain values of B for high enough occupation. The function g is zero at the region where only κ_0 is allowed. The dashed lines separate the same occupation regions which were previously analysed in Fig. 3.8. There are once again discontinuities at the regions where a new κ level appears and the occupation is high enough.

From the plots of f and g we can see once again (and by this point it should be expected) that we obtain the aforementioned discontinuities at fixed values of B for which the occupation number is high enough. The order of magnitude of the functions themselves results incredibly small (specially for g), but this is a result from having taken the small thickness of $L = 10\,\mathrm{nm}$, chosen both for computational and visual facility. One could in principle fine tune the variables through Eqs. (5.106) and (5.108) such that the orders of magnitude of both functions is increased.

Finally, we note that the function g in Fig. 5.6b presents a change of sign at

certain heights. This can be explained by analysing the expression of Eq. (5.104). As seen in Fig. 5.2b, the contribution that dominates is generally the $\kappa = \kappa_0$ and $\kappa' = \kappa_1$ term. As $\sigma_0 > \sigma_1$, then $\Delta = \sigma'^2 - \sigma^2$ is negative. Thus, at a low enough occupation number (low enough n_e), the constant 2 will dominate over the other terms in Eq. (5.104), producing a negative g. Now, if we increase the sum over n by increasing n_e, then the other terms will now dominate. As $\epsilon \gg 1$ then the denominators of these terms are generally negative and thus produce a positive result for the sum in g. By this conclusion we note that, although it appears like so, the place at which g changes of sign is not related at all to the occupation sectors of Fig. 3.7, as seen by the miss-match of the dashed lines and the region where the sign changes.

6 Conclusions

A diversity of quantum phenomena emerging from the effective theory of TIs under the action of external electromagnetic fields were studied. The initial motivation for this work was the Hall effect (reviewed in chapter 1), as the effective electromagnetic theory of a TI (reviewed in chapter 2) allowed a system which consisted on a plate of finite thickness of a TI under the presence of an external magnetic field to hold bound states and treat the system as a bi-dimensional plate, as an internal electric field was induced, and whose action in the Schrödinger equation was to produce a finite triangle potential that allowed this localization (demonstrated in chapter 3). Although a system which allowed the realisation of the QHE was replicated, additional unexpected phenomena were encountered.

First off, the quantization condition which depended on the dimensionless thickness Γ, and which was given by Eq. (3.15), produced a variable number of energy bands as a function of Γ. Thus, for a fixed thickness L there could be a spontaneous appearance of new bands at critical values of the magnetic field. The implications for this were first discussed in section 3.3.3, where a general algorithm for computing the Fermi energy was described, but whose important conclusion was that this macroscopic variable presented discontinuities at the aforementioned critical points. Nevertheless, it was noted that this discontinuity was found only when the occupation number was big enough and, as further discussed in section 3.3.4, for this to happen we would also need to restrict the system on a finite volume as dispersion states which could drain the system appeared. This also concluded that the calculations involving this transition would never be exact because when a new energy band appeared, some states would inevitably decay into dispersion states (that were nevertheless bound by the finite volume). The presence of these dispersion states was systematically ignored throughout this work, and thus the results can not be exact.

Having studied the basic quantum system, the natural next step was to calculate its magnetization because the energy bands depended on the external magnetic field through the induced electric field. This was done in chapter 4. First, the simpler case where there was only one energy band present was analysed (section 4.1). Having settled the way to compute the non-trivial magnetization terms, these were now computed for the first critical point. That is, just before the appearance of the second allowed energy band (section 4.2.1) and just after its appearance (section 4.2.2). With this, the presence of a quantum phase transition of first order was demonstrated, whose order parameter was computed in section 4.2.3. The general case for the critical point at which the nth energy band appears was computed in section 4.2.4.

The study finalized in chapter 5 with the analysis of realisation of the QHE on this system. For this a parallel electric field was introduced, which in turn induced an internal parallel magnetic field. This disrupted the conventional QHE system, but nevertheless we assumed that the general behaviour of the current was maintained as this magnetic field was of the order of the fine structure constant. Thus, a perturbation analysis was performed, for which the first order corrections were found to cancel exactly, while the second order corrections turned out to be non-trivial expressions. While from the front it was assumed that the original quantization of the current would still be present at leading order, correction functions were found which consistently turned out to be very small. When plotting these functions with a numerical analysis which followed a similar algorithm from section 3.3.3, the same discontinuities were found in correspondence to the phase transition.

In summary, a quantum phase transition of first order was found. The macroscopic variables studied which suffer this phase transition were the Fermi energy, the magnetization and the Hall current.

A Relevant parameters

All constants and expressions are described within the SI units system. Values taken from Ref. [5].

A.1 Constants

$$R_K = \frac{2\pi\hbar}{e^2} = 25812.80745...\Omega \quad \text{(von Klitzing constant)}.$$

$$\Phi_0 = \frac{2\pi\hbar}{e} = 4.13566773 \times 10^{-15}\,\text{T} \cdot \text{m}^2 \quad \text{(Quantum of Flux)}.$$

$$\alpha = \frac{1}{4\pi\epsilon_0}\frac{e^2}{\hbar c} = 1/137.035999084 \quad \text{(Fine-structure constant)}.$$

$$\lambdabar = \frac{\hbar}{mc} = 3.8615926796 \times 10^{-13}\,\text{m} \quad \text{(Electron's reduced Compton wavelength)}.$$

$$\mu_B = \frac{e\hbar}{2m} = 9.274009994 \times 10^{-24}\,\text{A} \cdot \text{m}^2 \quad \text{(Bohr magneton)}.$$

A.2 Variables

$$\tilde{B} = \alpha\frac{E}{c}, \quad \tilde{E} = -\alpha cB \quad \text{(Induced electromagnetic fields)}.$$

$$\omega_B = \frac{eB}{m}, \quad \omega_{\tilde{B}} = \frac{e\tilde{B}}{m} = \alpha\frac{eE}{mc} \quad \text{(Cyclotron frequencies)}.$$

$$\ell_B = \sqrt{\frac{\hbar}{eB}} = \sqrt{\frac{\hbar}{m\omega_B}}, \quad \ell_{\tilde{B}} = \sqrt{\frac{\hbar}{e\tilde{B}}} = \sqrt{\frac{\hbar}{m\omega_{\tilde{B}}}} \quad \text{(Magnetic lengths)}.$$

$$\ell_E = \left(\frac{\hbar^2}{2meE}\right)^{1/3}, \quad \ell_{\tilde{E}} = \left(\frac{\hbar^2}{2me\tilde{E}}\right)^{1/3} \quad \text{(Electric lengths)}.$$

$$g = \frac{A}{2\pi\ell_B^2} = \frac{eBA}{2\pi\hbar} = \frac{AB}{\Phi_0} \quad \text{(Landau level's degeneracy)}.$$

$$n_e = N/A \quad \text{(Electron surface density)}.$$

$$n_e^{3D} = N/V = N/(AL) \quad \text{(Electron volume density)}.$$

$$\sigma_{DC} = \frac{n_e e\tau}{m} \quad \text{(Drude conductivity)}.$$

A.2.1 Dimensionless variables

$$\sigma = \ell_{\tilde{E}}\kappa, \quad \sigma' = \ell_{\tilde{E}}\kappa', \quad \Delta = \sigma'^2 - \sigma^2 \quad \text{(Dimensionless momenta)}.$$

$$\Gamma = \frac{L}{\ell_{\tilde{E}}} \quad \text{(Dimensionless thickness)}.$$

$$\epsilon = \frac{1}{\hbar\omega_B}\frac{\hbar^2}{2m\ell_{\tilde{E}}^2} = -\alpha\frac{\ell_{\tilde{E}}}{\lambdabar} = \left(\frac{\alpha^2}{4\pi\lambdabar^2}\frac{\Phi_0}{B}\right)^{1/3} \quad \text{(Dimensionless } \kappa\text{-}n \text{ energy ratio)}.$$

$$\mathcal{E}_{n,\kappa} = (n + 1/2) - \epsilon\sigma^2 \quad \text{(Dimensionless energy)}.$$

B Spin corrections

Throughout every past calculation we have completely ignored the presence of spin, both as an additional quantum number, and also as the responsible operator for the Zeeman interaction. In this appendix we redo the calculations for which its presence does affect the results.

B.1 Spin in Landau Levels

The presence of spin introduces the Zeeman interaction

$$\hat{H}_Z = \mathfrak{g}\mu_B\hat{\mathbf{s}} \cdot \mathbf{B} \tag{B.1}$$

where $\mathbf{B} = B\hat{e}_z$, $\hat{\mathbf{s}} = \pm\frac{1}{2}\hat{e}_z$ is the spin operator and $\mathfrak{g}$ is the *anomalous gyromagnetic ratio*, which classically possesses the value of $\mathfrak{g} = 2$, but in reality acquires corrections both from quantum field theory and from the crystalline structure [3]. This has important effects, for the Zeeman-splitting of the energies

$$\Delta\mathcal{E}_Z = \mathfrak{g}\mu_B B = \frac{\mathfrak{g}}{2}\hbar\omega_B \tag{B.2}$$

would mix the spin up states of the level n with the spin down states of the level $n+1$ if we had $\mathfrak{g} = 2$. Nevertheless, its modified value turns out to produce a Zeeman splitting much smaller than the energy difference of the Landau levels [3].

If the Zeeman-splitting is so small that it cannot be resolved, the up and down states will effectively correspond to the same energy. In this case, the degeneracy of each Landau level g_s, with spin taken into account, doubles:

$$g_s \equiv 2g = \frac{2AB}{\Phi_0}. \tag{B.3}$$

This means that, in general, the number of occupied Landau levels is halved:

$$\nu^s \equiv \nu/2. \tag{B.4}$$

This applies to all of the ν defined throughout this work. For example,

$$\nu^s_{\text{tot}} = \left\lfloor \frac{n_e}{2}\frac{\Phi_0}{B} \right\rfloor, \quad \nu^s_m = \nu_m/2, \quad n^s_m = n_m/2. \tag{B.5}$$

This also implies that Eq. (3.41) will now take the form

$$\left\lfloor \frac{n_e}{2}\frac{\Phi_0}{B} \right\rfloor > m + b_m \left(n_C \frac{\Phi_0}{B} \right)^{1/3}, \quad b_m \equiv m(2m+1)^{2/3} - \sum_{l=0}^{m-1}(2l+1)^{2/3}. \quad \text{(B.6)}$$

This can be effectively accounted for by always dividing n_e by two in all of our results. For example, in Figs. 3.8 and 3.9 just divide the n_e axis by two to account for the spin corrections.

B.2 Spin in Magnetization

Chapter 4 is the one that presents the most noticeably spin corrections. The energies are now modified as

$$\mathcal{E}_{n,k,s} = -\frac{\hbar^2}{2m\ell_{\tilde{E}}^2}\sigma_k^2(\Gamma) + \hbar\omega_B(n+1/2) + \mathfrak{g}\mu_B s B, \quad n = 0, 1, ..., \quad k = 0, 1, ..., \quad s = \pm\frac{1}{2}, \quad \text{(B.7)}$$

so there will be another magnetization term which corresponds to the Pauli paramagnetism. For the 3D free electron gas one obtains that this term is [41]

$$\chi_{\text{Pauli}} = -\frac{3}{4}\mathfrak{g}^2\chi_{\text{Landau}}, \quad \text{(B.8)}$$

such that for $\mathfrak{g} = 2$ one obtains the well known relation $\chi_{\text{Landau}} = -\frac{1}{3}\chi_{\text{Pauli}}$. Once again, we remark that the effects of the material change this relation. In principle, they could even render the Pauli term negligible with respect to the Landau term [41]. Nevertheless, we keep this term for generality.

In our effective 2D case, the same way as it happened for the Landau term (4.30), we obtain a susceptibility given by

$$\tilde{\chi}_{\text{Pauli}} = \frac{\pi}{Lk_F}\chi_{\text{Pauli}}. \quad \text{(B.9)}$$

Thus, in all of our results of this section we must make

$$\tilde{\chi}_{\text{Landau}} \longrightarrow \left(1 - \frac{3}{4}\mathfrak{g}^2\right)\tilde{\chi}_{\text{Landau}} \quad \text{(B.10)}$$

to take spin into account.

With spin, the degeneracies of the 2D and 3D electron gas with spin also change:

$$g_0^s \equiv 2g_0 = \frac{mV^{2/3}}{\pi\hbar^2}, \quad g_{3D}^s(\mathcal{E}_F) = \frac{mk_F}{\pi^2\hbar^2}. \quad \text{(B.11)}$$

This doubles the explicit value of the Landau susceptibility:

$$\tilde{\chi}_{\text{Landau}}^s = -2\frac{m\mu_0\mu_B^2}{6\pi\hbar^2 L}. \quad \text{(B.12)}$$

Note that nevertheless we still obtain that $g_0^s \hbar \omega_B = g_s$, which was necessary when discretizing integrals, so all of our results still hold. The relationship

$$\frac{g_0^s(\mathcal{E}_F)}{V} = \frac{\pi}{L k_F} g_{3D}^s(\mathcal{E}_F), \tag{B.13}$$

which was needed to relate the 3D Landau (and Pauli) susceptibility with the one we obtained, also holds when taking spin into account. That is,

$$\boxed{\tilde{\chi}_{\text{Landau}} = \frac{\pi}{L k_F} \chi_{\text{Landau}}}. \tag{B.14}$$

still holds, as χ_{Landau} also doubled.

The $\chi_{\tilde{\theta}}$ term in all of our equations acquires no corrections as long as we take into account that, for a fixed particle number (or electronic density n_e^{3D}), the number of occupied Landau levels ν_m is halved and the degeneracies are doubled with respect to the spinless case. In particular, the thin-plate magneto-electric susceptibility

$$\boxed{\chi_{\tilde{\theta}} = \frac{m}{4\hbar^2 \epsilon_0} e^2 L^4 \alpha^2 n_e^{3D}}, \tag{B.15}$$

remains unchanged. The one before the critical point,

$$\boxed{\chi_{\tilde{\theta}}^- = \frac{2m}{\hbar^2 \epsilon_0} e^2 \alpha^2 L \left[\frac{2}{9} \frac{a_0}{\Gamma^4} L^3 n_e^{3D} + \frac{2}{4\pi} \left(1 - \frac{2}{3} \frac{a_0}{|\Gamma|} \right)^2 \right]}, \tag{B.16}$$

changes by a factor of two in the second term, as we now take $g_0^s = 2g_0$ in Eq. (4.49). The one after the critical point,

$$\boxed{\chi_{\tilde{\theta}}^+ = \frac{2m}{\hbar^2 \epsilon_0} e^2 \alpha^2 L \left[\frac{2}{9} \frac{L^3}{\Gamma_c^4} \left(a_0(n_e^{3D} - n_1^s g_s/V) + \Gamma_c m_1^2 n_1^s g_s/V \right) + \frac{2}{4\pi} \left(1 - \frac{2}{3} \frac{a_0}{\Gamma_c} \right)^2 \right]}, \tag{B.17}$$

changes in the same way just in the second term, as for the first terms we have that $n_m^s g_s = n_m g$.

The general discontinuity of the magnetization at a critical point of Eq. (4.83), in which we explicitly substituted the degeneracies, is now

$$\boxed{\Delta M^{(m)} = -\frac{2\mu_B}{2\pi} \frac{\Gamma_c^{(m)3}}{L^3} \left[\left(m - \frac{2}{3} \frac{1}{\Gamma_c^{(m)}} (a_0 + ... + a_{m-1}) \right) n_m^s + \frac{\lambda}{12\alpha L} \left(1 - \frac{3}{4} \mathfrak{g}^2 \right) h(\mathcal{E}_F) \right]}, \tag{B.18}$$

when taking spin into account. Technically only the last term explicitly doubles, as in the first term, the number n_m^s is halved.

B.3 Spin in the QHE of TI

If we keep in mind that the Zeeman effect is negligible such that each Landau level is doubly degenerate, just as we have done, nothing particularly noticeably changes

in chapter 5. The perturbation Hamiltonian $\hat{H}'$ of Eq. (5.8) does not possess spin operators that mix spin states, while the Zeeman interaction just enters in the free Hamiltonian $\hat{H}_0$ and does not change the spatial components of the free solutions. Therefore all of the perturbation matrix elements are diagonal in spin space, and thus the Energy differences in the perturbation expansion cancel the Zeeman splitting.

At the end all of the expressions stay the same, and the only thing that changes is the degeneracy of each Landau level $g_s = 2g$, which implicitly changes the sum over the occupied states in all of our expressions. This can just be taken into account by taking $n_e \longrightarrow n_e/2$, just as before. For example, the n_e axis in Figs. 5.6a and 5.6b should be halved to take spin into account.

C Airy Functions

C.1 Overview

The Airy functions were first introduced by G. B. Airy when studying the intensity of light in the neighbourhood of a caustic [44, 45]. Under the modern notation (first introduced by H. Jeffreys in 1928 [36, 46]), these are given by

$$\text{Ai}(z) = \frac{1}{\pi} \int_0^\infty \cos\left(\frac{t^3}{3} + zt\right) dt, \qquad \text{Bi}(z) = \frac{1}{\pi} \int_0^\infty \left[e^{-t^3/3+zt} + \sin\left(\frac{t^3}{3} + zt\right)\right] dt, \tag{C.1}$$

and are the solutions to the homogeneous differential equation

$$y''(z) = zy, \tag{C.2}$$

which is called the Airy equation. A plot for these functions is shown in Fig. C.1. Both of the functions are oscillatory for negative values of z, while $\text{Ai}(z)$ exponentially decays and $\text{Bi}(z)$ exponentially grows for positive values of z.
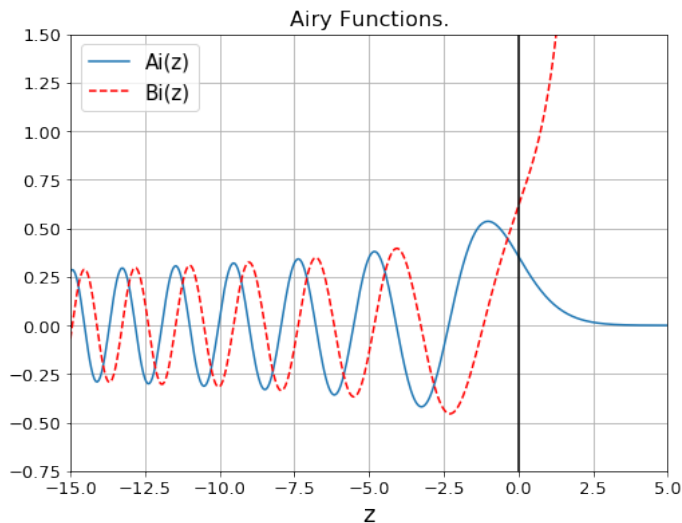

Figure C.1: Plot of the Airy functions.

The Wronskian between these functions is [36]

$$W\{\text{Ai}(z), \text{Bi}(z)\} \equiv \text{Ai}(z)\frac{d\,\text{Bi}(z)}{dz} - \text{Bi}(z)\frac{d\,\text{Ai}(z)}{dz} = \frac{1}{\pi}, \tag{C.3}$$

and thus these are the two independent solutions of the Airy equation (C.2).

C.1.1   Useful integrals

If we define arbitrary linear combinations of the Airy functions given by

$$A(\xi) = a_1 \operatorname{Ai}(\xi) + a_2 \operatorname{Bi}(\xi), \tag{C.4}$$

and

$$B(\xi) = b_1 \operatorname{Ai}(\xi) + b_2 \operatorname{Bi}(\xi) \tag{C.5}$$

(where in the main text we take $a_1 = C$, $a_2 = D$, $b_1 = C^*$ and $b_2 = D^*$), then there exist some general primitives for combinations of these functions. Some of them, which are used throughout this work (specially in Chapter 5), are

As well as the integrals (C.6) and (C.7), we will also need the ones at next order in ξ, which are also present in [36]. These are

$$\bar{I}_1 = \int A(\xi)B(\xi)\,\mathrm{d}\xi = \xi A(\xi)B(\xi) - A'(\xi)B'(\xi), \tag{C.6}$$

$$I_1 = \int A(\xi)B(\xi + \Delta)\,\mathrm{d}\xi = \frac{1}{\Delta}\big[B'(\xi + \Delta)A(\xi) - B(\xi + \Delta)A'(\xi)\big], \tag{C.7}$$

$$\bar{I}_2 = \int \xi A(\xi)B(\xi)\,\mathrm{d}\xi = \frac{\xi^2}{3}A(\xi)B(\xi) + \frac{1}{6}\big[A'(\xi)B(\xi) + A(\xi)B'(\xi)\big] - \frac{\xi}{3}A'(\xi)B'(\xi), \tag{C.8}$$

and

$$\begin{aligned}
I_2 &= \int \xi A(\xi)B(\xi + \Delta)\,\mathrm{d}\xi \\
&= -\frac{\Delta + 2\xi}{\Delta^2}A(\xi)B(\xi + \Delta) + \frac{1}{\Delta^3}(2 + \xi\Delta^2)\big[B'(\xi + \Delta)A(\xi) - B(\xi + \Delta)A'(\xi)\big] \\
&\quad + \frac{2}{\Delta^2}B'(\xi + \Delta)A'(\xi).
\end{aligned} \tag{C.9}$$

C.2   Wave functions under a constant electric field

Take the 1D time-independent Schrödinger equation $\hat{H}\Psi(z) = \mathcal{E}\Psi(z)$. Under the action of a constant electric field E, the Hamiltonian is

$$\hat{H} = \frac{\hat{p}_z^2}{2m} + eE\hat{z}. \tag{C.10}$$

This gives the differential equation

$$-\frac{\hbar^2}{2m}\frac{\mathrm{d}^2}{\mathrm{d}z^2}\Psi(z) + (eEz - \mathcal{E})\Psi(z) = 0. \tag{C.11}$$

We assume that the wave functions are bound states (just like in Chapter 3). This means that the energies are negative and so can be expressed as

$$\mathcal{E} \equiv \mathcal{E}_\kappa = -\frac{\hbar^2\kappa^2}{2m}, \qquad \kappa \in \mathbb{R}^+. \tag{C.12}$$

If we further define the dimensionless variable

$$\xi = \left(\frac{\hbar^2}{2meE}\right)^{2/3}\left(\kappa^2 + \frac{2meE}{\hbar^2}z\right), \tag{C.13}$$

then

$$\frac{\mathrm{d}^2}{\mathrm{d}z^2} = \left(\frac{2meE}{\hbar^2}\right)^{2/3}\frac{\mathrm{d}^2}{\mathrm{d}\xi^2}, \tag{C.14}$$

and thus Eq.(C.11) transforms into

$$\Psi''(\xi) - \xi\Psi(\xi) = 0. \tag{C.15}$$

This is the Airy equation and so the solutions are

$$\Psi(\xi) = a\,\mathrm{Ai}(\xi) + b\,\mathrm{Bi}(\xi). \tag{C.16}$$

This is the reason why the bound-state solutions (3.5b) are given by Airy functions in their z-component, where in that case the electric field is the induced field $\tilde{E}$.

D The WKB approximation

D.1 Overview

The WKB approximation consists of approximating the Schrödinger equation in one dimension (the z direction in our context) by assuming that the de Broglie wavelength of the wave function is smaller than the characteristic length at which the potential $V(z)$ noticeably varies [11]. This is done by defining the classical momentum

$$p(z) = \sqrt{2m(E - V(z))} \tag{D.1}$$

which is real for the so-called classical region $E > V(z)$, and imaginary for the non-classical region $E < V(z)$.

Thus, the Schrödinger equation can be written as

$$\frac{d^2\psi}{dz^2} = -\frac{p^2(z)}{\hbar^2}\psi(z). \tag{D.2}$$

Expressing the wave function as

$$\psi(z) = A(z)e^{i\phi(z)}, \tag{D.3}$$

where $A(z)$ and $\phi(z)$ are real functions then Eq. (D.2) becomes

$$A'' + i\left(A^2\phi'\right)' - A(\phi')^2 = -\frac{p^2(z)}{\hbar^2}A. \tag{D.4}$$

Separating the real and imaginary parts we get the following two sets of equations, so far completely equivalent to the Schrödinger equation,

$$A'' = A\left[(\phi')^2 - \frac{p^2(z)}{\hbar^2}\right], \qquad \left(A^2\phi'\right)' = 0. \tag{D.5}$$

Now we suppose that the term A''/A can be neglected with respect to $(\phi')^2$ and p^2, which this tells us that the wave function's amplitude does not oscillate very much [12]. In the first equation, this implies that

$$\phi'(z) \approx \pm\frac{p(z)}{\hbar}. \tag{D.6}$$

97

Thus, from the second equation of (D.5),

$$A(z) = \frac{C}{\sqrt{\phi'(z)}} \approx \frac{C}{\sqrt{p(z)}}. \tag{D.7}$$

With this, we now see what was mentioned at the beginning of this section about the meaning of this approximation, for the condition $A''/A \ll p^2/\hbar^2$, alongside with supposing that $V''(z) \approx 0$ (the potential varies slowly), is equivalent to

$$\frac{\hbar}{p} \ll \frac{p^2}{m|V'|} = \frac{2[E - V(z)]}{|\mathrm{d}V/\mathrm{d}z|}. \tag{D.8}$$

That is, once again, we assume that de Broglie wave length is much smaller than the characteristic length at which the potential varies. Notice, nonetheless, that this condition will irrevocably break close to the turning points for which $E = V(z)$.

Far from the turning points, in the classical region ($p(z)$ real) the wave function is approximately

$$\psi(z) = \frac{C}{\sqrt{p(z)}} \exp\left[\pm \frac{i}{\hbar} \int p(z')\,\mathrm{d}z'\right], \tag{D.9}$$

and in the non-classical region ($p(z)$ imaginary),

$$\psi(z) = \frac{C}{\sqrt{|p(z)|}} \exp\left[\pm \frac{1}{\hbar} \int |p(z')|\,\mathrm{d}z'\right]. \tag{D.10}$$

These account for oscillating and exponentially decreasing respectively functions as expected. The choice on the limits of integration can always be absorbed in the normalization constant.
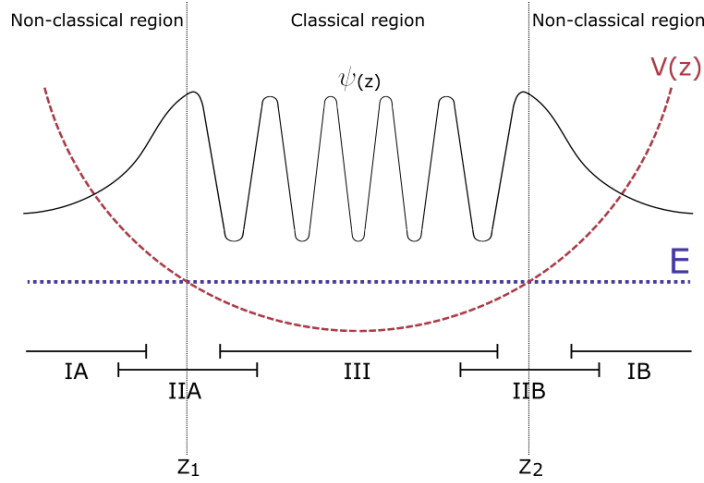

Figure D.1: Regions of interest for a potential well in the WKB method and their approximations. IA & IB: Non-classical regions with wave functions given by Eq. (D.10) and $p(z)$ imaginary. III: Classical region with wave function given by Eq. (D.9) and $p(z)$ real. IIA & IIB: Turning-point regions where the WKB approximation breaks. $V(z)$ is approximated as a linear function, such that the wave functions are given by Eq. (D.12) around each turning point z_1 and z_2. For $|z| > z_i$ we have positive $\xi_i \equiv \alpha_i(z - z_i)$. For $|z| < z_i$ we have negative ξ_i, $i = 1, 2$.

Close to the turning points we cannot use the WKB approximation, but can instead directly approximate the potential at first order around each turning point. That is, if we assume a potential well with turning points z_1 and z_2 (see Fig. D.1), then we can take

$$V(z) \approx E + V'(z_i)(z - z_i), \quad z \approx z_i, \quad i = 1, 2. \tag{D.11}$$

As this is a linear potential, the solutions to the Schrödinger equation are composed of Airy functions [12]. That is, close to the turning points,

$$\psi_i(z) = a \operatorname{Ai}(\alpha_i[z - z_i]) + b \operatorname{Bi}(\alpha_i[z - z_i]), \quad \alpha_i = \left[\frac{2m}{\hbar^2} V'(z_i) \right]^{1/3}, \quad i = 1, 2. \tag{D.12}$$

Note that for a potential well α_1 is negative, while α_2 is positive. In total, setting the integration limits and taking into account the convergence of the wave functions, the approximate solutions in each region are (see Fig. D.1)

$$\psi(z) \approx \begin{cases} \frac{C_1}{\sqrt{|p(z)|}} \exp\left[-\frac{1}{\hbar} \int_z^{z_1} |p(z')| \, \mathrm{d}z' \right], & z \ll z_1, \\ a_1 \operatorname{Ai}(\alpha_1[z - z_1]) + b_1 \operatorname{Bi}(\alpha_1[z - z_1]), & z \approx z_1, \\ \frac{1}{\sqrt{p(z)}} \left(A e^{\frac{i}{\hbar} \int_{z_1}^z p(z') \, \mathrm{d}z'} + B e^{-\frac{i}{\hbar} \int_{z_1}^z p(z') \, \mathrm{d}z'} \right), & z_1 \ll z \ll z_2, \\ a_2 \operatorname{Ai}(\alpha_2[z - z_2]) + b_2 \operatorname{Bi}(\alpha_2[z - z_2]), & z \approx z_2, \\ \frac{C_2}{\sqrt{|p(z)|}} \exp\left[-\frac{1}{\hbar} \int_{z_2}^z |p(z')| \, \mathrm{d}z' \right], & z_2 \ll z. \end{cases} \tag{D.13}$$

Now we stick each solution by mixing the conditions that define each region. First we stick the non classical regions to the turning points. For the Airy functions we use the asymptotic expressions corresponding to large positive values of $\xi_i \equiv \alpha_i(z - z_i)$ (that is, $z \ll z_1$ with z negative for $i = 1$ and $z_2 \ll z$ with z positive for $i = 2$), for which [36]

$$a_i \operatorname{Ai}(\xi_i) + b_1 \operatorname{Bi}(\xi_i) \approx \frac{a_i}{2\sqrt{\pi}\xi_i^{1/4}} e^{-\frac{2}{3}\xi_i^{3/2}} + \frac{b_i}{\sqrt{\pi}\xi_i^{1/4}} e^{\frac{2}{3}\xi_i^{3/2}}. \tag{D.14}$$

For the solutions in the non classical region we assume $z \approx z_i$ (with $z < z_1$ and $z > z_2$ respectively) such that the potential is given by (D.11). This gives $p(z) \approx \sqrt{2m[E - E - V'(z_i)(z - z_i)]}$ and thus

$$\int_z^{z_i} |p(z')| \, \mathrm{d}z' \approx \hbar \int_z^{z_i} \left| \sqrt{-\alpha_i^3(z' - z_i)} \right| \, \mathrm{d}z' = -(-1)^i \frac{2}{3} \hbar \xi_i^{3/2}, \tag{D.15}$$

so the corresponding wave functions are approximately

$$\frac{C_i}{\sqrt{|p(z)|}} \exp\left[(-1)^i \frac{1}{\hbar} \int_z^{z_i} |p(z')| \, \mathrm{d}z' \right] \approx \frac{C_i}{\sqrt{\hbar}(\alpha_i^3[z - z_i])^{1/4}} e^{-\frac{2}{3}\xi_i^{3/2}} \tag{D.16}$$

Comparing the asymptotic forms of Eqs. (D.14) and (D.16), we obtain that

$$a_i = \sqrt{\frac{4\pi}{|\alpha_i|\hbar}} C_i, \quad b_i = 0. \tag{D.17}$$

Now we stick the classical region to the turning points. For the oscillating solutions we take once again $z \approx z_i$ such that $V(z)$ is given by Eq. (D.11), alongside with $z > z_1$ and $z < z_2$ respectively for each point. In this case, both ξ_i are now negative. For $z \approx z_1$ we obtain

$$\int_{z_1}^{z} p(z')\,\mathrm{d}z' \approx \hbar \int_{z_1}^{z} \sqrt{-\alpha_1^3 (z' - z_1)}\,\mathrm{d}z' = \frac{2}{3}\hbar(-\xi_1)^{3/2}, \tag{D.18}$$

For $z \approx z_2$ we need to separate the limits of integration, as they needn't be close,

$$\begin{aligned}
\int_{z_1}^{z} p(z')\,\mathrm{d}z' &= \int_{z_1}^{z_2} p(z')\,\mathrm{d}z' - \int_{z}^{z_2} p(z')\,\mathrm{d}z' \\
&= \hbar\Omega - \hbar \int_{z}^{z_2} \sqrt{-\alpha_2^3 (z' - z_2)}\,\mathrm{d}z', \quad \Omega \equiv \frac{1}{\hbar} \int_{z_1}^{z_2} p(z')\,\mathrm{d}z' \tag{D.19} \\
&= \hbar\Omega - \frac{2}{3}\hbar(-\xi_2)^{3/2}.
\end{aligned}$$

Thus, for $z \approx z_1$,

$$\frac{1}{\sqrt{p(z)}} e^{\pm \frac{i}{\hbar} \int_{z_1}^{z} p(z')\,\mathrm{d}z'} \approx \frac{1}{\sqrt{\hbar|\alpha_1|}(-\xi_1)^{1/4}} e^{\pm \frac{2}{3}i(-\xi_1)^{3/2}}, \tag{D.20}$$

and for $z \approx z_2$,

$$\frac{1}{\sqrt{p(z)}} e^{\pm \frac{i}{\hbar} \int_{z_1}^{z} p(z')\,\mathrm{d}z'} \approx \frac{1}{\sqrt{\hbar|\alpha_2|}(-\xi_2)^{1/4}} e^{\pm i\left[\Omega - \frac{2}{3}(-\xi_2)^{3/2}\right]}. \tag{D.21}$$

For the remaining Airy functions we use the asymptotic expressions for large negative ξ_i, which now give [36]

$$\begin{aligned}
a_i \operatorname{Ai}(\xi_i) &\approx \frac{a_i}{\sqrt{\pi}(-\xi_i)^{1/4}} \sin\left[\frac{2}{3}(-\xi_i)^{3/2} + \frac{\pi}{4}\right] \\
&= \frac{a_i}{2i\sqrt{\pi}(-\xi_i)^{1/4}} \left[e^{i\frac{2}{3}(-\xi_i)^{3/2} + i\pi/4} - e^{-i\frac{2}{3}(-\xi_i)^{3/2} - i\pi/4}\right]
\end{aligned} \tag{D.22}$$

At the $z \approx z_1$ region the functions of Eqs. (D.20) and (D.22) match naturally, and so

$$\frac{a_1}{2i\sqrt{\pi}} e^{i\pi/4} = \frac{A}{\sqrt{\hbar|\alpha_1|}}, \quad -\frac{a_1}{2i\sqrt{\pi}} e^{-i\pi/4} = \frac{B}{\sqrt{\hbar|\alpha_1|}}, \tag{D.23}$$

so that with Eq. (D.17),

$$A = -ie^{i\pi/4}C_1, \quad B = ie^{-i\pi/4}C_1. \tag{D.24}$$

At the $z \approx z_2$ region, not only do the constants swap, but we also obtain an extra factor,

$$\frac{a_2}{2i\sqrt{\pi}} e^{i\pi/4} = \frac{B}{\sqrt{\hbar|\alpha_2|}} e^{-i\Omega}, \quad -\frac{a_2}{2i\sqrt{\pi}} e^{-i\pi/4} = \frac{A}{\sqrt{\hbar|\alpha_2|}} e^{i\Omega}, \tag{D.25}$$

so that with Eq. (D.17),

$$A = ie^{-i\Omega - i\pi/4} C_2, \quad B = -ie^{i\Omega + i\pi/4} C_2. \tag{D.26}$$

Using Eqs. (D.24) and (D.26) we obtain that

$$\frac{A}{B} = -e^{-2i\Omega - i\pi/2} = -e^{i\pi/2}. \tag{D.27}$$

At most, the arguments must differ by $2\pi i k$, $k \in \mathbb{Z}$. As Ω is positive, we must have that $\Omega = \pi(k + 1/2)$, $k = 0, 1, 2....$ This gives us the approximate quantization condition, and the main result of the WKB approximation,

$$\boxed{\int_{z_1}^{z_2} p(z)\, \mathrm{d}z = \pi \hbar \left(k + \frac{1}{2} \right), \quad k = 0, 1, 2...} \tag{D.28}$$

D.2   Application for the bound-state energies

In the context of chapter 3, we have that

$$p(z) = \sqrt{-\kappa^2 - 2me\tilde{E}z}, \tag{D.29}$$

where we must remember that $\tilde{E} < 0$. From Fig. 3.1 we can see that the first turning point is the one that fulfills $p(z_1) = 0$. The second one is $z_2 = L$. With these conditions we obtain that

$$z_1/\ell_{\tilde{E}} = -\sigma^2, \quad z_2/\ell_{\tilde{E}} = \Gamma. \tag{D.30}$$

Having fixed the turning points in terms of the bound momentum κ, we can compute the integral of the WKB quantization condition of Eq. (D.28),

$$\frac{1}{\hbar} \int_{z_1}^{z_2} p(z)\, \mathrm{d}z = \int_{z_1}^{z_2} \sqrt{-\kappa^2 - z/\ell_{\tilde{E}}^3}\, \mathrm{d}z = -\frac{2}{3}(-\sigma^2 - \Gamma)^{3/2}. \tag{D.31}$$

With the right hand side of Eq. (D.28), and taking in mind that Γ and σ are negative, we thus obtain

$$\boxed{|\sigma| = \sqrt{|\Gamma| - (3\pi/2)^{2/3}(k + 1/2)^{2/3}},} \tag{D.32}$$

which is the desired formula of Eq. (3.18).

E Limits

In chapters 3 and 5, not only does it looks like the limit $\Delta \longrightarrow 0$ of equations (C.7) and (C.9) does not imply equations (C.6) and (C.8) respectively, but it even seems that the limit diverges. This is subsequently inherited to the integral $I_{\kappa,\kappa'}$. In this section we will show that the undetermined integrals diverge by a constant term which is not dependent on ξ, and so any definite integral does not diverge. Furthermore, the finite term will coincide with the desired limit. Even so, the limit $\kappa = \kappa'$ on the definite integral $I_{\kappa,\kappa'}$ does not hold. We will see that this is due to the fact that taking the limit does not commute with imposing the boundary conditions.

By a direct calculation,

$$
\begin{aligned}
\lim_{\Delta \longrightarrow 0} I_1 &= \lim_{\Delta \longrightarrow 0} \frac{1}{\Delta} \big[B'(\xi + \Delta) A(\xi) - B(\xi + \Delta) A'(\xi) \big] \\
&= \lim_{\Delta \longrightarrow 0} \left\{ \frac{B'(\xi + \Delta) - B'(\xi)}{\Delta} A(\xi) - \frac{B(\xi + \Delta) - B(\xi)}{\Delta} A'(\xi) \right. \\
&\qquad\qquad\qquad\qquad\qquad \left. + \frac{A(\xi) B'(\xi) - A'(\xi) B(\xi)}{\Delta} \right\} \\
&= B''(\xi) A(\xi) - B'(\xi) A'(\xi) + \frac{W(A, B)}{\Delta},
\end{aligned}
\tag{E.1}
$$

where $W(A, B)$ is the Wronskian between the two functions. Because $A(\xi)$ and $B(\xi)$ are linear combinations of Airy functions, they satisfy the Airy equation $y''(\xi) = \xi y(\xi)$. Thus, if we have $A(\xi) = aAi(\xi) + bBi(\xi)$ and $B(\xi) = cAi(\xi) + dBi(\xi)$, then

$$
W(A, B) = (ad - bc)\frac{1}{\pi},
\tag{E.2}
$$

which is a constant independent of ξ. Thus

$$
\lim_{\Delta \longrightarrow 0} I_1 = \bar{I}_1 + C,
\tag{E.3}
$$

where C is an infinite constant that nullifies itself when computing the definite integral. Something similar happens when taking the limit of I_2 to obtain $\bar{I}_2$.

This motivates us to think that $I_{\kappa,\kappa}$ of equation (5.42), being the result of a definite integral, should be recovered when taking the limit of $I_{\kappa,\kappa'}$ in equation (5.43). This is not the case. The limit still results in a pole, even after already having eliminated

the infinite constant of the indefinite integral. The reason for this is that **taking the limit does not commute with imposing the boundary conditions**.

A simple way to see this to take a term similar to the ones that appear in equation (E.1),

$$x \equiv \frac{A'(\tau') - A'(\tau)}{\Delta}, \tag{E.4}$$

with $\tau' = \tau + \Delta$.

If we first take the limit,

$$x_1 = \lim_{\Delta \to 0} \frac{A'(\tau + \Delta) - A'(\tau)}{\Delta} = A''(\tau), \tag{E.5}$$

where $A(\tau)$ fulfills the Airy equation, so

$$x_1 = \tau A(\tau) = (\sigma^2 + \Gamma)A(\tau), \tag{E.6}$$

where we have also taken the definition of τ in terms of the other dimensionless constants σ and Γ.

Now, if we instead first (like we did when calculating $I_{\kappa,\kappa'}$) impose the boundary conditions (5.22) and (5.23), then

$$x_2 = -\frac{\sigma' A(\tau') - \sigma A(\tau)}{\Delta}. \tag{E.7}$$

Taking the limit $\Delta \to 0$, $\sigma = \sigma'$, then

$$x_2 = -\sigma \lim_{\Delta \to 0} \frac{A(\tau + \Delta) - A(\tau)}{\Delta} = -\sigma A'(\tau). \tag{E.8}$$

Using the boundary conditions once again,

$$x_2 = \sigma^2 A(\tau). \tag{E.9}$$

Comparing both expressions,

$$x_1 - x_2 = \Gamma A(\tau) \neq 0. \tag{E.10}$$

So the limit does not commute with taking the boundary conditions. Because in the final expressions of $I_{\kappa,\kappa'}$ we have already imposed the boundary conditions, it is not expected that the limit $\kappa \to \kappa'$ from one should recover the other.

Bibliography

[1] C. Kittel. *Introduction to Solid State Physics*. John Wiley & Sons Inc, 8th edition, 2005.

[2] E.H. Hall. On a new action of the magnet on electric currents. *American Journal of Mathematics*, 2(287), 1879.

[3] David Tong. The quantum Hall effect, January 2016.

[4] K. v. Klitzing, G. Dorda, and M. Pepper. New method for high-accuracy determination of the fine-structure constant based on quantized Hall resistance. *Physical Review Letters*, 45(494), 1980.

[5] International Science Council. Comitee on Data. Fundamental physical constants, June 2019.

[6] D.C. Tsui, H.L. Stormer, and A.C. Gossard. Two-dimensional magnetotransport in the extreme quantum limit. *Physical Review Letters*, 48(1559), 1982.

[7] S. Meng. Integer Quantum Hall Effect, May 2018, hep-th/2011.13601.

[8] K. Fujikawa and H. Suzuki. *Path Integrals and Quantum Anomalies*. Oxford University Press, 1st edition, 2004.

[9] P. Drude. Zur Elektronentheorie der Metalle. (German) [Towards a theory of electrons in metals]. *Annalen der Physik*, 306(3):566–613, 1900.

[10] P. Drude. Zur Elektronentheorie der Metalle; II. Teil. Galvanomagnetische und thermomagnetische Effecte. (German) [Towards a theory of electrons in metals; part II. Galvanomagnetic and thermodynamic effects.]. *Annalen der Physik*, 308(11):369–402, 1900.

[11] J. J. Sakurai. *Modern Quantum Mechanics*. Addison Wesley Publishing Company, revised edition, 1994.

[12] D. J. Griffiths. *Introduction to Quantum Mechanics*. Pearson Education International, 2nd edition, 2005.

[13] I.D. Vagner, V.M. Gvozdikov, and P. Wyder. Quantum mechanics of electrons in strong magnetic field. *Journal of Science and Engineering*, 3(1):5–55, 2006.

[14] G. B. Arfken and H. J. Weber. *Mathematical Methods for Physicists*. Elsevier Academic Press, 6th edition, 2005.

[15] T. Ando. Theory of quantum transport in a two-dimensional electron system under magnetic fields. III. many-site approximation. *Journal of the Physical Society of Japan*, 37(3), 1974.

[16] O.M. Corbino. Azione elettro-magnetica degli ioni dei metalli, deviati dalla traiettoria normale per effetto di un campo magnetico. (Italian) [Electromagnetic action of metal ions, deviated from the normal trajectory due to the effect of a magnetic field]. *Atti R. Accad. Lincei*, 20:342–344, 1911.

[17] C. L. Kane and E. J. Mele. Z_2 topological order and the quantum spin Hall effect. *Phys. Rev. Lett.*, 95:146802, Sep 2005.

[18] C. L. Kane and E. J. Mele. Quantum Spin Hall Effect in Graphene. *Phys. Rev. Lett.*, 95(22):226801, 2005, cond-mat/0411737.

[19] L. Fu, C. L. Kane, and E. J. Mele. Topological insulators in three dimensions. *Phys. Rev. Lett.*, 98:106803, Mar 2007.

[20] J. E. Moore and L. Balents. Topological invariants of time-reversal-invariant band structures. *Phys. Rev. B*, 75:121306, Mar 2007.

[21] R. Roy. Topological phases and the quantum spin Hall effect in three dimensions. *Phys. Rev. B*, 79:195322, May 2009.

[22] B.A. Bernevig and S.C. Zhang. Quantum spin Hall effect. *Phys. Rev. Lett.*, 96:106802, Mar 2006.

[23] L. Fu and C.L. Kane. Topological insulators with inversion symmetry. *Phys. Rev. B*, 76:045302, Jul 2007.

[24] B.A. Bernevig, T.L. Hughes, and S.C. Zhang. Quantum spin Hall effect and topological phase transition in HgTe quantum wells. *Science*, 314:1757–1761, Dec 2006.

[25] H. Zhang, CX. Liu, XL. Qi, et al. Topological insulators in $Bi_2 Se_3$, $Bi_2 Te_3$ and $Sb_2 Te_3$ with a single Dirac cone on the surface. *Nature*, 5:438–442, May 2009.

[26] D. Hsieh, D Qian, L. Wray, et al. A topological Dirac insulator in a quantum spin Hall phase. *Nature*, 452:970–974, Apr 2008.

[27] M. König, S. Wiedmann, C. Brüne, et al. Quantum spin Hall insulator state in HgTe quantum wells. *Science*, 318:766–770, Nov 2007.

[28] J. D. Jackson. *Classical Electrodynamics*. John Wiley & Sons Inc, 3rd edition, 1999.

[29] H. A. Kramers. Théorie générale de la rotation paramagnétique dans les cristaux. (French) [General theory of the paramagnetic rotation in a crystal]. *Proceedings of the Royal Netherlands Academy of Arts and Sciences*, 33(6–10):959–972, Nov 1930.

[30] E. P. Wigner. *Group Theory and its Application to the Quantum Mechanics of Atomic Spectra*. Academic Press Inc., 1st edition, 1960.

[31] X.L. Qi, T.L. Hughes, and S.C. Zhang. Topological field theory of time-reversal invariant insulators. *Phys. Rev. B*, 78:195424, Nov 2008.

[32] V. Dziom, A. Shuvaev, A. Pimenov, et al. Observation of the universal magnetoelectric effect in a 3D topological insulator. *Nat. Commun*, 8:15197, May 2017.

[33] D.A. Bonilla. Problemas clásicos y cuánticos en electrodinámica θ. (Spanish) [Classical and quantum problems in θ electrodynamics]. Master's thesis, Universidad Nacional Autónoma de México, 2017.

[34] A. Sekine and K. Nomura. Axion Electrodynamics in Topological Materials, Nov 2020, cond-mat.mes-hall/2011.13601.

[35] M. Fiebig. Revival of the magnetoelectric effect. *J. Phys. D: Appl. Phys.*, 38(8):123–152, Apr 2005.

[36] O. Vallée and M. Soares. *Airy Functions and Applications to Physics*. Imperial College Press, 1st edition, 2004.

[37] D. Baasanjav, O. A. Tretiakov, and K. Nomura. Magnetoelectric effect in topological insulator films beyond the linear response regime. *Phys. Rev. B*, 90:045149, Jul 2014.

[38] N. W. Ashcroft and N. D. Mermin. *Solid State Physics*. Harcourt, 1st edition, 1976.

[39] R. M. White. *Quantum Theory of Magnetism*. Springer, 3rd edition, 2007.

[40] M. Abramowitz and I. A. Stegun. *Handbook of Mathematical Functions with Formulas, Graphs, and Mathematical Tables*. Dover Publications, 10th edition, 1972.

[41] D. Arovas. Lecture notes on condensed matter physics, March 2010.

[42] C. Pfleiderer. Why first order quantum phase transitions are interesting. *J. Phys.: Condens. Matter.*, 17(11):987–997, Mar 2005.

[43] M.Z. Hasan and C.L. Kane. Colloquium: Topological Insulators. *Rev. Mod. Phys.*, 82:3045, 2010, 1002.3895.

[44] G. B. Airy. On the intensity of light in the neighbourhood of a caustic. *Trans. Camb. Phil. Soc.*, 6:379–402, Jan 1838.

[45] G. B. Airy. *Supplement to a paper "On the intensity of light in the neighbourhood of a caustic"*. Pitt Press by JW Parker, 1848.

[46] H. Jeffreys. Asymptotic solutions of linear differential equations. *The Lond., Edinb., and Dub. Phil. Mag. and Jour. of Sci.*, 33(221):451–456, Mar 1942.